DYNAMIC LIGHT SCATTERING FROM A SYSTEM OF INTERACTING COLLOIDAL PARTICLES

By

THOMAS WARREN TAYLOR

Bachelor of Science

Larmar University

Beaumont, Texas

1977

Submitted to the Faculty of the Graduate College
of the Oklahoma State University
in partial fulfillment of the requirements
for the Degree of
DOCTOR OF PHILOSOPHY
July, 1983

DYNAMIC LIGHT SCATTERING FROM A SYSTEM OF

INTERACTING COLLOIDAL PARTICLES

Thesis Approved:

Bruce J. Ackerson
Thesis Adviser

Hugh L. Scott

H. Olin Spivey

Norman N. Durham
Dean of the Graduate College

ACKNOWLEDGMENTS

Many people deserve credit for this work, however, I wish to express my sincere appreciation and respect for my major adviser, Dr. Bruce J. Ackerson. Bruce first brought the problem to my attention and continued to lend a great deal of insight throughout the work. His discussions and support helped me through the difficult times. Appreciation is also extended to the other committee members, Dr. H. L. Scott, Dr. G. P. Summers, and Dr. H. O. Spivey for their invaluable assistance and suggestions in the preparation of this manuscript.

To my colleagues in the department who put up with my rambling about the problems and difficulties I encountered, I am also grateful. Among them are Dr. Mahendra Jani, Dr. R. B. "Bubba" Bossoli, Robert Ruokolainen, and Jimmy Robbins.

I owe a great thanks to Mrs. Janet Sallee for typing the final manuscript and to Heinz Hall for his excellent help in designing and machining much of the apparatus used in the experiments.

I owe a special thanks to my parents, Mr. and Mrs. E. C. Beasley and the late Dr. T. W. Taylor, for encouraging and supporting me even when no end was in sight and for instilling in me the desire for knowledge.

We gratefully acknowledge support by the National Science Foundation Division of Materials Research, Low Temperature Physics (Grant No. DMR 81-11619) and the Water Research Institute. Without their support this thesis would not have been written.

Finally to my wife, Karen, I owe my deepest thanks for the many sacrifices she had to make to allow me to pursue my dreams. Without her patience and understanding, the long hours and nights spent in the lab and preparing this thesis would have been unbearable.

TABLE OF CONTENTS

LIST OF TABLES

LIST OF FIGURES

CHAPTER I

INTRODUCTION

Interacting Brownian Particles and Thesis Summary

The technique of dynamic light scattering has been used in the past to investigate the dynamical properties of macromolecules in solution. The interpretation of the experimental results is only straight forward at low concentrations where the particles move without interaction. In many instances it is of interest to extend these investigations to higher concentrations where the particles begin to interact. There are several types of interactions that may be important, however, the repulsive screened Coulomb interaction is of particular interest in suspensions of latex spheres. These Coulombic forces can cause an ordering of the charged particles over distances much larger than the average interparticle spacing.

Light scattering is a useful tool to investigate colloidal suspensions like this because the size of the particles and the interparticle spacing is of the order of 100 - 1000A and 1000A - 1.0 μm, respectively. The configuration of the system depends on several parameters, including the temperature and the interaction range. The interaction range, or the strength of the interaction, can be altered by changing the amount of counter-ions shielding the Coulomb potential. When the interaction

range is much greater than the mean interparticle spacing, the Brownian particles exhibit a crystalline structure. As the interaction range is reduced, the colloidal crystals "melt" and the Brownian particles exhibit a liquid-like form.

Experiments in the liquid-like phase show that the dynamic structure factor, or the intermediate scattering function, is not a single exponential as it is for non-interacting particles. The initial decay rate, for times much smaller than the typical collision time, satisfies the relation

$$K_1 = Dk^2/S(\bar{k}) \tag{1.1}$$

where $S(k)$ is the static structure factor, $\bar{k}$ is the scattered wave vector and D is the infinite dilution diffusion coefficient. This was found experimentally by Brown, Pusey, Goodwin and Ottewill (1975) and Schaefer and Ackerson (1975) and supported by the theoretical results of Pusey (1975) and Ackerson (1976). The interpretation of this short time response is that the initial decay is determined by the independent Brownian motion of the particles.

Although the short time behavior seems to be well understood, the long time behavior is not understood. An expression for the time dependence of the intermediate scattering function has been derived from the Smoluchowski equation using

$$\dot{S}(k,t) = - K_1 S(k,t) + 1/S(k) \int_o^t dt' M(k,t-t') S(k,t') \tag{1.2}$$

where $M(k,t)$ is called the memory function. It has been shown, assuming pairwise additive interaction, that in the limits $k << k_m$ and $k >> k_m$,

where k_m is the value of the scattered wave vector where the static structure factor shows its first peak, that S(k,t) should be a single exponential. Thus M(k,t) must be zero in these limits. In general, however, a finite memory function will lead to a nonexponential decay.

Gruner and Lehmann (1979, 1980) have made extensive measurements of the intermediate scattering function for suspensions of polystyrene spheres in water at five different concentrations. At the concentrations they used multiple scattering was a problem for which severe corrections had to be made. After correcting the correlation function the time decay was analyzed using the Siegart relation and a multiple exponential fitting routine

$$S(k,t) = \sum_i a_i \exp(-\Gamma_i t) \tag{1.3}$$

with the constraint $\sum_i a_i = 1$. Using this they extracted a reduced memory function

$$M'(k,O) = \frac{\tilde{M}(k,O)}{K_1 S(k)} = 1 - \left(\sum_i a_i/\Gamma_i\right)\left(\sum_i a_i \Gamma_i\right) \tag{1.4}$$

where:

$$\tilde{M}(k,O) = \int_O^\infty dt\, M(k,t).$$

They plotted this function against k/k_m and as expected M'(k,O) approached zero in the limits $k << k_m$ and $k >> k_m$. They also found the surprising result that for all the concentrations studied, M'(k,O) seemed to lie on a universal curve.

The cause for this nonexponentiality was not understood at that time. Explanations were sought in the frequency dependence of the hydrodynamic interactions (Berne, 1977) and in the dynamics of the

counterions (Altenberger, 1980). These explanations are ruled out because their typical relaxation frequencies are much larger than the experimentally determined first cumulant. The deviation from a single exponential must be due to processes that occur on a slower time scale.

Although the memory function accounts for the nonexponential behavior, the question remains as to the physical significance of the memory function. Hess and Klein (1981) used a phenomenological Navier-Stokes equation with an external friction force for the "Browian particle fluid" to suggest that in the limit of small wavevectors, $k \to 0$, the memory function is related to the intrinsic longitudinal viscosity of the Brownian particles

$$\eta_{ll} = \lim_{k \to o} \frac{c\, k_B T}{(Dk^2)^2} \int_o^\infty dt\, M(k,t). \qquad (1.5)$$

The longitudinal viscosity is identified as $\eta_{ll} = 4/3\, \eta_s + \eta_B$ with η_s the shear viscosity and η_B the bulk viscosity of the Brownian particles. The particle density or concentration is denoted by c. In order to reach this regime, light scattering experiments must be performed in the extreme forward direction which is very difficult to do.

The connection between the viscosity and the memory function seemed to be a step in the right direction, so the next move was to generalize this result to larger scattering wavevectors. Hess (1981a) solved the problem for a system of particles that obeyed the Smoluchowski equation and again showed the relationship between the longitudinal viscosity of the particles and the memory function. Questioning the restrictions of the Smoluchowski equation for strongly interacting systems, he also investigated the problem for a system that obeyed the more general

Fokker-Planck equation (Hess, 1981b). In both cases he found the effect could be understood as a visco-elastic relaxation of the longitudinal component of the stress due to the strong interactions between the particles. The problem can only be solved by introducing a frequency and wavevector dependent longitudinal viscosity. He found in both cases that the memory function was related to this longitudinal viscosity and that the result of the Fokker-Planck approach reduced to that of the Smoluchoski approach in the appropriate limit (see Chapter II). Then this Fokker-Planck result, coupled with a mode-mode coupling calculation of the intrinsic longitudinal viscosity based on the experimentally determined static structure factor of Gruner and Lehmann (1979b) showed qualitatively good agreement between theory and experiment.

While everything seems to work well, the existence of a universal curve for the reduced memory function is puzzling. It would seem that as the interactions increased in strength that the viscosity should also increase and this increase should be seen in the memory function. One cause for the universal behavior could be that the ratio of the interaction range to the mean interparticle spacing remained constant at all the concentrations studied. However, this seems highly unlikely. A second cause might be in their method of correcting for multiple scattering. If there was a systematic error in the method, then it could cause a systematic error in their results.

The purpose of the thesis is:

1. To investigate multiple scattering in interacting systems and devise a more precise method of correcting for multiple scattering or to suppress its effects.

2. To measure the memory function for a suspension of latex

spheres at different strengths of interactions. In so doing determine if the reduced memory function increases as the ionic strength of the suspension increases.

Correlation Functions

As most of this thesis deals with correlation functions of one kind or another it is useful to give a brief and general description of them. Martin (1968) gives a good and complete review of these functions as well as their applicability to many situations. The reader is directed to his book for a more thorough discussion.

Time dependent correlation functions have been familiar for a long time in the theory of noise and stochastic processes. These functions provide a concise method for expressing the degree to which two dynamical properties are correlated over a period of time. Here we will discuss some of their basic properties that will help in the understanding of the remainder of the thesis.

Consider a property A that depends on the positions and momenta of all the constituent particles in the system. The particles are constantly in motion due to their thermal excitations so their positions and momenta are constantly changing. The property A then is also constantly changing. Although the particles are moving according to Newton's equations, their vast number cause the motion to appear randomly thus, the property A changes randomly and resembles a noise pattern (Figure 1).

If we wished to measure this property, we would take many measurements over a period of time and average them. Thus, the measured bulk property for an equilibrium system is defined as the time average

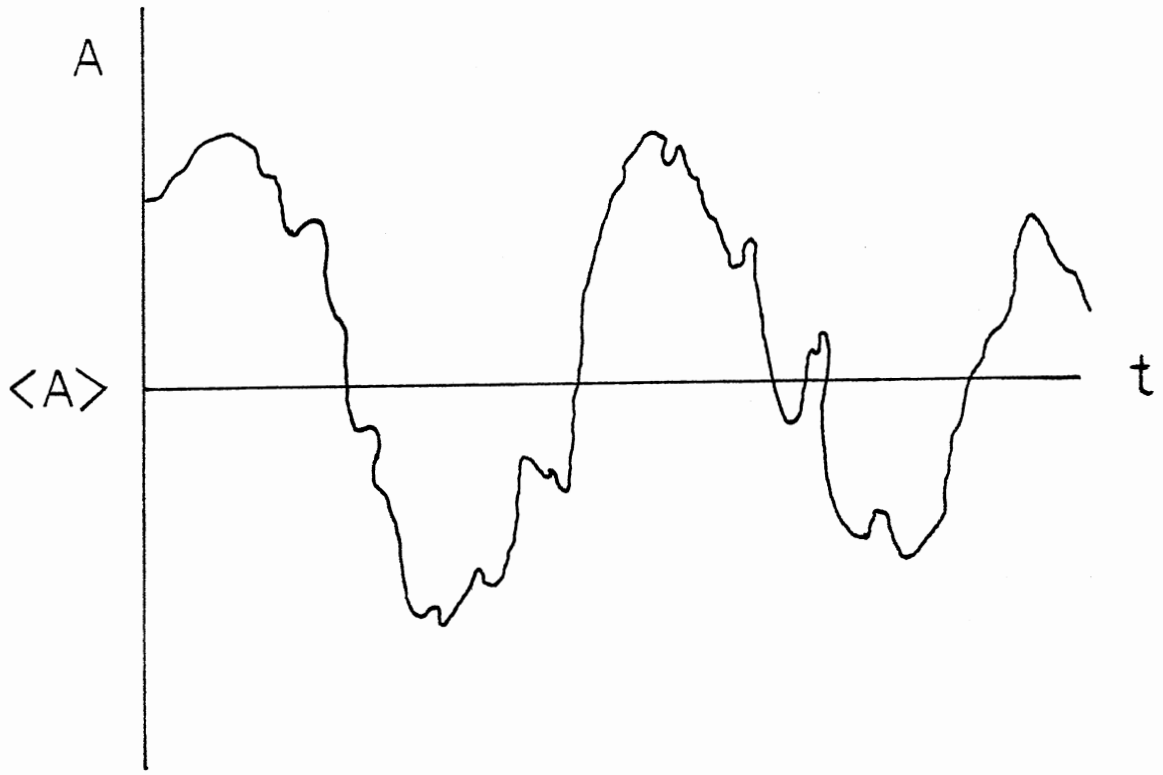

Figure 1. The Fluctuation of Property A in Time

$$A(t_o) = \lim_{T\to\infty} 1/T \int_{t_o}^{t_o+T} dt\, A(t) \qquad (1.6)$$

where t_o is the time when the measurement is initiated and T the length of time over which the property is averaged. We introduce the limit $T\to\infty$ to ensure that the averaging takes place over a time much longer than the period of the fluctuations.

Under certain general conditions, the system is metrically indecomposable or ergodic, so that the infinite time average is independent of the time in which the measurement was initiated. This property is referred to as stationarity and allows us to set $t_o = 0$ in Eq. (1.6).

$$A(o) = \lim_{T\to\infty} \frac{1}{T} \int_o^T dt\, A(t) \qquad (1.7)$$

Referring again to Figure 1 and for simplicity setting $\langle A\rangle = 0$, we see that in general $A(t) \neq A(t+t')$. However, for t' very small compared to the average fluctuation time, the two values of A will be very close. As t' grows the deviation of A(t+t') from A(t) also grows. Thus, we can say that A(t+t') is correlated with A(t) when t' is small but this correlation is lost as t' grows large compared to the typical fluctuation time of A.

A measure of this correlation is the autocorrelation function of A which is defined as

$$\langle A(t)A(o)\rangle = \lim_{T\to\infty} \frac{1}{T} \int_o^T dt'\, A(t')A(t+t') \qquad (1.8)$$

For t = 0 this becomes $\langle A^2(0)\rangle$ and is always positive. For other values of t, the product A(t')A(t+t') is negative at certain values of t' and

positive at other values. There is some cancellation between these positive and negative terms in the averaging process. This implies that

$$\langle A^2(0)\rangle \geq \langle A(t)A(0)\rangle \tag{1.9}$$

Thus, if A is a constant of the motion, the autocorrelation function remains constant in time, otherwise it decays from its initial value which is a maximum. For a nonconserved, nonperiodic property we expect that for t very large compared to the typical fluctuation time that A(t') and A(t+t') will become totally uncorrelated. This enables us to write

$$\lim_{t\to\infty} \langle A(t)A(0)\rangle = \langle A(t)\rangle \langle A(0)\rangle = \langle A(0)\rangle^2 \tag{1.10}$$

Therefore the time correlation function of A decays from $\langle A^2\rangle$ to $\langle A\rangle^2$.

In most cases, spectroscopy measures a time averaged correlation function whereas most theoretical calculations deal with the ensemble averaged correlation function. Birkhoffs ergodic theorem (Uhlenbeck and Ford, 1963) say that these two correlation functions are identical if the systems studied are ergodic. Although it has never been proven that real systems are ergodic, the predictions of the ensemble theory have been so consistent with experiment that the equivalence of the time averaged and ensemble averaged correlation functions is assumed. We, therefore, define the equilibrium ensemble averaged time correlation function as

$$\langle A(t)A(0)\rangle = \int d\bar{\Gamma}\, \rho_o\, A(\Gamma,t)A(\Gamma,0). \tag{1.11}$$

Here Γ is the state of the system and is dependent on the position and momenta of the constituent particles, ρ_o is the equilibrium probability

distribution of the particles and the property A is dependent on the state of the system. Thus, $A(\Gamma,0)$ is the value of the property A when the system is in its initial state $\Gamma(0)$ and $A(\Gamma,t)$ is the value at time t when the system is in the state $\Gamma(t)$.

Light Scattering

The main experimental technique involved in this work is dynamic light scattering, sometimes called quasi-elastic light scattering. For this reason a brief outline of light scattering theory is given in this section, along with some examples of the information that can be determined from it. In order to simplify the discussion, the following assumptions are applied.

1. The scattering volume contains a large number of particles so that the amplitude of the scattered electric field is a complex gaussian random variable.

2. The intensity of the scattered light from the liquid and small ions is negligible compared to the light scattered from the particles.

3. The particles are small, spherical, and identical so that their individual scattering amplitudes are independent of time.

4. The incident light is polarized perpendicular to the scattering plane and the scattered light has the same polarization.

5. The suspension is sufficiently transparent so that the Born approximation can be applied.

Under these assumptions the electric field at the particle is given by

$$E_p = E_o \hat{\varepsilon} \exp(i\bar{k}_I \cdot \bar{r}_1 - i\omega t) \quad . \tag{1.12}$$

Here E_o is the amplitude of the incident wave with frequency, ω, and wavevector $k_I = 2\pi n/\lambda$. The wavelength in vacuum is λ, the polarization is ε and index of refraction in the liquid is n. The position of the particle is r_1. The field at the detector can be written

$$\bar{E}_s = \frac{E_p}{|\bar{r}_2-\bar{r}_1|}\,\hat{\varepsilon}\,\exp(i\bar{k}_s\cdot(\bar{r}_2-\bar{r}_1) \tag{1.13}$$

where $\bar{k}_s$ is the scattered wavevector and $\bar{r}_2$ is the position of the detector.

Now if $r_2 >> r_1$, which is generally true, then $\hat{r}_2 \approx \hat{k}_s$ or $\bar{r}_2$ and $\bar{k}_s$ are in the same direction. This enables us to write the vector difference

$$|\bar{r}_2-\bar{r}_1| = r_2 - \bar{r}_1\cdot\bar{r}_2/r_2 \,. \tag{1.14}$$

The electric field at the detector can now be written

$$\bar{E}_s = E_o/r_2\,\hat{\varepsilon}\,\exp(ik_s r_2 - i\omega t)\,\exp[i(\bar{k}_I-\bar{k}_s)\cdot r_1] \tag{1.15}$$

Elastic scattering implies that no energy change occurs in the scattering process, hence $|\bar{k}_I| = |\bar{k}_S|$. We can now define the scattered wave vector as

$$\bar{k} = \bar{k}_I - \bar{k}_S \tag{1.16}$$

and the amplitude of k is given by

$$|k| = |\bar{k}_I - \bar{k}_S| = 2k_I \sin(\theta/2) \tag{1.17}$$

where θ is the angle between $\bar{k}_I$ and $\bar{k}_S$. Using this the scattered elec-

tric field is simplified to

$$\bar{E}_s(r_2,t) = \hat{\varepsilon}\, E_o/r_2 \exp(ik_s r_2 - i\omega t) \exp(ik\cdot r_1) \qquad (1.18)$$

Now consider all the N particles in the scattering volume and write the electric field autocorrelation function

$$\langle E_s(r_2,t)\, E_s^*(r_2,0)\rangle = \left\langle \sum_{i,j=1}^{N} \frac{E_o^2}{r_2^2} \exp(-i\omega t) \exp[ik\cdot(r_i(t) - r_j(0))] \right\rangle \qquad (1.19)$$

The photomultiplier tube is insensitive to high frequency oscillations so that the term $\exp(-i\omega t)$ can be neglected. In most experimental situations the distance r_2 is approximately the same for all particles. This means that the detector will see the relatively slowly varying envelope caused by the motions of the particles.

We can now define a normalized electric field autocorrelation function

$$g^{(1)}(t) = S(k,t)/S(k) \qquad (1.20)$$

with the dynamic structure factor given by

$$S(k,t) = \langle E_s(r_2,t)\, E_s^*(r_2,0)\rangle/C \qquad (1.21)$$

and the static structure factor

$$S(k) = \langle E_s(r_2,0)\, E_s^*(r_2,0)\rangle/C \qquad (1.22)$$

where the constant $C = NE_o^2/r_2^2$.

The static structure factor is identified as the average scattered intensity. Using Eq. (1.19) for a system of uniform identical scatterers

the static structure factor reduces to

$$S(k) = \sum_j \langle \exp[ik\cdot(\bar{r}_1 - \bar{r}_j)] \rangle \tag{1.23}$$

This factor can also be written in terms of the pair correlation function, g(r) (Hanson and McDonald, 1976).

$$S(k) = 1 + 4\pi C/k \int_o^\infty dr[g(r)-1]\, r\sin(kr) \tag{1.24}$$

In the absence of interactions the cross terms in Eqs. (1.19) and (1.23) are zero, and

$$S^I(k) = 1 \tag{1.25}$$

and

$$S^I(k,t) = \langle \exp[ik\cdot(\bar{r}(t) - \bar{r}(0))] \rangle \tag{1.26}$$

The superscript I indicates the ideal or noninteracting case.

With this brief background we can now make a few statements about the high and low k limits. From Eq. (1.24) we see that in the high k regime, the rapid oscillations in sin(kr) will cause the second term to be zero so that S(k) = 1. This is the same as neglecting the cross terms in Eq. (1.23) and implies that $S(k) = S^I(k)$. Applying the same arguments to S(k,t) yields

$$S(k,t) = S^I(k,t) = \langle \exp[ik\cdot(\bar{r}(t)-\bar{r}(0))] \rangle \tag{1.27}$$

Thus in the high k limit dynamic light scattering measurements will provide information on the self diffusion of the particles, even in strongly interacting systems.

In the low k limit dynamic light scattering probes large scale low motions in the suspension. When investigating these fluctuations of large spatial extent, it is useful to write the dynamic structure factor in the form

$$S(k,t) = \langle a(k,t)a(-k,0)\rangle \tag{1.28}$$

where a(k,t) is the spatial Fourier transform of the particle number density

$$a(k,t) = \int d\bar{r}\, \exp(i\bar{k}\cdot\bar{r}) \left[\sum_{i=1}^{N} \delta(\bar{r}-\bar{r}(t)\right] \tag{1.29}$$

or

$$a(k,t) = \sum_{i=1}^{N} \exp\left[i\bar{k}\cdot\bar{r}_i(t)\right] \tag{1.30}$$

Thus in the low k limit, light scattering directly measures the particle concentration fluctuations. The time correlation of the particle concentration in this limit is calculable from hydrodynamics. As an example the temperature diffusion mode in a simple liquid behaves like

$$\langle a(k,t)a(-k,0)\rangle \alpha \exp\left[-T/cC_p\, k^2 t\right] \tag{1.31}$$

where T is the thermal conductivity, c the average particle concentration and C_p the specific heat. Thus dynamic light scattering enables one to measure either the specific heat of the thermal conductivity of the sample, depending on what is known.

Another example is the diffusion of particles. In this case the correlation function is ensemble averaged to obtain

$$\langle \exp[i\bar{k}\cdot(\bar{r}(t) - \bar{r}(0))]\rangle = \int d\bar{r}(t)d\bar{r}(0)\ P(\bar{r}(t),\bar{r}(0))\ \exp[i\bar{k}\cdot(\bar{r}(t) - \bar{r}(0))] \tag{1.32}$$

where $P(\bar{r}(t),\bar{r}(0))$ is the probability that a particle will be at the position $\bar{r}(t)$ at time t given that it was initially at $\bar{r}(0)$. In diffusion the position dependencies in the probability distribution function appear only in the form $|\bar{r}(t)-\bar{r}(0)|$, see Eq. (1.36). This enables us to simplify Eq. (1.32) to

$$\langle \exp[ik\cdot(\bar{r}(t)-\bar{r}(0))]\rangle = \int d\bar{r}\ P(\bar{r},t)\ \exp(i\bar{k},\bar{r}) = P(\bar{k},t) \tag{1.33}$$

Thus the correlation function measured in dynamic light scattering is the spatial Fourier transform of the probability P(r,t).

To find this in terms of the particle properties we go to the diffusion equation

$$\dot{P}(\bar{r},t) = D\nabla^2 P(\bar{r},t) \tag{1.34}$$

where D is the infinite dilution diffusion coefficient given by the Stokes-Einstein relation for independent diffusing particles

$$D = k_B T/6\pi\eta a \tag{1.35}$$

Here a is the particle radius and η is the viscosity of the system. The fundamental solution to this equation is

$$P(\bar{r}(t),\bar{r}(0)) = \exp[-(\bar{r}(t)-\bar{r}(0))^2/4Dt]/(4\pi Dt)^{3/2} \tag{1.36}$$

However, the Fourier transform of this function is measured in DLS. DLS = dynamic light scattering. The easiest way to determine the

Fourier transformed probability function is to take the Fourier transform of the diffusion equation (1.34).

$$\dot{P}(k,t) = -Dk^2 P(k,t) \tag{1.37}$$

The solution to this equation is easily found to be

$$P(k,t) = \exp(-Dk^2 t) \tag{1.38}$$

Thus with dynamic light scattering we can measure the diffusion coefficient and hence the particle size or viscosity of the fluid.

These are but two examples of the many uses of dynamic light scattering but they demonstrate the wide applicability and usefulness of the technique.

Thesis Overview

With this brief background we can proceed with the main purpose of the thesis. In Chapter II we present the theory connecting the memory function to the viscosity of the colloidal particle fluid. It is primarily a review of the work of Hess (1981a, 1981b). We also review some of the techniques and theorems that are used in the theory.

Chapter III is dedicated to the study of multiple scattering. It begins with a review of Sorensen, Mockler and O'Sullivan's (1976, 1978) work on noninteracting systems. This multiple scattering theory is then extended to all available polarizations and also to interacting systems. The extension to interacting systems shows the difficulties involved in separating the effects of interactions from the effects of multiple scattering. We also present a method to reduce multiple

scattering to a minimum.

The experimental lore is given in Chapter IV along with data analysis techniques and a brief description of the problems inherent in the study of colloidal suspensions.

The last chapter, Chapter V, gives the experimental results obtained. It contains a brief discussion of them as well as further work that should be done in this area.

CHAPTER II

THEORY OF INTERACTING PARTICLES

Introduction

With the advent of the laser, dynamic light scattering has become a very useful technique to study many body interactions, particularly in suspensions of charged colloidal particles. Different formalisms have been developed to connect the intermediate scattering function, the quantity measured by dynamic light scattering, with the "hydrodynamic" properties of the system under study. The purpose of this chapter is to present a review of one of the more useful formalisms used to accomplish this.

We begin with a brief review of Liouville space and linear response theory. This includes the general form of the fluctuation-dissipation theory as discussed by Kubo (1966). A classical example of a particle undergoing Brownian motion is used to demonstrate the fluctuation-dissipation theorem. Projection operator techniques are then used on the same example to find an exact solution and to elucidate the assumptions involved in both cases. These same techniques are then used on a distribution function that obeys the Smoluchowski equation (SE), the equation that is generally used for interacting Brownian particles. Next the microscopic expression for the longitudinal stress tensor in a liquid is used to make a connection between the memory function of the

previous discussion and the longitudinal intrinsic viscosity. Finally the results obtained by starting with the complete Fokker-Planck equation (FPE) from which the SE is derived in perturbation, are given as well as a discussion of the differences. A connection is also made between the parameters actually extracted in a typical experiment with the longitudinal intrinsic viscosity. These last two sections are meant to be a brief review of the work of Hess (1981a, 1981b) and one should go to these papers for a more complete discussion.

Linear Response and the Fluctuation-Dissipation Theory

Much of this section deals with the Liouville operator, hence, it is helpful to give a brief review of this operator and the Liouville space. The state of an N-particle system is specified by a vector $\bar{\Gamma}(\bar{q}_1,\bar{q}_2,\ldots\bar{q}_N,\bar{p}_1,\bar{p}_2,\ldots\bar{p}_N)$, where the $\bar{q}$'s are the generalized position vectors andthe $\bar{p}$'s are the corresponding conjugate momenta. The state of the system is represented as a point in the 2N-dimensional phase space. The state, $\bar{\Gamma}$, evolves in time according to the canonical equations of motion,

$$\dot{\bar{q}}_i = \frac{\delta H}{\delta \bar{p}_i} \; ; \; \dot{\bar{p}}_1 = -\frac{\delta H}{\delta \bar{q}_i} \tag{2.1}$$

The state Γ must obey the equation

$$\dot{\bar{\Gamma}} = \sum_{i=1}^{N} \left(\frac{\delta \bar{\Gamma}}{\delta \dot{\bar{q}}_1} \dot{q}_i + \frac{\alpha \bar{\Gamma}}{\delta \dot{\bar{p}}_i} \dot{\bar{p}}_i\right)$$

$$= \sum_{i=1}^{N} \left(\frac{\delta \bar{\Gamma}}{\delta \dot{\bar{q}}_i} \frac{\delta H}{\delta \bar{p}_i} - \frac{\delta \bar{\Gamma}}{\delta \bar{p}_i} \frac{\delta H}{\delta \bar{q}_i}\right)$$

or

$$\dot{\bar{\Gamma}} = \sum_{i=1}^{N} [\bar{\Gamma},H] \tag{2.2}$$

where $[\bar{\Gamma},H]$ is the Poisson bracket of $\bar{\Gamma}$ with the Hamiltonian, H. The Liouville operator, $\hat{L}$ is defined as

$$i\hat{L}\bar{\Gamma} = [\bar{\Gamma},H] \tag{2.3}$$

This operator is a linear partial differential operator, that is also Hermitian. Equation (2.2) can be written in terms of the Liouville operator as

$$\dot{\bar{\Gamma}} = i\hat{L}\Gamma \tag{2.4}$$

with the formal solution

$$\bar{\Gamma}(t) = \exp(i\hat{L}t)\bar{\Gamma}(0) \tag{2.5}$$

The propagator, $\exp(i\hat{L}t)$, is a time evolution operator that defines a mapping in phase space.

We now consider a mechanical property of the system, $\bar{A}(\bar{p}_i,\bar{q}_i)$. As the state of the system changes the mechanical property $\bar{A}$ also changes. The property $\bar{A}$ is an implicit function of time through its phase dependence. Therefore, we can write the equation of motion of $\bar{A}$ as

$$\dot{\bar{A}} = i\hat{L}\bar{A} \tag{2.6}$$

with the solution

$$\bar{A}(\bar{\Gamma},t) = \exp(i\hat{L}t)\bar{A}(\bar{\Gamma},0) \tag{2.7}$$

The time correlation function of property $\bar{A}$ is defined as the

ensemble average of the product of the property A at some initial time and at a later time

$$\langle\bar{A}(t+t')\bar{A}(t')\rangle = \int d\Gamma\, \ell_o\, \bar{A}(t+t')\, \bar{A}(t') = \int d\Gamma\, \ell_o\, A(\bar{\Gamma},t')\, \exp(i\hat{L}t)A(\bar{\Gamma},t') \tag{2.8}$$

where ℓ_o is the equilibrium distribution function. The correlation function may be identified as a scalar product and has the following properties:

1. $$\langle\bar{A}\,\bar{B}\rangle^* = \langle\bar{B}\,\bar{A}\rangle \tag{2.9}$$

2. if $\bar{A} = C_1\bar{A}_1 + C_2\bar{A}_2$ where C_1 and C_2 are constants, then

$$\langle\bar{B}\,\bar{A}\rangle = C_1\langle\bar{B}\,\bar{A}_1\rangle + C_2\langle\bar{B}\,\bar{A}_2\rangle \text{ , and} \tag{2.10}$$

$$\langle\bar{A}\,\bar{B}\rangle = C_1^*\langle\bar{A}_1\bar{B}\rangle + C_2^*\langle\bar{A}_2\bar{B}\rangle$$

3. $$\langle\bar{A}\,\bar{A}\rangle \geq 0 \tag{2.11}$$

The equality holds only in the case $\bar{A} = 0$. All functions of finite norm, $||\bar{A}|| = \langle AA\rangle^{\frac{1}{2}}$, that obey the above definitions define a Hilbert space. This space is denoted Liouville space because the Liouville operator generates motion in this space.

Some of the properties of time correlations include:

1. They are stationary, or

$$\frac{\delta}{\delta t'}\langle X(t+t')Y(t')\rangle = 0, \text{ or}$$

$$\langle X(t+t')Y(t')\rangle = \langle X(t)Y(0)\rangle \tag{2.12}$$

2. They are real if X and Y are real.

3. $$\langle X\,Y\rangle = \langle Y\,X\rangle, \text{ thus } \langle X(t)Y(0)\rangle = \langle Y(-t)X(0)\rangle \tag{2.13}$$

or in particular $\langle X(t)X(0)\rangle = \langle X(-t)X(0)\rangle$.

Consider a suspended mirror that is turned by an electromagnetic device. The motion is slowed by a frictional force due to impacts with the air molecules. Although the collisions are random, a number of the collisions produce a systematic effect proportional to the angular velocity of the mirror. The randomness of the collisions can be seen when the mirror simply hangs with no external force applied. The collisions cause a small and eratic random motion of the mirror.

These random impacts generally cause two different results. They act as a random driving force to maintain the incessant irregular motion of the mirror, and they also give rise to a systematic frictional force in forced motion. Kubo (1966) noted that these two parts must be related as they arise from the same source. This relationship between the systematic and random parts of microscopic forces is called the fluctuation-dissipation theorem.

To determine the general form of this theorem linear response theory will be used. Consider a system to which an external force, $K(t)$, is applied in the infinite past, $t = -\infty$, when the system was initially in equilibrium. The total Hamiltonian can be written

$$\begin{aligned} H_T &= H + H_{ext} \\ H_T &= H - \bar{A}K(t) \end{aligned} \tag{2.14}$$

where $\bar{A}$ is the dynamical quantity conjugate to the applied external force. The equation of motion for the distribution function, ρ, is

$$\dot{\rho} = i\hat{L}_T\rho = i\hat{L}\rho + i\hat{L}_{ext}\rho \tag{2.15}$$

where the L_i's are the Liouville operators associated with the corresponding Hamiltonians. The equilibrium distribution function, ρ_o, must satisfy the initial condition

$$\rho_o = C \exp(-\beta H) \tag{2.16}$$

where β is the Boltzmann factor, $1/k_B T$.

To the first order in the external force, the distribution becomes

$$\rho(t) = \rho_o + \Delta\rho(t) \tag{2.17}$$

where

$$\Delta\rho(t) = \int_{-\infty}^{t} dt' \exp[i(t-t')\hat{L}]\cdot i\hat{L}_{ext}(t')\rho_o \tag{2.18}$$

Consider now the reaction of a physical quantity of the system, $\bar{B}$, to the external force. Its response is

$$\Delta\bar{B}(t) = \int d\bar{\Gamma}\, B(\bar{q},\bar{p})\Delta\rho(t) \tag{2.19}$$

With the use of Eqs. (2.14) and (2.19) and partial integration, the response of B can be written

$$\Delta\bar{B}(t) = \int_{-\infty}^{t} dt' \int d\Gamma\, K(t')\rho_o[A(0)B(t-t')] \tag{2.20}$$

Here $\bar{B}(t) = \exp(i\hat{L}t)\bar{B}(0)$ and $[\bar{A}(0),\bar{B}(t)]$ is the Poisson bracket. The response function is defined as

$$\phi_{BA}(t) = \int d\bar{\Gamma}\, \rho_o[\bar{A}(0),\bar{B}(t)]$$

$$= <[\bar{A}(0),\bar{B}(t)]> \tag{2.21}$$

Therefore, the response of $\bar{B}$ can be written as

$$\Delta\bar{B}(t) = \int_{-\infty}^{t} dt' \; K(t') \; \phi_{BA}(t-t') \tag{2.22}$$

This shows that the response, $\Delta\bar{B}$, is linear in the external force and a superposition of the delayed effects. The response function ϕ_{BA} represents the response of the system at time t to an impulsive force, $K(t) \propto \delta(t)$, exerted at time $t = 0$. To demonstrate this let the external force $K(t) = \delta(t)$. The change in momentum of particle i is then

$$\Delta\bar{p}_i = \int_{o}^{t} dt' \; \frac{\delta H_{ext}(t')}{\delta\bar{q}_i} = \frac{\delta \bar{A}(0)}{\delta\dot{\bar{q}}_i} \tag{2.23}$$

similarly,

$$\Delta\bar{q}_i = -\frac{\delta A(0)}{\delta\bar{p}_i} \tag{2.24}$$

Thus, the resulting change in the quantity $\bar{B}$ can be written

$$\Delta\bar{B}(t) = \sum_{i=1}^{N} \left(\frac{\delta B(t)}{\delta\bar{p}_i} \Delta\bar{p}_i + \frac{\delta B(t)}{\delta\bar{q}_i} \Delta\bar{q}_i\right)$$

$$= [A(0), B(t)] \tag{2.25}$$

The response function ϕ_{BA} is just this change averaged over the initial distribution of the phase. The response function means the effect of an impulsive force conjugate to quantity $\bar{A}$ on another quantity $\bar{B}$ at a later time.

This is the main result of linear response theory. The response of a system to an external force can be related back to the equilibrium

properties of the system.

We now consider a periodic force, $K(t) = \mathrm{Re}(K_o e^{i\omega t})$. The response of quantity $\bar{B}$ can be written

$$\Delta\bar{B} = \mathrm{Re}[\chi_{BA}(\omega) K_o \exp(i\omega t)] \tag{2.26}$$

where the admittance

$$\chi_{BA}(\omega) = \frac{\delta\bar{B}(\omega)}{\delta\bar{A}(\omega)} \tag{2.27}$$

is the Fourier transform of the response function

$$\chi_{BA}(\omega) = \int_o^\infty dt\ \phi_{BA} \exp(-i\omega t) = \int_o^\infty dt\ \langle[A(O)B(t)]\rangle \exp(-i\omega t) \tag{2.28}$$

To obtain the true form of the fluctuation-dissipation theorem this admittance should be separated into dissipative and non-dissipative parts. However, the fluctuation-dissipation theorem may be used in a wider sense to include the non-dissipative parts of the admittance. In this form one makes use of the time correlation function and we may regard Eqs. (2.21) or (2.28) as the exact expression of the fluctuation-dissipation theorem. Although the formalism may cloud the significance of this theorem, it says that dissipative properties of a system can be related to fluctuations in the microscopic forces acting on the system.

It has been shown that linear response theory results in the fluctuation-dissipation theorem. Guided by the fluctuation-dissipation theorem we will show how the theorem manifests itself in a system of Brownian particles suspended in a fluid.

Consider the forces on a particle in a quiescent fluid. A particle

undergoing Brownian motion is randomly moving around in the fluid. This random motion is caused by impacts of the fluid molecules with the particle. These impacts are described by a random force, f(t). It is also known that a particle moving through a medium experiences a drag force that is proportional to the velocity of the particle. The proportionality constant, γ, is understood to be a drag or friction coefficient. With these forces we can now use Newton's second law to write down the equation of motion for the particle

$$m\dot{\bar{v}}(t) = -\gamma\bar{v}(t) + f(t) \; . \tag{2.29}$$

Here m is the mass of the particle.

The fluctuation-dissipation theorem says that the friction coefficient should be related to the fluctuations in the random force. This at first appears strange. The forces that cause the motion also slow it down. However, after more thought it is seen that the drag is caused by impacts with the fluid molecules just as the motion is caused by impacts with the fluid molecules. Since the two effects have the same source, they must be related. Led by this we want to see if

$$\gamma \propto \int_o^\infty dt \, \langle f(t) f(0) \rangle \tag{2.30}$$

To start, Equation (2.29) is solved for the random force. This is then substituted into Eq. (2.30) to obtain

$$\int_o^\infty dt \, \langle f(t) f(0) \rangle = m^2 \int_o^\infty dt \, \langle \dot{\bar{v}}(t) \dot{\bar{v}}(0) \rangle + \gamma^2 \int_o^\infty dt \, \langle \bar{v}(t) \bar{v}(0) \rangle$$

$$+ \gamma m \int_o^\infty dt \left[\langle \dot{\bar{v}}(t) \bar{v}(0) \rangle + \langle \dot{\bar{v}}(0) \bar{v}(t) \rangle \right] \tag{2.31}$$

Recall that correlation functions have the property of stationarity or

$$\frac{\delta}{\delta t'} \langle v(t+t')v(t') \rangle = 0$$

and

$$\langle \dot{v}(t+t')v(t') \rangle + \langle v(t+t')\dot{v}(t') \rangle = 0 \tag{2.32}$$

Note that in v(t+t'), t' shows up only in the form of t + t' so

$$\frac{d}{dt'} v(t+t') = \frac{d}{dt} v(t+t') \tag{2.33}$$

Hence in the limit as t' goes to zero 2.32 becomes

$$\langle \dot{v}(t)v(0) \rangle + \langle \dot{v}(0)v(t) \rangle = 0 \tag{2.34}$$

Thus the integrand of the third term in 2.31 is zero.

Next consider the correlation of the particle velocities. To determine this the solution of the equation of motion (2.29) is needed. The solution is

$$\bar{v}(t) = \bar{v}(0) \exp(-\gamma t/m) + 1/m \int_0^t dt' \, \bar{f}(t') \exp\left[-\frac{\gamma(t-t')}{m}\right] \tag{2.35}$$

Using this expression for the velocity, the velocity correlation function is written as

$$\langle \bar{v}(t)\bar{v}(0) \rangle = \langle \bar{v}(0)^2 \rangle \exp(-\gamma t/m) + 1/m \int_0^t dt' \exp\left[-\frac{\gamma(t-t')}{m}\right] \langle \bar{f}(t')\dot{v}(0) \rangle \tag{2.36}$$

Normally when thinking of Brownian motion one envisions a particle that is much larger than the surrounding molecules. Then the force

imparted by a single impact has a very short duration. This means that the random force on a particle and the particle's velocity should be uncorrelated or

$$\langle f(t)v(0)\rangle = 0 \tag{2.37}$$

Using this noncorrelation, the velocity correlation function reduces to the simple form

$$\langle v(t)v(0)\rangle = \langle v(0)^2\rangle \exp[-\gamma/m\ t] \tag{2.38}$$

Doing the integration over time, the second term in 2.31 becomes

$$\gamma^2 \int_0^\infty dt\ \langle v(t)v(0)\rangle = m\gamma\ \langle v(0)^2\rangle \tag{2.39}$$

This is what was expected. This term is proportional to the friction coefficient, γ.

The determination of the acceleration correlation function is left. To solve this, note that stationarity allows this term to be rewritten as

$$m^2 \int_0^\infty dt\ \langle \dot{v}(t)\dot{v}(0)\rangle = m^2 \int_0^\infty dt\ \langle \frac{d}{dt} v(t+t')\ \dot{v}(t')\rangle \tag{2.40}$$

Exchanging the order of integration yields

$$m^2 \langle \int_0^\infty d[v(t+t')]\ v(t')\rangle = m^2[\langle v(\infty)\dot{v}(t')\rangle - \langle v(0)\dot{v}(t')\rangle] \tag{2.41}$$

The term $\langle v(\infty)\dot{v}(t')\rangle$ must be zero because this function should have a finite correlation time and eventually decay to zero.

To find an expression for the second term we multiply 2.29 by $v(0)$

and ensemble average. Making use of the non-correlation of the force and velocity discussed earlier, we find

$$- m^2\langle v(0)\dot{v}(t')\rangle = m\gamma \langle v(0)^2\rangle = m^2 \int_0^\infty dt\langle \dot{v}(t)\dot{v}(0)\rangle \tag{2.42}$$

This term is also proportional to the friction coefficient. Using 2.31, 2.39 and 2.42, we can solve for the friction coefficient to find

$$\gamma = \frac{1}{2m\langle v(0)^2\rangle} \int_0^\infty dt\langle f(t)f(0)\rangle \tag{2.43}$$

The fluctuation-dissipation theorem holds true in this case. The friction coefficient, or the drag force, is indeed related to the random forces on the particles. More exactly, the friction coefficient is related to the fluctuations in the random forces that cause the Brownian motion. However, this is true only under the assumptions made in the derivation. These were:

1. The system is in equilibrium so that the stationarity condition holds.
2. The random force on the particle and the particle velocity are on two different time scales and they are uncorrelated.

The first assumption causes no problems, but the second assumption seems to limit the result to specific cases.

The problem can be solved using a more elegant formlaism to shed some light on these assumptions. To do this projection operator techniques are employed. The Liouville equation for the velocity of the Brownian particle is the appropriate starting place.

$$\dot{\bar{v}}(t) = i\hat{L}\,\bar{v}(t) \tag{2.44}$$

The solution to this equation is

$$\bar{v}(t) = \exp(i\hat{L}t)\ \bar{v}(0) \tag{2.45}$$

Using this result the Liouville equation is rewritten as

$$\dot{\bar{v}}(t) = \exp(i\hat{L}t)\ i\hat{L}\ \bar{v}(0) \tag{2.46}$$

Using operator identities and Laplace transforms, the time propagator $\exp(i\hat{L}t)$ is written as

$$\exp(i\hat{L}t) = \exp(i\hat{O}_1\hat{L}t) + \int_o^t dt'\ \exp(i\hat{L}t')\ i\hat{O}_2\hat{L}\ \exp[i\hat{O}_1(t-t')\hat{L}] \tag{2.47}$$

where $\hat{O}_1$ and $\hat{O}_2$ are any two operators that have the property $\hat{O}_1 + \hat{O}_2 = 1$. One of the operators is chosen to be the projection operator $\hat{P}$, which projects any arbitrary vector onto the initial velocity $\bar{v}(0)$. $\hat{P}$ is defined as

$$\hat{P}\bar{A} = \frac{\langle \bar{v}(0)\bar{A}\rangle}{\langle \bar{v}(0)^2\rangle}\ \bar{v}(0) \tag{2.48}$$

The other operator is $\hat{Q} = 1-\hat{P}$. $\hat{Q}$ is also a projection operator because it is Hermitian and has the property $\hat{Q}^2 = \hat{Q}$. Using the definitions of $\hat{P}$ and $\hat{Q}$ it is seen that

$$\langle \hat{Q}\bar{A}\cdot\bar{v}(0)\rangle = \langle (1-\hat{P})\bar{A}\ \bar{v}(0)\rangle = \langle \bar{A}\bar{v}(0)\rangle - \frac{\langle \bar{A}\ \bar{v}(0)\rangle}{\langle \bar{v}^2(0)\rangle}\langle v^2(0)\rangle \tag{2.49}$$

or $\langle \hat{Q}\bar{A}\cdot\bar{v}(0)\rangle = 0$. Therefore, $\hat{Q}$ projects onto a vector orthogonal to the initial velocity. The projection operators have the following properties:

$$\hat{Q}\bar{v}(0) = 0$$

$$\hat{P}\bar{v}(0) = \bar{v}(0)$$

$$(\hat{P} + \hat{Q})\bar{v}(0) = \bar{v}(0) \ .$$

Choosing $\hat{Q} = \hat{O}_1$ and $\hat{P} = \hat{O}_2$, the time propagator becomes

$$\exp(i\hat{L}t) = \exp(i\hat{Q}\hat{L}t) + \int_o^t dt' \exp(i\hat{L}t')(i\hat{P}\hat{L}) \exp[i\hat{Q}\hat{L}(t-t')] \qquad (2.50)$$

Recalling that $\hat{P} + \hat{Q} = 1$, 2.46 is rewritten as

$$\dot{\bar{v}}(t) = \exp(i\hat{L}t)\hat{P}i\hat{L}\ \bar{v}(0) + \exp(i\hat{L}t)\hat{Q}i\hat{L}\ \bar{v}(0) \qquad (2.51)$$

Using the definition of $\hat{P}$ the first term in this expression is written as

$$\exp(i\hat{L}t)\hat{P}i\hat{L}\ \bar{v}(0) = \frac{<i\hat{L}v(0)v(0)>}{<\bar{v}(0)>^2} \exp[i\hat{L}t\ \bar{v}(0)]$$

$$= \frac{<\dot{\bar{v}}(0)\bar{v}(0)>}{<v^2(0)>}\bar{v}(t) \qquad (2.52)$$

As in the previous example the discussion is limited to an equilibrium situation so that the stationarity condition (2.12) holds. This means $<\dot{\bar{v}}(0)\ \bar{v}(0)> = 0$ and the first term in 2.51 is zero.

Using the expansion for the time evolution operator (2.50), the particle acceleration is

$$\dot{\bar{v}}(t) = \exp(i\hat{Q}\hat{L}t)\hat{Q}i\hat{L}\ v(0) + \int_o^t dt' \exp(i\hat{L}t')i\hat{P}\hat{L} \exp[i\hat{Q}\hat{L}(t-t')]\ \hat{Q}i\hat{L}\ \bar{v}(0) \qquad (2.52)$$

Note that the velocity in this expression only appears in the form

$\hat{Q}i\hat{L}\bar{v}(0)$, so we define the quantity

$$\bar{G}(0) = \hat{Q}i\hat{L}\bar{v}(0) \tag{2.54}$$

Now $\bar{G}$ evolves in time according to

$$\bar{G}(t) = \hat{Q}i\hat{L}\bar{v}(t) = \exp(i\hat{L}t)\hat{G}(0) \; . \tag{2.55}$$

With this definition 2.53 simplifies to

$$\dot{\bar{v}}(t) = \exp(\hat{Q}i\hat{L}t)\bar{G}(0) + \int_o^t dt' \exp(i\hat{L}t)i\hat{P}\hat{L} \exp[i\hat{Q}\hat{L}(t+t')]\bar{G}(0) \tag{2.56}$$

It is seen that the propagators in this expression are not $\exp(i\hat{L}t)$ but rather $\exp(\hat{Q}i\hat{L}t)$ so another vector incorporating this propagator is defined

$$\bar{F}(t) = \exp(\hat{Q}i\hat{L}t)\bar{G}(0) \tag{2.57}$$

This vector should not be confused with the vector $\bar{G}(t)$ as in general $\bar{F}(t) \neq \bar{G}(t)$ except at t=0 where $\bar{F}(0) = \bar{G}(0)$. Examine this vector a little closer. Using the property $\hat{Q}^2 = \hat{Q}$ and the expansion of an exponential it is easy to show that $\exp(\hat{Q}i\hat{L}t)\hat{Q} = \hat{Q}\exp(\hat{Q}i\hat{L}t)\hat{Q}$. Applying this to the definition of $\bar{F}(t)$ we find

$$\bar{F}(t) = \exp(\hat{Q}i\hat{L}t)\hat{Q}i\hat{L}\bar{v}(0) = \hat{Q}\exp(\hat{Q}i\hat{L}t)\hat{Q}i\hat{L}\bar{v}(0)$$

or

$$\bar{F}(t) = \hat{Q}\bar{F}(t) \tag{2.58}$$

This means that $\bar{F}(t)$ is a vector orthogonal to the initial velocity so that $\langle\bar{F}(t)\ \bar{v}(0)\rangle = 0$.

Using these results 2.56 is rewritten as

$$\dot{\bar{v}}(t) = \bar{F}(t) + \int_o^t dt' \exp(i\hat{L}t')i\hat{P}\hat{L}\ \bar{F}(t-t') \tag{2.59}$$

By the position of $\bar{F}$ in this equation, it is suspected that $\bar{F}$ is a force. With a little insight it is recognized as the random force on the particles. Although F is defined strictly in the mathematical formalism and its definition doesn't look like a force, the fact that it stands alone in the equation of motion strongly suggests that it is indeed a force.

Now examine the term $i\hat{P}\hat{L}\bar{F}(t-t')$. Using 2.58 and the definition of $\hat{P}$ this term is written as

$$i\hat{P}\hat{L}\,\bar{F}(t) = i\hat{P}\hat{L}\hat{Q}\,\bar{F}(t) = \frac{\langle i\hat{L}\hat{Q}\bar{F}\,\bar{v}(0)\rangle}{\langle \bar{v}^2(0)\rangle}\,\bar{v}(0) \tag{2.60}$$

Since $\hat{L}$ and $\hat{Q}$ are both Hermitean operators, the ensemble average becomes

$$\langle i\hat{L}\hat{Q}\bar{F}\,\bar{v}(0)\rangle = -\langle \bar{F}(t)\hat{Q}i\hat{L}\,\bar{v}(0)\rangle = -\langle \bar{F}(t)\bar{F}(0)\rangle \tag{2.61}$$

Equation 2.60 becomes

$$i\hat{P}\hat{L}\,\bar{F}(t) = \frac{1}{m}\gamma(t-t')\bar{v}(0) \tag{2.62}$$

where the function $\gamma(t-t')$ is defined as

$$\gamma(t-t') = m\,\frac{\langle \bar{F}(t-t')\bar{F}(0)\rangle}{\langle \bar{v}^2(0)\rangle} \tag{2.63}$$

The equation of motion (2.59) becomes

$$m\dot{\bar{v}}(t) = -\int_0^t dt'\,\gamma(t-t')\bar{v}(t') + \bar{F}'(t) \tag{2.64}$$

where $\bar{F}'(t) = m\bar{F}(t)$ and m is the particle mass. This is recognized as the generalized Langevin equation and is very similar to the equation we found intuitively (2.29). The only assumption we used in arriving at this equation is that the system is in equilibrium so that the stationar-

ity condition holds. We found mathematically that the random force and the particle velocity are uncorrelated regardless of particle size. This was assumed in the intuitive case based on the particle being much larger than the fluid molecules. This neglect of particle size results in a time dependent frictional coefficient and a superposition of all previous effects. The system seems to have a "memory" of past impacts that contribute to the drag force. Thus an equation of this form is sometimes referred to as a memory function equation.

We can arrive at the results obtained earlier by imposing the condition that the particle is large compared to the surrounding fluid particles. Under this condition the correlation time of the random forces should be very small or

$$<\bar{F}(t)\bar{F}(0)> \propto \delta(t) \tag{2.65}$$

Using this the friction coefficient can be written as

$$\gamma(t) = \gamma_o \delta(t) \tag{2.66}$$

Equation 2.64 is integrated to obtain

$$m\dot{\bar{v}}(t) = \gamma_o \bar{v}(t) + \bar{F}(t) \ . \tag{2.67}$$

This is the equation we found using Newton's second law. Equation 2.67 holds only when the condition of large particles in a suspension of small fluid particles also holds.

Now that linear response theory and the fluctuation-dissipation theorem have been demonstrated, we move on to aspects more relevant to the study of interacting colloidal suspensions. Consider a quantity measured in dynamic light scattering, the intermediate scattering func-

tion. For an N-particle system, this function has the form

$$S(\bar{k},t) = \langle a(\bar{k},t)\, a(-\bar{k},0)\rangle \tag{2.68}$$

The static structure factor is defined as the t = 0 limit of the intermediate scattering function,

$$S(\bar{k}) = \langle a(\bar{k},0)\, a(-\bar{k},0)\rangle \tag{2.69}$$

Here $a(\bar{k},t)$ is the spatial Fourier transform of the particle number density at time t

$$a(\bar{k},t) = 1/\sqrt{N} \sum_{i=1}^{N} \exp(i\bar{k}\cdot\bar{r}_i) \tag{2.70}$$

The Liouville operator scheme discussed earlier works well for Brownian particles in the limit of short times, times of the order of velocity fluctuations. However, DLS probes the intermediate scattering function at longer times; times of the order of the decay time for concentration fluctuations. Thus it seems reasonable that one should use the same projection operator techniques with an equation of motion applicable to intermediate times. The Smoluchowski equation, (SE), is just such an equation and is generally used in the study of interacting Brownian particles. The N particle SE has the form

$$\dot{P}_N(\bar{R},\bar{R}_o,t) = \sum_{i=1}^{N} \left[D\bar{\nabla}_i^2 P_N - \beta D\bar{\nabla}_i\cdot\bar{F}_i(\bar{R}) P_N\right] \tag{2.71}$$

where $P_N(\bar{R},\bar{R}_o,t)$ is the probability of finding N particles at the positions $\bar{R} = (\bar{r}_1,\bar{r}_2,\ldots\bar{r}_N)$ at time t given their initial positions, $\bar{R}_o$. D is the diffusion constant for the particles at infinite dilution, β is the Boltzmann factor, and $\bar{F}_i(\bar{R})$ is the force on particle i due to the other Brownian particles as well as any other forces on the particle.

This equation is sometimes written as

$$\dot{P}_N = \hat{O} P_N \tag{2.72}$$

with the Smoluchowski time advancing operator defined as

$$\hat{O} = \sum_{i=1}^{N} [D\bar{\nabla}_i^2 - \beta D\bar{\nabla}_i \cdot \bar{F}(\bar{R})] \tag{2.73}$$

The operator $\hat{O}$ is not Hermitean, in contrast to the Liouville operator. Therefore, the time evolution operator is not the same operator $\hat{O}$. However, the time evolution operator has been found (Ackerson, 1978; Deitrich and Peschal, 1979) and has the form

$$\hat{\hat{O}} = \sum_{i=1}^{N} [D\bar{\nabla}_i^2 + \beta D\bar{F}_i(\bar{R}) \cdot \bar{\nabla}_i] \tag{2.74}$$

The potential $U(\bar{R})$ is defined to contain any particle interactions and other external forces on the ith particle

$$\bar{F}_i(\bar{R}) = - \bar{\nabla}_i U(\bar{R}) \tag{2.75}$$

The equilibrium correlation function between two dynamical variables is written as

$$\langle \bar{A}(0)\bar{B}(t) \rangle = 1/Z \int d\bar{R} \exp[-\beta U(\bar{R}_o)]\bar{B}(\bar{R},0) \exp(\hat{\hat{O}}t)\bar{A}(\bar{R},0) \tag{2.76}$$

where Z, the partition function, normalizes the initial distribution $\exp[-\beta U(R_o)]$.

As the particle number density is the only conserved quantity and fluctuates on the time scale of interest, we choose as the projection operator, the operator $\hat{P}$ which projects onto $a(\bar{k},0) = a(k)$ defined by

$$\hat{P}\bar{A} = \frac{\langle a(-k)\bar{A}\rangle}{S(\bar{k})}\, a(\bar{k}) \tag{2.77}$$

The equation of motion for the intermediate scattering function is written as

$$\dot{S}(\bar{k},t) = \frac{\delta}{\delta t}\left[\langle a(-\bar{k})\exp(\hat{\hat{O}}t)a(\bar{k})\rangle\right] \tag{2.78}$$

Using the same projection operator techniques described earlier a memory function equation similar to 2.64 is obtained.

$$\dot{S}(\bar{k},t) = -\mu_1 S(\bar{k},t) + 1/S(\bar{k}) \int_o^t dt' M(t-t')S(\bar{k},t) \tag{2.79}$$

Here μ_i is the first cumulant defined as

$$\mu_1 = Dk^2/S(\bar{k}) \tag{2.80}$$

The memory function is identified as

$$M(\bar{k},t) = \langle f(-\bar{k},O)\exp(\hat{\hat{Q}}\hat{\hat{O}}t)f(\bar{k},O)\rangle \tag{2.81}$$

where

$$f(\bar{k},O) = \hat{\hat{Q}}\hat{\hat{O}}a(\bar{k}) \tag{2.82}$$

and the generalized random force is related to the force in the SE by

$$f(\bar{k},O) = iD\beta \sum_{i=1}^{N} \bar{k}\cdot\bar{F}_i \exp(i\bar{k}\cdot r_i) - Dk^2(1 - 1/S(\bar{k})) \sum_{i=1}^{N} \exp(-i\bar{k}\cdot\bar{r}_i) \tag{2.83}$$

This is another manifestation of the fluctuation-dissipation theorem. We see that the memory function is related to the correlation of the

generalized random forces. After the previous example we also suspect that the memory function should be related to a dissipative property of the colloidal suspension, so the microscopic properties of a simple liquid will be investigated next.

Microscopic Expressions for a Simple Liquid

We would like to connect the memory function above to the properties of a suspension of interacting Brownian particles. We start by looking at some of the properties of a simple liquid. The longitudinal component of the stress tensor is defined as

$$\sigma_{ll}(\bar{k}) = \bar{k}\cdot\bar{\bar{\sigma}}\cdot\bar{k}/k^2 \tag{2.84}$$

From hydrodynamic arguments (Schofield, 1968; Eselstaff, 1967), it can be shown that the microscopic description of the stress tensor is given by

$$\sigma_{ll}(\bar{k}) = 1/k^2 \sum_{i=1}^{N} [(\bar{k}\cdot\bar{p}_i)^2/m + i\bar{k}\cdot\bar{F}_i]\exp(-i\bar{k}\cdot\bar{r}_i) \tag{2.85}$$

with m being the particle mass and $\bar{p}_i$ the momentum of particle i. In an overdamped system of Brownian particles, the momentum is assumed to vary rapidly on the time scale of the fluctuations of the particles positions. Hence, 2.85 can be averaged over the momenta, as only their mean values will contribute on this time scale. Doing this enables the stress tensor to be written as

$$\sigma_{ll}(\bar{k}) = \beta^{-1} \sum_{i=1}^{N} \exp(-i\bar{k}\cdot\bar{r}_i) + 1/k^2 \sum_{i=1}^{N} (i\bar{k}\cdot\bar{F}_i \exp(-i\bar{k}\cdot\bar{r}_i)] \tag{2.86}$$

Schofield shows that the stress in a liquid may be decomposed into

the local osmotic pressure and a fluctuating nonequilibrium component. The local osmotic pressure follows the concentration fluctuations instantaneously and is given by

$$\pi(\bar{k}) = \frac{\delta\pi(\bar{k})}{\delta a(\bar{k})}\Big|_T \sum_{j=1}^{N} \exp(-i\bar{k}\cdot\bar{r}_j) = [\beta S(\bar{k})]^{-1} \sum_{j=1}^{N} \exp(-i\bar{k}\cdot\bar{r}_j) \quad (2.87)$$

The fluctuating part is now written as

$$\sigma_{11}^{f}(\bar{k}) = \sigma_{11}(k) - \pi(k) = 1/k^2 \sum_{j=1}^{N} i\bar{k}\cdot\bar{F}_j \exp(ik\cdot r_j) - [1/S(k) - 1]\beta^{-1} \sum_{j=1}^{N}$$

$$x \exp(i\bar{k}\cdot\bar{r}_j) \quad (2.88)$$

Comparing this with the generalized random force in the Smoluchowski representation (2.83), it is noted that

$$f(\bar{k}) = -D\beta k^2 \sigma_{11}^{f}(\bar{k}) \; . \quad (2.89)$$

The memory function can now be written as

$$M(t) = (Dk^2\beta)^2 \langle \sigma_{11}^{f}(-\bar{k}) \exp(\hat{Q}\hat{\tilde{O}}t) \sigma_{11}^{f}(\bar{k}) \rangle \quad (2.90)$$

This is very similar to the response function discussed earlier. Recall Equation 2.21

$$\phi_{BA}(t) = \langle \bar{A}(0) \exp(i\hat{L}t) B(0) \rangle$$

Instead of having the full time evolution operator, $\hat{\tilde{O}}$, the reduced operator, $\hat{Q}\,\hat{\tilde{O}}$, determines the dynamics of the memory function.

We would like to find the origin of this response. P. C. Martin (1965) has shown that outside the hydrodynamic limit the k-ω dependent

transport coefficients are related to the response of the system to the local screened field rather than the externally applied field. Hess (1981) uses operator properties and linear response theory, to find the memory function in terms of a response to the externally applied velocity field. One is directed to his paper for the mathematical details. He finds the memory function can be written as

$$M(\bar{k},\omega) = (Dk^2)^2 \beta \chi_{\sigma^f_{11},\nabla\cdot\bar{v}_e} \Big/ \left[1+\frac{Dk^2}{S(k)}\right]\chi_{a,\bar{\nabla}\cdot\bar{v}_e} \qquad (2.91)$$

where $\chi_{A,\bar{\nabla}\cdot\bar{v}_e}$ is understood to be the response of $\bar{A}$ to the longitudinal gradient of the external velocity field. This has the form of a screened response, where the response of the stress fluctuations is screened by the concentration fluctuations. Thus the local velocity field is different from the external velocity field. In a system that obeys the SE, the velocity is not an independent variable so the local velocity field can be considered as a functional of the external field and the concentration fluctuations. The local state is determined by the slow variable or the concentration fluctuations. To linear order, the change in the gradient of the local velocity field can be written

$$\delta\bar{\nabla}\cdot\bar{v}_\ell(k,t) = \frac{\delta\bar{\nabla}\cdot\bar{v}_\ell}{\delta\bar{\nabla}\cdot\bar{v}_e}\bigg|_a \delta\bar{v}\cdot\bar{v}_e(\bar{k},t) + \frac{\delta\nabla\cdot\bar{v}_\ell}{\delta\, a}\bigg|_{\nabla\cdot\bar{v}_e} \delta a(\bar{k},t) \qquad (2.92)$$

Without concentration fluctuations the local velocity field should equal the external field so that

$$\frac{\delta\nabla\cdot v_\ell(\bar{k},t)}{\delta\nabla\cdot v_e(\bar{k},t')} = \delta(t-t') \qquad (2.93)$$

Therefore, the admittance becomes

$$\chi_{\bar{\nabla}\cdot\bar{v}_\ell(k,t),\nabla\cdot\bar{v}_e(k_1t')} = \delta(t-t') + \frac{\delta\nabla\cdot y_\ell(k,t)}{\delta a(k,t)} \cdot \frac{\delta a(k,t)}{\delta\nabla\cdot v_e(k,t')} \qquad (2.94)$$

The local velocity is defined by the continuity equation

$$\dot{a}(\bar{k},t) = - c\bar{\nabla}\cdot\bar{v}_\ell(k,t)$$

where $c = \langle a(\bar{k},t)\rangle$. Using these expressions and the Smoluchowski' time evolution operator, $\hat{\bar{O}} + \delta\hat{\bar{O}}$, where $\delta\hat{\bar{O}}$ is the additional term due to the externally applied velocity field, the gradient of the local velocity field is written as

$$\nabla\cdot\bar{v}_\ell(k,t) = - 1/c(\hat{\bar{O}} + \delta\hat{\bar{O}})\, a(\bar{k},t) \qquad (2.95)$$

Applying the projection operators $\hat{P} + \hat{Q} = 1$, this is rewritten as

$$\bar{\nabla}\cdot\bar{v}_\ell(k,t) = - 1/c[\hat{P}(\hat{\bar{O}} + \delta\hat{\bar{O}})\, a(\bar{k},t) + \hat{Q}(\hat{\bar{O}} + \delta\hat{\bar{O}})\, a(\bar{k},t)] \qquad (2.96)$$

Since $\hat{Q}$ projects onto a vector orthogonal to the concentration fluctuations, the last term will not contribute when differentiated with respect to the concentration fluctuations and may be ignored. Using the definition of $\hat{P}$ we obtain

$$\frac{\delta\nabla\cdot\bar{v}_\ell(k,t)}{\delta a(\bar{k},t)} = - 1/c\ \delta(\bar{k})\ \langle a(-\bar{k})(\hat{\bar{O}} + \delta\hat{\bar{O}})\, a(\bar{k})\rangle \qquad (2.97)$$

The external field is now turned off so that $\bar{\nabla}\cdot v_e = 0$ and $\delta\hat{\bar{O}} = 0$. Equation 2.97 becomes

$$\frac{\delta\bar{\nabla}\cdot\bar{v}_{\ell}(\bar{k},t)}{\delta a(\bar{k},t)} = -1/c\, S(k)\, [<a(-\bar{k})\hat{\bar{O}}\, a(\bar{k})>] = \frac{Dk^2}{cS(k)} \tag{2.98}$$

Thus the response of the longitudinal gradient of the local field to the longitudinal gradient of the external field is

$$\chi_{\nabla\cdot\bar{v}_{\ell},\bar{\nabla}\cdot\bar{v}_{e}} = [1 + Dk^2/cS(k)]\chi_{a,\bar{\nabla}\cdot\bar{v}_{e}} \tag{2.99}$$

Substituting this expression into 2.91 the memory function becomes

$$M(\bar{k},\omega) = \frac{(Dk^2)^2\beta}{c}\, \chi\sigma^{f}_{11},\, \nabla\cdot v_{\ell}(\bar{k},\omega) \tag{2.100}$$

We see that the memory function is dependent on the response to the local velocity field and not the external field. Therefore, a $\bar{k}$-ω dependent longitudinal viscosity is defined as the response of the fluctuating component of the longitudinal stress to the change in the local velocity gradient

$$\eta_{11}(k,\omega) = \chi_{\nabla^{f}_{11},\nabla\cdot\bar{v}_{\ell}} \tag{2.101}$$

The friction coefficient for a suspension of colloidal particles is $\xi = (D\beta)^{-1}$, so a normalized dimensionless memory function is defined

$$\tilde{M}(\bar{k},\omega) = M(\bar{k},\omega)/Dk^2 = \eta_{11}(k,\omega)\, k^2/c\xi \tag{2.102}$$

Hence the normalized memory function is proportional to the ratio of the longitudinal viscosity of the Brownian particles to a "friction density".

Using 2.101 and the definition of the admittance given earlier we

can write the longitudinal viscosity as

$$\eta_{11} = \lim_{k,\omega \to o} \eta_{11}(k,\omega) = \beta \int_o^\infty dt \, \langle \sigma^f_{11}(\bar{k},t)\sigma_{11}(-k,O)\rangle \qquad (2.103)$$

This is the familiar fluctuation dissipation theorem. The viscosity is related to fluctuations in the local stress on the system.

Thus the Fourier transformed memory function equation (2.79) can be written

$$S(k,\omega) = \frac{S(k)}{i\omega + \frac{Dk^2}{S(k)}\left[1-\eta_{11}(k,\omega)k^2/c\xi\right]} \qquad (2.104)$$

The SE is derived from the Fokkar Planck equation (FPE) using the inverse friction coefficient as a small parameter. This expansion has been questioned recently (Hess, 1981b) for systems with strong interactions. Although this derivation is only assymptotically valid, it has been widely accepted for experimentally used frequencies and systems in which $\omega m/\xi << 1$. Thus expansions in $1/\xi$ seem reliable. Wilemski (1976) and Titulaer (1978) have shown that the corrections to the SE are of the order of $\{M/\xi^2 \, d\bar{F}(r_1)/d\bar{r}_1\}$. For an harmonic system with spring constant α, this becomes $m\alpha/\xi^2$. Thus corrections for strongly interacting systems may be important.

Led by this Hess (1981b) has used projection operator techniques similar to those used in the SE approach on the FPE. He arrives at an expression for the Fourier transform of the intermediate scattering function which is

$$S(k,\omega) = \frac{S(k)}{i\omega + \frac{Dk^2}{S(k)}\left[1 + \eta_{11}(k,\omega)k^2/c\xi\right]^{-1}} \qquad (2.105)$$

To arrive at this result, the assumption that the system is strongly overdamped is used. For the frequency range of interest ($\omega < 10^6 s^{-1}$) this is a valid assumption.

It is noted that to arrive at the SE result not only must the system be overdamped, but $\eta_{ll} k^2/c\xi << 1$. This condition may not hold for strongly interacting systems as the longitudinal viscosity is an intrinsic property of the system under study. The experimental data of Gruner and Lehmann (1979) show that at $k = k_m$, where k_m is the wave vector where $S(k)$ has its first maximum, $\eta_{ll} k_m^2/c\xi = 1$. Thus this condition does not hold and the SE should not be used.

The projection operator techniques used to obtain the results are rather complicated and may tend to cloud them. The results can be formulated in a rather simple way using the continuity equation

$$\dot{a}(\bar{k},t) = ci\bar{k}\cdot\bar{v}_\ell(\bar{k},t) \tag{2.106}$$

and the linear Navier-Stokes equation with an additional external friction force density

$$mc\,\dot{\bar{v}}_\ell(\bar{k},t) = i\bar{k}\cdot\overleftrightarrow{\sigma}_{ll}(\bar{k},t) - c\xi\, v_\ell(\bar{k},t) \tag{2.107}$$

This friction force density is due to the interactions with the fluid particles. In a system of Brownian particles, the friction term is much greater than the acceleration term so that 2.107 may be written as

$$\bar{v}_\ell(\bar{k},t) = i\bar{k}\cdot\overleftrightarrow{\sigma}_{ll}(\bar{k},t) \tag{2.108}$$

The longitudinal component of the stress tensor is again separated into a

pressure and fluctuating terms. The local velocity becomes

$$\bar{v}_{\ell}(\bar{k},t) = D/cS(k)\ i\bar{k}\ \bar{a}(\bar{k},t) + i\bar{k}\cdot\overleftrightarrow{\sigma}^{f}_{11}(\bar{k},t) \tag{2.109}$$

The fluctuating stress tensor is written in general form. In terms of the viscosity and the strain rate tensor it is

$$\overleftrightarrow{\sigma}^{f}_{\alpha\beta}(\bar{k},t) = \int_{o}^{t} dt'\ \eta_{\alpha\beta\gamma\delta}(\bar{k},t-t')\varepsilon^{\ell}_{\gamma\delta}(\bar{k},t) \tag{2.110}$$

Here $\varepsilon^{\ell}(\bar{k},t)$ is the spatial Fourier transform of the local strain rate tensor

$$\varepsilon^{\ell}_{\gamma\delta}(\bar{r},t) = \delta/\delta\bar{r}_{\gamma}\ \bar{v}^{\ell}_{\delta}(\bar{r},t) \tag{2.111}$$

It is possible to use linear response theory to find expressions for the components of the viscosity tensor, but we are only interested in finding the longitudinal component in terms of the concentrations fluctuations. Solving 2.106, 2.108-2.111 and 2.78 for the concentration fluctuations, the Fourier transformed concentration autocorrelation function is

$$S(\bar{k},\omega) = \frac{S(k)}{i\omega + \frac{Dk^2}{S(k)}\left[1 + \eta_{11}(k,\omega)k^2/\xi c\right]^{-1}} \tag{2.112}$$

This expression is exactly the same as that found using the FPE and projection operator techniques, so that everything seems consistent.

Connection With Experimentally Determined Parameters

The reason for experimentation in this area is now evident: to use

a non-perturbative method to measure the viscosity in a "fluid". Gruner and Lehmann (1979) have studied several systems of interacting colloidal particles. They analyzed the nonexponentiality of the intermediate scattering function in terms of the inverse first cumulant, μ_1, and a mean relaxation frequency, ν_1. Using these they can calculate a "reduced memory function" given by

$$M' = \frac{\mu_1 - \nu_1}{\mu_1} \tag{2.113}$$

where

$$\mu_1 = - \partial/\partial t \ln[S(\bar{k},t)]\Big|_{t=0} \tag{2.114}$$

and

$$\nu_1(k) = 1/\int_0^\infty dt' \, S(\bar{k},t') \tag{2.115}$$

Using these definitions and the expressions for the correlation functions (2.104, 2.105), the reduced memory function becomes

$$M'(k) = \begin{cases} \eta_{11}(\bar{k},0)k^2/c\xi & \text{SE} \\ \dfrac{\eta_{11}(k,0)k^2/c\xi}{1 + \eta_{11}(k,0)k^2/c\xi} & \text{FPE} \end{cases} \tag{2.116}$$

Thus by measuring the correlation function for a strongly interacting colloidal system of particles, the reduced memory function can be extracted and the longitudinal intrinsic viscosity determined.

CHAPTER III

MULTIPLE SCATTERING

Introduction

Many problems arise in the analysis of dynamic light scattering (DLS) data. Among those most often encountered in the study of colloidal suspensions are polydispersity and multiple scattering. Multiple scattering is a major problem when investigating interacting systems. This is due to the large particle size and a high concentration of particles needed to cause the suspensions to interact. Since we are trying to measure the nonexponentiality of the intensity autocorrelation function that is produced by the interactions we need to be able to resolve the effects caused by multiple scattering from those caused by the interactions. The multiple scattering problem is therefore of great concern.

A number of papers concerning multiple scattering from suspensions of particles undergoing Brownian motion have recently been published (Sorensen, Mockler and O'Sullivan, 1976, 1978; Boe and Lohne, 1978; Siano, Berne and Flynn, 1978; Colby, Narducci, Bluemel, and Beer, 1975). These papers have mainly been concerned with non-interacting point particles. Sorensen et al. (1976) have developed a procedure for determining the double scattered field exactly. They have also proposed (Sorensen et al. 1978) an approximation to determine the effects of the full multiple scattered field on the average scattered intensity and the first cumulant. These

procedures pertain only to non-interacting systems. Our interest, however, lies in the effects interactions have on the multiple scattered field and on the measured intensities and first cumulants.

In this chapter we will review the procedures of Sorensen and present some experimental data that agrees rather well with their predictions. We also extend their procedure for the double scattered field to include the effects of interactions. Experimental data is presented to detail the problems in analyzing data obtained on interacting colloidal suspensions. We also investigate the thin film cell as a method of reducing the effects of multiple scattering to a negligible level.

Non-interacting Particles

We first envision an experiment where light is scattered from independent uncorrelated particles. The incident light is scattered by a particle in the system to a second particle. The light scattered by the second particle is then directed into the detector. Since the two particles are uncorrelated, the double scattered correlation function is expected to be equal to the product of two single scattered correlation functions. Although the far field approximation has not yet been mentioned, one might expect this result would only hold if the conditions for the far field approximation are also met.

The total scattered field for a system of particles can be written

$$\bar{E}(\bar{r}_1,t) = \bar{E}_o(\bar{r}_1,t) + \sum_{n=1}^{\infty} \bar{E}_n(\bar{r}_1,t) \qquad (3.1)$$

where $\bar{E}_n$ denotes an electric field that has been scattered n times with a wave vector $\bar{k}(n)$.

For the processes with which we are concerned, the full electric field autocorrelation function must be evaluated. This function is defined as

$$\langle \bar{E}^*(\bar{r}_1,t)\cdot\bar{E}(\bar{r}_1,0)\rangle = \sum_{n=1}^{\infty}\langle \bar{E}_n^*(\bar{r}_1,t)\bar{E}_n(\bar{r}_1,0)\rangle + \sum_{i\neq j}^{\infty}\langle \bar{E}_i^*(\bar{r}_1,t)\bar{E}_j(\bar{r}_1,0)\rangle \quad (3.2)$$

The lowest ordered term in the series is the single scattered correlation function $\langle \bar{E}_1^*(\bar{r}_1,t)\bar{E}_1(\bar{r}_1,0)\rangle$. This is a totally "polarized" term as its polarization will be in the same direction as the polarization of the incident beam.

The next higher order term is the correlation of the single scattered field with the double scattered field, $\langle E_1^*(\bar{r}_1,t)E_2(\bar{r}_1,0)\rangle$. This term is also totally polarized as will be any term of the form $\langle \bar{E}_1^*(\bar{r}_1,t)\bar{E}_j(\bar{r}_1,0)\rangle$, because of the inner product with the single scattered field.

If the condition of independent uncorrelated particles is used, the individual scattering events are uncorrelated and all terms of the form $\langle \bar{E}_i^*\bar{E}_j\rangle$ for $j\neq i$ are zero. This is a result of the fact that there are j-i extra uncorrelated events in $\bar{E}_j$ than there are in $\bar{E}_i$. Hence $\bar{E}_i$ and $\bar{E}_j$ are uncorrelated. With these arguments the double scattered correlation function can be considered the lowest order contribution to the multiple scattered field.

Single Scattered Electric Field

The derivation is started by evaluating the single scattered term. This term has been well studied, but the assumptions needed and the formalism used will help illuminate the procedures and assumptions used to evaluate the higher order terms. Consider the geometry shown in Figure 2. The single scattered electric field can be written

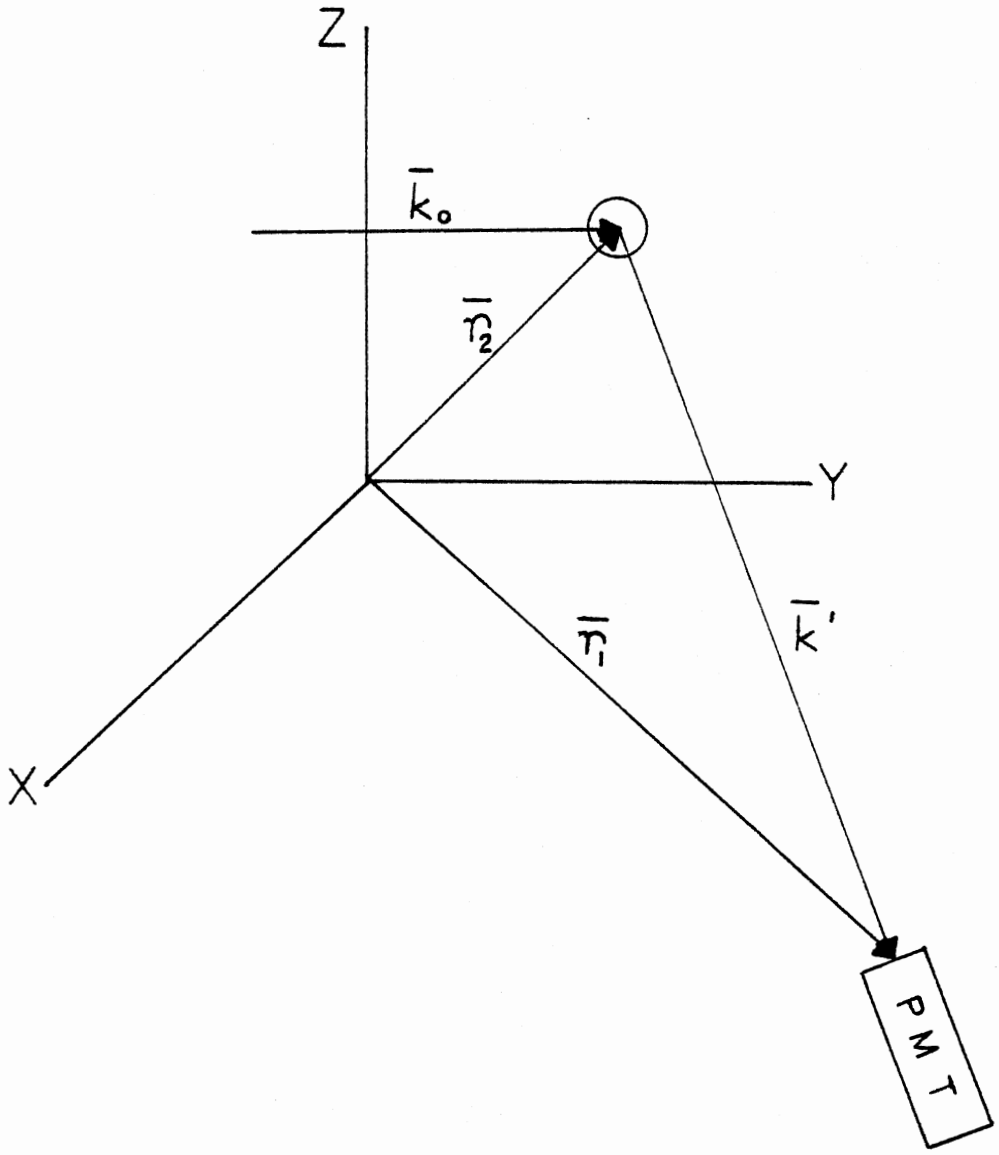

Figure 2. Single Scattering Geometry

$$\bar{E}_1(\bar{r}_1,t) = k'^2 \int d\bar{r}_2 \overleftrightarrow{T}(\bar{r}_{12}) \cdot \overleftrightarrow{\alpha}(\bar{r}_2,t)\cdot\bar{E}_o(\bar{r}_2,t) \tag{3.3}$$

With $\overleftrightarrow{T}(\bar{r}_{12})$ as the electric dipole field propagator and $\overleftrightarrow{\alpha}(r_2,t)$ as the polarizability tensor. The incident electric field $\bar{E}_o$ is written as a wave of frequency ω and wave vector $\bar{k}_o$, with polarization $\hat{\varepsilon}$ and amplitude E_o.

$$\bar{E}_o(\bar{r}_2,t) = \hat{\varepsilon}\, E_o \exp(i\bar{k}_o\cdot\bar{r}_2 - i\omega t) \tag{3.4}$$

If the polarizability of the medium is isotropic, the induced moment is parallel to the incident field. Thus the polarizability can be written as the diad

$$\overleftrightarrow{\alpha}(\bar{r},t) = a(\bar{r},t)\hat{\varepsilon}\hat{\varepsilon} \tag{3.5}$$

We now examine the far field approximation. In most scattering experiments the detector is far removed from the scattering volume, so that $\bar{r}_1 >> \bar{r}_2$. Hence

$$|\bar{r}_{12}| = |\bar{r}_1 - \bar{r}_2| = \bar{r}_1 - \bar{r}_2\cdot\hat{r}_1 \tag{3.6}$$

To first order this gives

$$|\bar{r}_{12}| = r_1$$

so that

$$|\bar{r}_{12}|\, k_o = r_1 k_o >> 1 \tag{3.7}$$

and

$$\bar{k}' = k'\hat{r}_1$$

With this approximation, the electric dipole field propagator takes on the form

$$\overleftrightarrow{T}(\bar{r}_{12}) = \frac{\exp(ik'r_1)}{r_1} \exp(-i\bar{k}_o \cdot \bar{r}_2)(\overleftrightarrow{I} - \hat{r}_1\hat{r}_1) \tag{3.8}$$

where $\overleftrightarrow{I}$ is the unit tensor. The single scattered electric field can now be simplified to

$$\bar{E}_1(\bar{r},t) = E_o(k'^2) \exp(-i\omega t) [\hat{r}_1 x(\hat{\varepsilon} x \hat{r}_1)] \int d\bar{r}_2 \, a(\bar{r}_2,t) \exp[i(\bar{k}_o - \bar{k}') \cdot \bar{r}_2] \tag{3.9}$$

This is the usual result for the single scattered field, with the proper polarization requirements and the $1/r$ and $1/\lambda^2$ dependencies.

If the derivation is limited to a system of small scattering particles with a radius much less than λ, then the particles will scatter isotropically in the plane perpendicular to the incident polarization. With this restriction the amplitude of the polarizability becomes

$$a(r,t) = \sigma \sum_{i=1}^{N} \delta[r - r_i(t)] \tag{3.10}$$

where σ is the electric field scattering cross section for one particle. The electric field autocorrelation function in the scattering plane, the plane perpendicular to the incident polarization, can now be written as

$$\langle \bar{E}_1^*(\bar{r}_1,t) \bar{E}_1(\bar{r}_1,0) \rangle = \frac{E_o^2 k'^4 \sigma^2}{r_1^2} \left\langle \sum_{i=1}^{N} \exp[-i(\bar{k}_o - \bar{k}') \cdot \bar{r}_i(t)] \sum_{j=1}^{N} \right.$$

$$\left. x \exp[i(\bar{k}_o - \bar{k}') \cdot \bar{r}_j(0)] \right\rangle \tag{3.11}$$

Now the condition of no interparticle correlations is imposed so that the ensemble average is zero unless i=j. For identical particles all i=j terms are equal, so the correlation function simplifies to

$$\langle \bar{E}_1^*(\bar{r}_1,t)\bar{E}_1(\bar{r}_1,0)\rangle = \frac{N E_o^2 k'^4 \sigma^2}{r^2} \langle \exp\left[i(\bar{k}_o-\bar{k}')\cdot(\bar{r}_2(0)-\bar{r}_2(t))\right]\rangle \qquad (3.12)$$

This is the standard result for the single scattered electric field auto-correlation function. In the case of freely diffusing Brownian particles with diffusion constant D, the ensemble average reduces to

$$\langle \exp\left[i(\bar{k}_o-\bar{k}')\cdot(\bar{r}_2 IO) - \bar{r}_2(t))\right]\rangle = \exp\left[-D(\bar{k}_o-\bar{k}')^2 t\right] \qquad (3.13)$$

and the correlation function becomes

$$\langle \bar{E}_1^*(\bar{r}_1,t)E_1(\bar{r}_1,0)\rangle = \frac{N E_o^2 k'^4 \sigma^2}{r_1^2} \exp\left[-D|\bar{k}_o-\bar{k}'|^2 t\right] \qquad (3.14)$$

This is the well documented result for freely diffusing Brownian particles. There is a constant amplitude that is exponentially damped by a single exponential. The decay rate is dependent on the diffusion constant of the particles.

Double Scattered Electric Field

With the results given previously for single scattering, it is a fairly simple process to determine the double scattered field. As stated earlier the double scattered field is expected to be a product of two single scattering events, however, the approximations used and the conditions under which they apply need to be examined. Sorenson et al. (1976) has shown that the double scattered field may be written

$$\bar{E}_2(\bar{r}_1,t) = k'^2 \int d\bar{r}_2 \overleftrightarrow{T}(\bar{r}_{12})\cdot\overleftrightarrow{\alpha}(\bar{r}_2,t)\cdot k''^2 \int d\bar{r}_3 \overleftrightarrow{T}(\bar{r}_{23})\cdot\overleftrightarrow{\alpha}(\bar{r}_3,t)\cdot\bar{E}_o(\bar{r}_3,t) \qquad (3.15)$$

where $\bar{r}_3$ is the position of the first scatterer, $\bar{r}_2$ is the position of the second scatterer, and $\bar{r}_1$ is the position of the detector. The scattering wave vectors are shown in Figure 3. As was seen above it is possible to use the far field approximation for $\overleftrightarrow{T}(\bar{r}_{12})$. However, we must justify the approximation for the scattering from particle 1 to particle 2. In order to do so the following assumptions are made:

1. $|\bar{r}_3-\bar{r}_2|k' >> 1$, or the interparticle spacing is much greater than the wavelength of the scattered field.

2. $|\bar{r}_2| >> |\bar{r}_3|$

Assumption 1 is easy to satisfy by adjusting the k-space in which the experiments are done. Assumption 2 can be satisfied by choosing the origin arbitrarily close to the first scatterer. It should also be noted that the particles must move slowly enough so that this condition holds true for times of the order of the correlation time. This assumption holds true for aqueous suspensions of colloidal particles undergoing Brownian motion. Hence the far field approximation can also be used for $\overleftrightarrow{T}(\bar{r}_{23})$.

Since $\bar{k}"$ is the scattered wave vector to the second particle, it must be parallel to $\bar{r}_2-\bar{r}_3$. By the far field approximation

$$|\bar{r}_2-\bar{r}_3| \approx \bar{r}_2$$

and

$$\bar{k}" \cdot \bar{r}_2 \approx k"r_2 \tag{3.15}$$

The double scattered field can then be written

$$\bar{E}_2(\bar{r},t) = E_o \frac{\exp(ik'r_1)}{r_1} \exp(-i\omega t)k'^2k"^2 \hat{\varepsilon}' \int d\bar{r}_2 \frac{a(\bar{r}_2,t)}{r_2}$$

$$x \exp[i(\bar{k}"-\bar{k}')\cdot\bar{r}_2] \cdot \int d\bar{r}_3 \, a(r_3,t) \exp[i(\bar{k}_o-\bar{k}")\cdot\bar{r}_3] \tag{3.16}$$

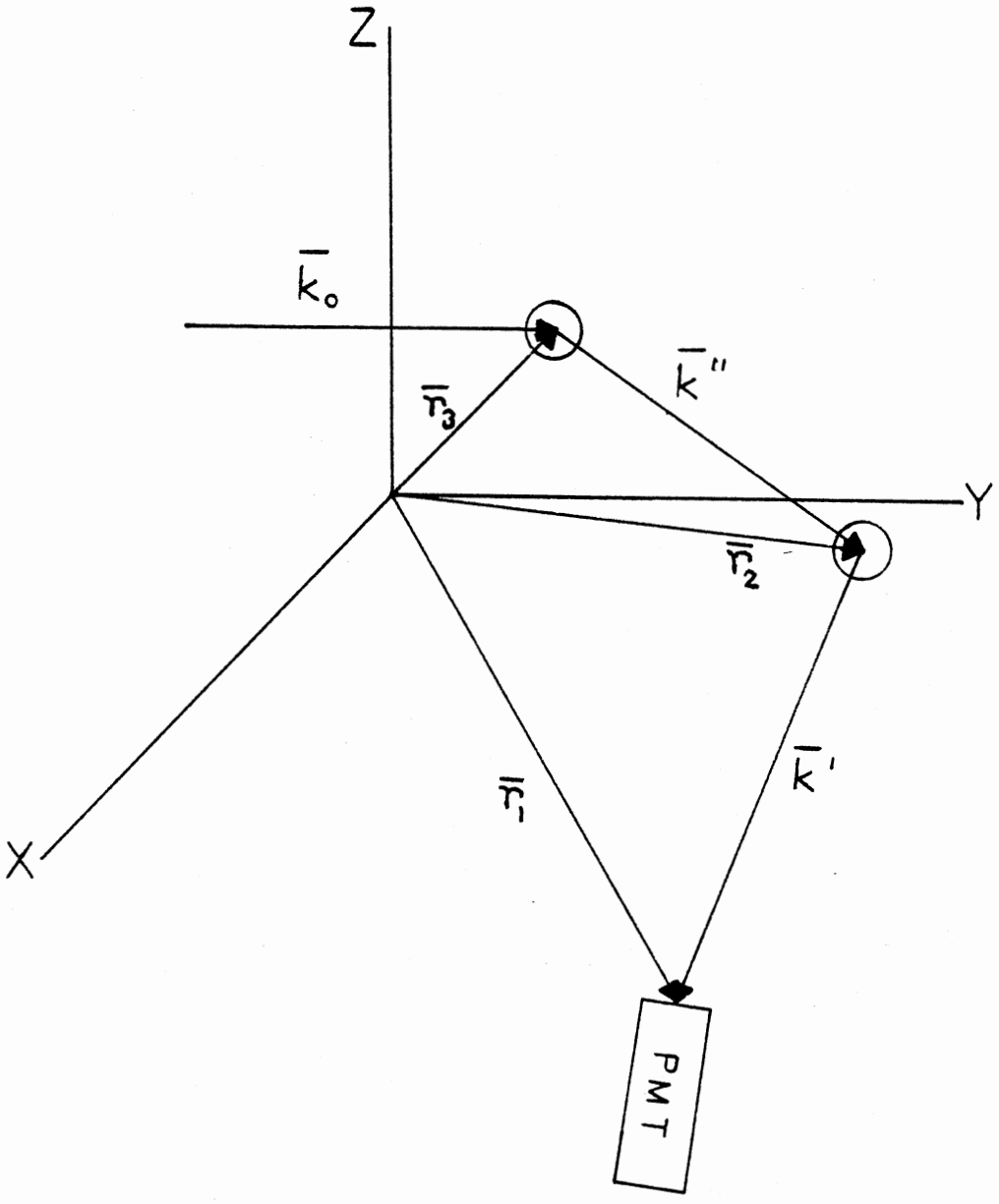

Figure 3. Double Scattering Geometry

Here $\hat{\varepsilon}'$ is the polarization of the double scattered wave vector and is given by $[\hat{r}_1 x(\hat{\varepsilon}'' x \hat{r}_2)]$. In this expression $\hat{\varepsilon}''$ is the polarization of the intermediate scattered wave vector, $\hat{\varepsilon}'' = [\hat{r}_2 x(\hat{\varepsilon} x \hat{r}_2)]$. The derivation is again limited to the case of small isotropic scatters. The double scattered electric field then reduces to

$$\bar{E}_2(\bar{r}_1,t) = E_o \frac{\exp(ik'r_1)}{r_1} \exp(-\omega t)(k'k'')^2 \sigma^2 \hat{\varepsilon}' \sum_{i=1}^{N} \left[\frac{1}{r_{2i}(t)}\right.$$

$$\left. x \exp(i(\bar{k}''-\bar{k}')\cdot\bar{r}_{2i}(t))\right] \cdot \sum_{\ell=1}^{N} \exp[i(\bar{k}_o-\bar{k}'')\cdot\bar{r}_{3\ell}(t)] \qquad (3.17)$$

As expected this has the form of two independent successive scattering events. The assumptions implicit in this result are: the far field approximation holds for both scattering events, the polarizability is isotropic, and the particles are small, isotropic scatterers.

The double scattered electric field autocorrelation function $\langle E_2^*(\bar{r}_1,t)E_2(\bar{r}_1,0)\rangle$ is now evaluated. As was done for the single scattered field, the condition of a noncorrelative, identical particle system is invoked. This allows us to do two things:

1. The single ensemble average of the phase terms can be written as the products of the ensemble average of the first and second scattering phase terms, or

$$\left\langle \sum_{i,j} \frac{1}{r_{2i}(0)r_{2j}(t)} \exp[i(\bar{k}''-\bar{k}')\cdot(\bar{r}_{2i}(0)-\bar{r}_{2j}(t))]\varepsilon_{\ell m}\right.$$

$$\left. x \exp[i(\bar{k}_o-\bar{k}'')\cdot(r_{3\ell}(0)-\bar{r}_{3m}(t))]\right\rangle$$

$$= \left\langle \sum_{i,j} \frac{1}{r_{2i}(0)r_{2j}(t)} \exp[i(\bar{k}''-\bar{k}')\cdot(\bar{r}_{2i}(0)-\bar{r}_{2j}(t))]\right\rangle$$

$$x \left\langle \sum_{\ell m} \exp[i(\bar{k}_o-\bar{k}'')\cdot(\bar{r}_{3\ell}(0)-\bar{r}_{3m}(t))]\right\rangle \qquad (3.18)$$

2. The ensemble averages are zero unless i=j or l=m respectively. The sum also becomes N times the summand.

The double scattered field correlation function can now be written as

$$\langle \bar{E}_2^*(\bar{r}_1,t)\bar{E}_2(\bar{r}_1,0)\rangle = \frac{E_o^2}{r_1^2} k''^4 k'^4 \sigma^4 \hat{\varepsilon}'^2 N^2 \frac{1}{\langle r_2\rangle^2} \langle \exp[i(\bar{k}''-\bar{k}') \cdot (\bar{r}(0)-\bar{r}(t))]\rangle \cdot \langle \exp[i(\bar{k}_o-\bar{k}'') \cdot (\bar{r}(0)-\bar{r}(t))]\rangle \quad (3.19)$$

Again the form of two distinct, independent scattering events is noted. Each event modulates the incident wave and the resultant waves correlation function is the product of two individual correlation functions.

For a system of particles undergoing Brownian motion, the ensemble averages in 3.19 reduce to $\exp(-D|\bar{k}''-\bar{k}'|^2 t)$ and $\exp(-D|\bar{k}_o-\bar{k}''|^2 t)$, respectively. Here D is Stokes Einstein diffusion coefficient. The electric field correlation function then reduces to the simple form

$$\langle \bar{E}_2^*(\bar{r}_1,t)\bar{E}_2(r_1,0)\rangle = \frac{E_o^2}{r_1^2} k''^4 k'^4 \sigma^4 \hat{\varepsilon}'^2 \frac{N^2}{\langle r_2\rangle^2} \exp[-D|\bar{k}''-\bar{k}'|^2 t] \times \exp[-D|\bar{k}_o-\bar{k}''|^2 t] \quad (3.20)$$

Integration Over Intermediate Scattered Wave Vector

We now need to extend this result into what one would observe in a real experiment on a system of identical particles. The final scattered wave vector, $\bar{k}'$, is determined by the positioning of the detector and

the incident beam, however the intermediate scattered wave vector may assume any direction. Therefore, 3.19 must be integrated over all possible orientations of $\bar{k}$". In doing this we will assume a spherical symmetry of second scatters about the first scatter. The final scattered wave vector will be taken to be in the scattering plane. Figure 4 defines the four different polarizations schemes that apply to this system and the geometries used for the integration procedures. The scattered wave vectors can now be defined as

$$\hat{k}" = \hat{r}_2 = \hat{i}\,\sin\theta"\,\cos\phi" + \hat{j}\,\sin\theta"\,\sin\phi" - \hat{k}\,\cos\theta"$$

$$\hat{k}' = \hat{r}_1 = \hat{i}\,\cos\phi' + \hat{j}\,\sin\phi' \qquad (3.21)$$

$$\hat{k}_o = \hat{j}$$

For vertical incident polarization, the polarization vector $\hat{\varepsilon} = k$. To determine the polarization of the final scattered field we must first determine the polarization of the intermediate scattered field, $\hat{\varepsilon}"$. It is

$$\hat{\varepsilon}" = [\hat{k}" \times (\hat{\varepsilon}\times\hat{k}")] = \hat{i}[-\sin\theta"\,\cos\phi"\,\cos\theta"] + \hat{j}[-\sin\theta"\,\sin\phi"\,\cos\theta"]$$

$$+ \hat{k}(\sin^2\theta") \qquad (3.22)$$

The final polarization is then

$$\hat{\varepsilon}' = [\hat{k}' \times (\hat{\varepsilon}" \times \hat{k}')] = \hat{i}\,\sin\theta"\,\cos\theta"\,\cos\phi'\,[\cos(\phi'-\phi")-1]$$

$$+ \hat{j}\,\sin\theta"\,\cos\theta"\,[\sin\phi'\,\cos(\phi'-\phi")-\cos\phi']$$

$$+ \hat{k}\,\sin^2\theta" \qquad (3.23)$$

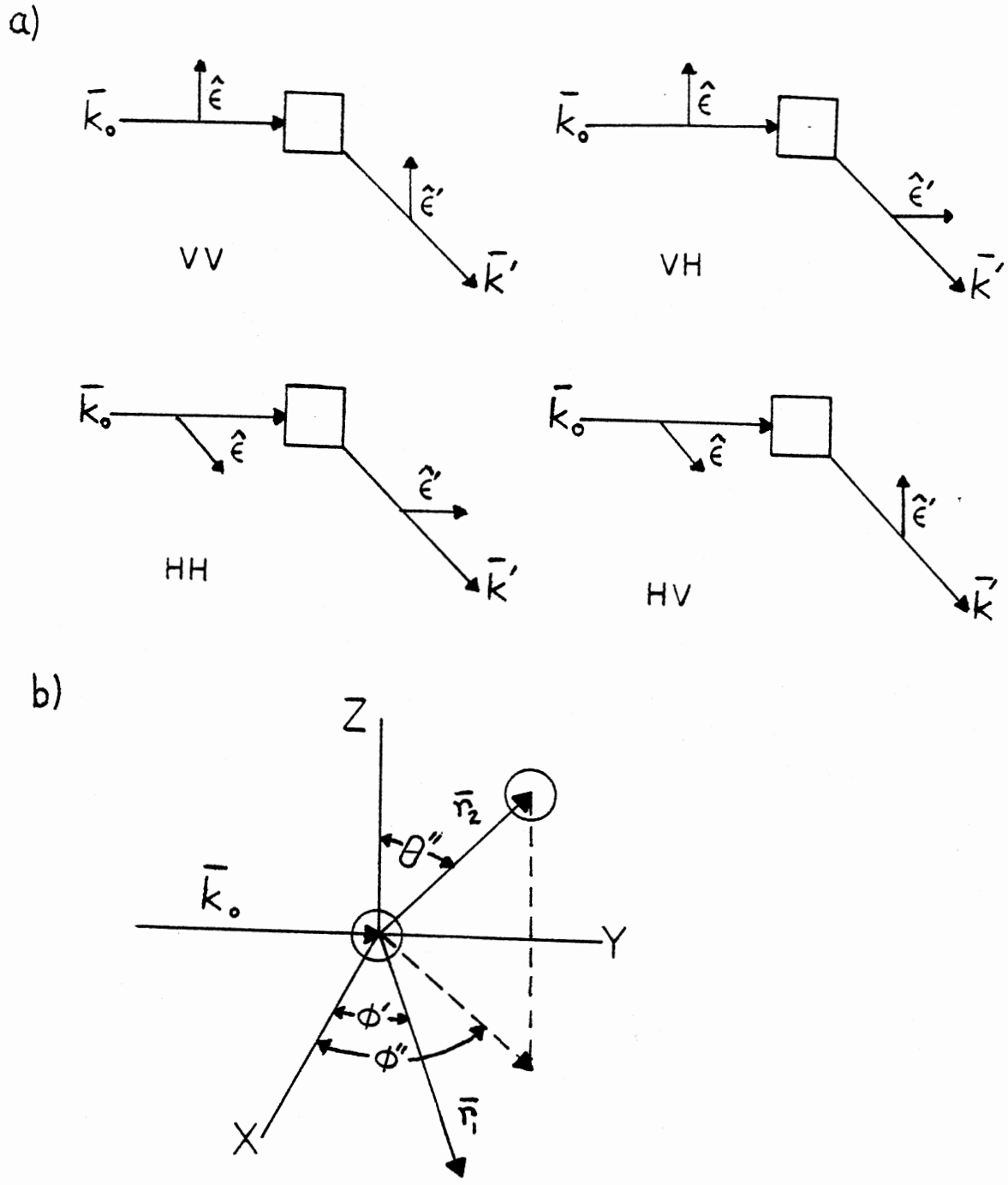

Figure 4. Definition of Polarization Schemes (a) and Integration Parameters (b)

Thus for the vertical incident polarization, we find the polarization factors to be $\varepsilon'^2_{VV} = \sin^4\theta''$ for the VV polarization and $\varepsilon'^2_{VH} = \sin^2\theta'' \cos^2\theta'' \sin^2(\phi'-\phi'')$ for the VH polarization. The same procedures may be followed to find the polarization factors for horizontal incident polarization, $\hat{\varepsilon} = \hat{i}$, to obtain

$$\varepsilon'^2_{HH} = [\sin^2\theta'' \cos\phi'' \sin(\phi'-\phi'') - \sin\phi']^2$$

$$\varepsilon'^2_{HV} = \sin^2\theta'' \cos^2\theta'' \cos^2\phi''$$

The assumption of quasi-elastic scattering is now applied. This allows us to use the approximations

$$|k_o| \cong |k| \cong |k''|.$$

Thus,
$$|\bar{k}_o - \bar{k}''|^2 = 2k_o^2(1-\sin\theta'' \sin\phi'') \tag{3.24}$$

$$|\bar{k}'' - \bar{k}'|^2 = 2k_o^2[1-\sin\theta'' \cos(\phi'-\phi'')]$$

When these results are substituted into 3.20, a rather complex relationship is obtained that is not easily integrated over k". However the first cumulant and the average scattered intensity can be determined. To find the average scattered intensity the integrals are performed at t=0

$$I^{(2)} = \langle E_2^*(r_1 0) E_2(r_1, 0)\rangle = A \int_o^{4\pi} d\Omega'' \, \hat{\varepsilon}'^2 \tag{3.25}$$

where
$$A = \frac{E_o^2 N^2}{r_1^2 \langle r_2^2 \rangle} k_o^8 \sigma^4 \tag{3.26}$$

Performing the integral for the four different polarizations the double scattered intensities are

$$I_{VV}^{(2)} = \frac{32\pi}{15} A$$

$$I_{VH}^{(2)} = I_{HV}^{(2)} = \frac{4\pi}{15} A \qquad (3.27)$$

$$I_{HH}^{(2)} = \frac{4\pi}{15} A \left[1+7 \sin^2\phi'\right]$$

We see that both the "depolarized" components (I_{VH}, I_{HV}) are equal and constant, independent of scattering angle. The VV polarized component is also independent of scattering angle. The double scattered depolarization ratio, the ratio of $I_{vh}^{(2)}$ to $I_{vv}^{(2)}$, is 1/8. However, the HH polarization is dependent on the scattering angle. For forward and backward scattering the intensity is equal to the VV polarized component. As you move away from these extremes the intensity decreases until at 90^o it becomes equal to the depolarized components.

The double scattered first cumulant, the initial slope of the double scattered correlation function is defined as

$$K_1^{(2)} = -\lim_{t\to O} \frac{\partial}{\partial t} \frac{\langle \bar{E}_2^*(r,t)\bar{E}_2(r,O)\rangle}{\langle \bar{E}_2^*(r,O)\bar{E}_2(r,O)\rangle} \qquad (3.28)$$

or
$$K_1^{(2)} = \frac{D \int_o^{4\pi} d\Omega'' \, \varepsilon'^2 \left[(\bar{k}_o-\bar{k}'')^2 + (\bar{k}''-\bar{k}')^2\right]}{\int_o^{4\pi} d\Omega'' \, \varepsilon'^2} \qquad (3.29)$$

Performing the integrals for all polarizations schemes gives

$$K_{1vv}^{(2)} = K_{1vh}^{(2)} = K_{1hv}^{(2)} = K_{1hh}^{(2)} = 4Dk_o^2 \qquad (3.30)$$

Thus for non-interacting pointlike particles we find that the double scattered first cumulant is independent of both scattering angle and polarization. In addition it is twice the decay rate of single scattering at 90°.

Higher Order Scattering

At the concentrations we are using, higher order scattering should also be present. Following Sorensen et al. (1978) we proceed theoretically by considering independent scattering events in succe-ssion for the nth order scattered correlation function. However, for $n > 2$, this becomes quite complex and integration over the n-1 intermediate scattered wave vectors is difficult. Instead a qualitative procedure will be introduced based on the results of the double scattering problem.

As noted earlier, the double scattered first cumulant was twice that of single scattering at 90°. This may be understood by visualizing that each event may scatter at any angle between 0° and 180°. For pointlike particles the scattering is isotropic and any angle is equally likely. This results in an average scattering angle of 90°. On the average each scattering event would contribute a decay rate equal to a single scattering event at 90°. Hence two events should give a decay rate twice that of single scattering at 90° which was found when the double scattering problem was solved exactly.

Generalizing to higher order scattering, we look at n scattering events. Each event will contribute a decay rate equal to single scattering at 90°. The single scattered first cumulant at 90° is $K_1^{(1)}(90)$ and $K_1^{(n)}$ is the nth scattered first cumulant. As with double scattering $K_1^{(n)}$ is expected to be independent of scattering angle. The first

cumulant for the nth order scattered light can be written simply as

$$K_1^{(n)} = nK_1^{(1)} \quad (90^o) \tag{3.31}$$

To investigate the additive effects of higher order scattering, consider the scattering to be a random process. Then each scattering event is independent of the next. Although the probability of each event is small, there are many possible events so that the average number of scattering events is finite. The Poisson distribution describes these random processes. The probability of having n scattering events is

$$P(n) = \frac{\bar{n}^n \exp(-\bar{n})}{n!} \tag{3.32}$$

where $\bar{n}$ denotes the average number of scattering events.

The intensity of the nth order scattered light should be proportional to the probability of n scattering events or

$$I_n \propto P(n) \tag{3.33}$$

Thus any measured first cumulant will be an average of the correlation times with the average weighted by the Poisson distribution. All events will be characterized by the average number of scattering events, $\bar{n}$. To determine $\bar{n}$, a depolarization ratio is defined,

$$R = \frac{I_{vH}}{I_{vv}} = \frac{\sum_{n=1}^{\infty} I_{vH}^{(n)}}{\sum_{n=1}^{\infty} I_{vv}^{(n)}} \tag{3.34}$$

$I_{vH}^{(n)}$ and $I_{vv}^{(n)}$ denote the VH and VV polarized components of the nth order

scattered light respectively. Also

$$I^{(n)} = I_{vv}^{(n)} + I_{vH}^{(n)} \propto P(n) \tag{3.35}$$

The nth order depolarization ratio is defined as

$$R_n = \frac{I_{vh}^{(n)}}{I_{vv}^{(n)}} \tag{3.36}$$

It was seen that this ratio is .125 for n=2 and Sorensen et al. (1978) has estimated that $R_3 = .266$. One would suspect that $R_n = 1$ for $n >> 1$ as the polarization should be completely random after many scattering events.

Gruner and Lehmann (1980) have suggested a method for determining the higher order depolarization ratios. The procedure begins by noting that the double scattered intensity should be proportional to the single scattered intensity, the proportionality constant depending on the concentration of scatterers,

$$I^{(2)} = \gamma I^{(1)} \tag{3.37}$$

The double scattered intensity is split as

$$I_{vv}^{(2)} = 8/9\ \gamma I^{(1)};\ I_{vH}^{(2)} = 1/9\ \gamma I^{(1)} \tag{3.38}$$

Assuming the same splitting and the same proportionality constant, the triple scattered intensity is

$$I_{vv}^{(3)} = 8/9\ \gamma\ I_{vv}^{(2)} + \frac{1}{9}\gamma I_{vH}^{(2)} = 65/81\ \gamma^2 I_1^{(1)} \tag{3.39}$$

$$I_{vH}^{(3)} = 8/9\ \gamma I_{vH}^{(2)} + \frac{1}{9}\gamma I_{vv}^{(2)} = 16/81\ \gamma^2 I^{(1)} \qquad (3.39)$$

The depolarization ratio, $R_3 = .246$, obtained in this method is in good agreement with Sorensen's value. The higher order values obtained in this manner are shown in Table I. It should be noted that although we followed the same procedure as Grüner and Lehmann to find these ratios, we arrived at different values.

TABLE I

THE N ORDER DEPOLARIZATION RATIOS

n	R_n
2	.125
3	.246
4	.360
5	.464
6	.557
7	.637
8	.706
9	.764
10	.811
11	.850
12	.881
13	.906
14	.927
15	.942
16	.955
17	.965
18	.972
19	.978
20	.983

With these defintions we can proceed to write the nth order intensity components as

$$I_{vv}^{n} \propto 1/(1+R_n)\ P(n)$$
$$I_{vH}^{n} \propto R_n/(1+R_n)\ P(n)\ . \tag{3.40}$$

The full depolarization ratio is then given by

$$R = \frac{\sum_{n=1}^{\infty} R_n/R_n+1\ P(n)}{\sum_{n=1}^{\infty} 1/R_n+1\ P(n)} \tag{3.41}$$

This expression can be evaluated numerically to find R as a function of $\bar{n}$. Thus, an experimentally measured depolarization ratio can be used to determine $\bar{n}$ for a given situation. It is then possible to predict the measured first cumulant for that experimental situation. The measured first cumulant is written as

$$\bar{K}_{1xy} = \frac{\sum_{n=1}^{\infty} I_{xy}^{(n)}\ K_1^{(n)}}{\sum_{n=1}^{\infty} I_{xy}^{(n)}} \tag{3.42}$$

where the bar over $\bar{K}_{1xy}$ denotes the measured value and the subscripts x,y denote the polarization. Using 3.31 and the expressions for the nth order intensities (3.40) 3.42 becomes

$$\bar{K}_{1vv}(90^{o}) = K_1^{(1)}(90^{o})\ \frac{\sum_{n=1}^{\infty} n/1+R_n\ P(n)}{\sum_{n=1}^{\infty} 1/1+R_n\ P(n)} \tag{3.43}$$

$$\bar{K}_{1vH}(90^{o}) = K_1^{(1)}(90^{o})\ \frac{\sum_{n=1}^{\infty} \frac{n\ R_n}{1+R_n} P(n)}{\sum_{n=1}^{\infty} \frac{R_n}{1+R_n} P(n)} \tag{3.44}$$

Hence knowing $\bar{n}$, we are able to predict the effects of multiple scattering on systems of non-interacting particles. Through careful experimentation it is possible to obtain information from a concentrated system of particles.

Interacting Particles

The next step is to determine the effects of multiple scattering in systems of interacting particles. Sorensen et al. have given a good procedure to look at non-interacting particle systems, so we will extend the procedure to interacting particle systems.

To achieve this we need to make the following assumptions:

1. The sample is composed of many correlated regions which are statistically independent from one another.

2. The double scattered field is a result of two successive single scattering events in different regions. Any double scattering within a single region is neglected.

The last assumption may be neglecting significant terms as the intensity of multiple scattered light depends on the separation distance of the two regions. In double scattering, light double scattered within a single region and light scattered from two separate regions seem to be of the same order in intensity. We neglect the single cell double scattered terms because we have no knowledge of the many body correlation function necessary to evaluate them.

Under these assumptions we can proceed in the same manner as before by exchanging the independent particles with independent correlation regions.

The double scattered electric field is written as

$$\bar{E}_2(\bar{r}_1,t) = E_o \exp(ik'r_1)\exp(-i\omega t)\ k_o^4\sigma^2\ \hat{\varepsilon}'\ \sum_{i=1}^{N} \frac{1}{r_{2i}(t)}$$

$$x\ \exp[i(\bar{k}"-\bar{k}')\cdot\bar{r}_{2i}(t)] \qquad (3.45)$$

The correlation function of the double scattered field is

$$\langle E_2^*(r_1,t)E_2(r_1,0)\rangle = \frac{E_o^2}{r_1^2} k_o^8\sigma^4\ \frac{\varepsilon'^2}{\langle r_2\rangle^2}\ \langle \sum_{i,j} \exp[i(\bar{k}"-\bar{k}')\cdot(\bar{r}_i(0)-\bar{r}_j(t))]\rangle$$

$$x\ \langle \sum_{\ell m} \exp[i(\bar{k}_o-\bar{k}")\cdot(\bar{r}_\ell(0)-\bar{r}_m(t))]\rangle \qquad (3.46)$$

The separation of the average over a 4 point correlation function into the product of pair correlation averages is done because we have two separate correlation regions. These pair correlation averages are defined as dynamic structure factors,

$$S(\bar{k},t) = \langle \sum_{i,j} \exp[ik\cdot(r_i(0)-r_j(t))]\rangle \qquad (3.47)$$

The static structure factor is defined as the t=0 limit of the dynamic structure factor or

$$S(k) = \langle \sum_{i,j} \exp[ik\cdot(r_i(0) - r_j(t))]\rangle \qquad (3.48)$$

Using these expressions the double scattered electric field correlation function is given by

$$\langle \varepsilon_2^*(r_1,t)\varepsilon_2(r_1,0)\rangle = \frac{E_o^2}{r_1^2} k_o^8\ \sigma^4\ \frac{\varepsilon'^2}{\langle r_2\rangle^2}\ S(\bar{k}"-\bar{k}',t)\ \ S(\bar{k}_o-\bar{k}",t) \qquad (3.49)$$

The intensity of the double scattered field, the t=0 limit of the

correlation function, is

$$I^{(2)} = \frac{E_o^2}{r_1^2} k_o^8 \sigma^4 \frac{\varepsilon'^2}{\langle r_2 \rangle^2} S(\bar{k}''-\bar{k}') \; S(\bar{k}_o-\bar{k}'') \tag{3.50}$$

In a liquid the static structure factor depends only on the magnitude of the difference in the scattered wave vectors $|\bar{k}''-\bar{k}'| = 2k_o \sin(\gamma/2)$, where γ' is the angle between k" and k'. It is also known that the dynamic structure factor has the form at least initially (Ackerson, 1976),

$$S(k,t) = S(k) \exp[-DK^2 4/S(k)] \tag{3.51}$$

Using 3.28, 3.49 and 3.50, the double scattered first cumulant is

$$K_1^{(2)} = \frac{AD}{I_2} \varepsilon'^2 [S(\bar{k}_o-\bar{k}'')(\bar{k}''-\bar{k}')^2 + S(\bar{k}''-\bar{k}')(\bar{k}_o-\bar{k}')^2] \tag{3.52}$$

where A is defined as

$$A = \frac{E_o^2 N^2}{r_1^2 \langle r_2 \rangle^2} k_o^8 \sigma^4$$

If γ is defined as the angle between k_o and k" and γ" as the angle between k" and k', the assumption of elastic scattering allows us to write

$$(\bar{k}_o-\bar{k}'')^2 = 2k_o^2(1-\cos\gamma)$$

$$(\bar{k}''-\bar{k}')^2 = 2k_o^2(1-\cos\gamma') \tag{3.53}$$

Using these expressions, the first cumulant is simplified to

$$\bar{K}_1^{(2)} = \frac{2ADK_o^2}{I^{(2)}} \varepsilon'^2 [S(\bar{k}_o - \bar{k}")(1-\cos\gamma') + S(\bar{k}"-\bar{k}')(1-\cos\gamma)] \quad (3.54)$$

with the intensity given by

$$I^{(2)} = A \varepsilon'^2 S(\bar{k}"-\bar{k}') S(\bar{k}_o - \bar{k}") \quad (3.55)$$

We again need to integrate these expressions over $\bar{k}"$ to find what one observes in an actual experiment. This is not easily done as the structure factor can in general be a complicated function. However, they can be numerically integrated to determine the properties of the double scattered field.

We have done this for the non-interacting case, S(k)=1, and for several different static structure factors. All the results for the more complicated structure factors had the same general features, so thus the discussion is limited to the most interesting one, an experimentally determined structure factor for an aqueous suspension of interacting latex spheres. The static structure factor and the double scattered intensities for a non-interacting particle system as well as the experimental system are shown in Figures 5 and 6. Figure 5a shows the static structure factor for a noninteracting system. This structure factor was input into 3.55 and numerically integrated. The resulting intensities are shown in Figure 5b. We find that $I_{vH} = I_{Hv}$. One should also note that $I_{vH} = I_{HH}$ (90^o), in contrast to the assumption of Gruner and Lehmann (1980). Both I_{vv} and I_{vH} are constant with depolarization ratio, $R_2 = .125$. The intensity in the HH polarization shows an

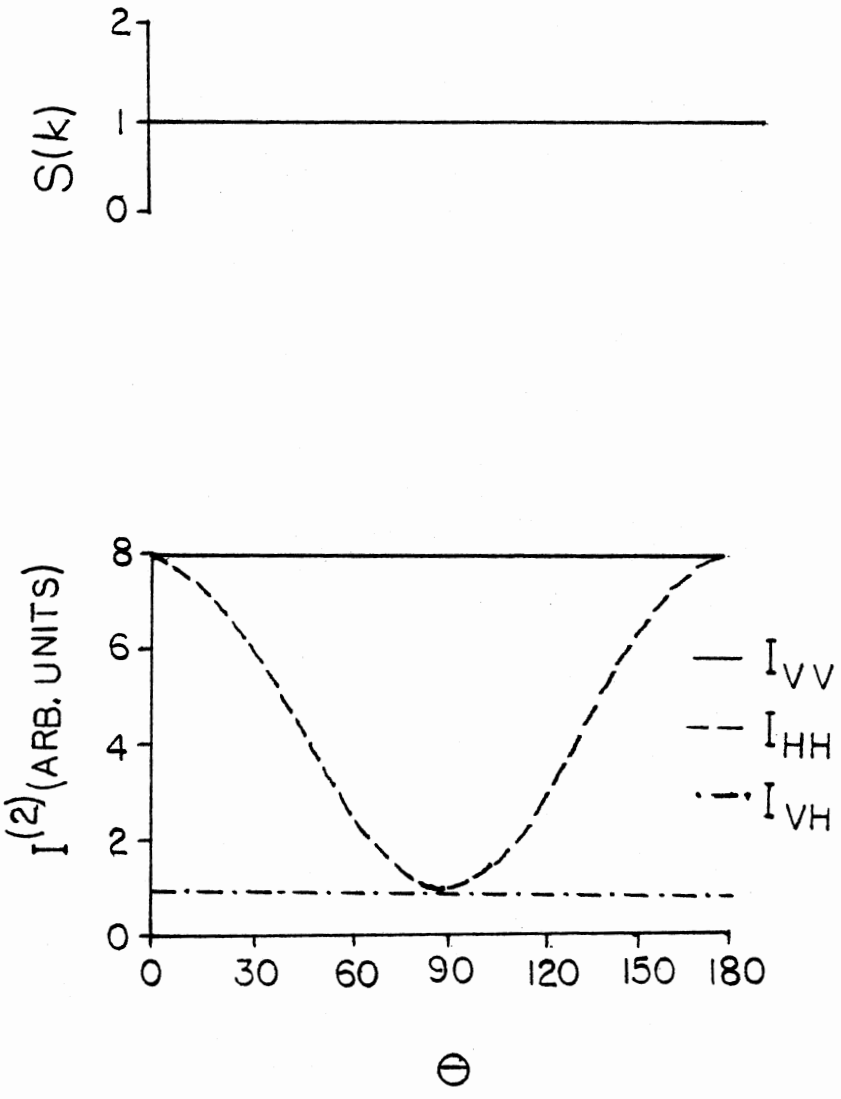

Figure 5. Static Structure Factors and Double Scattered Intensities for a Non-Interacting System of Particles

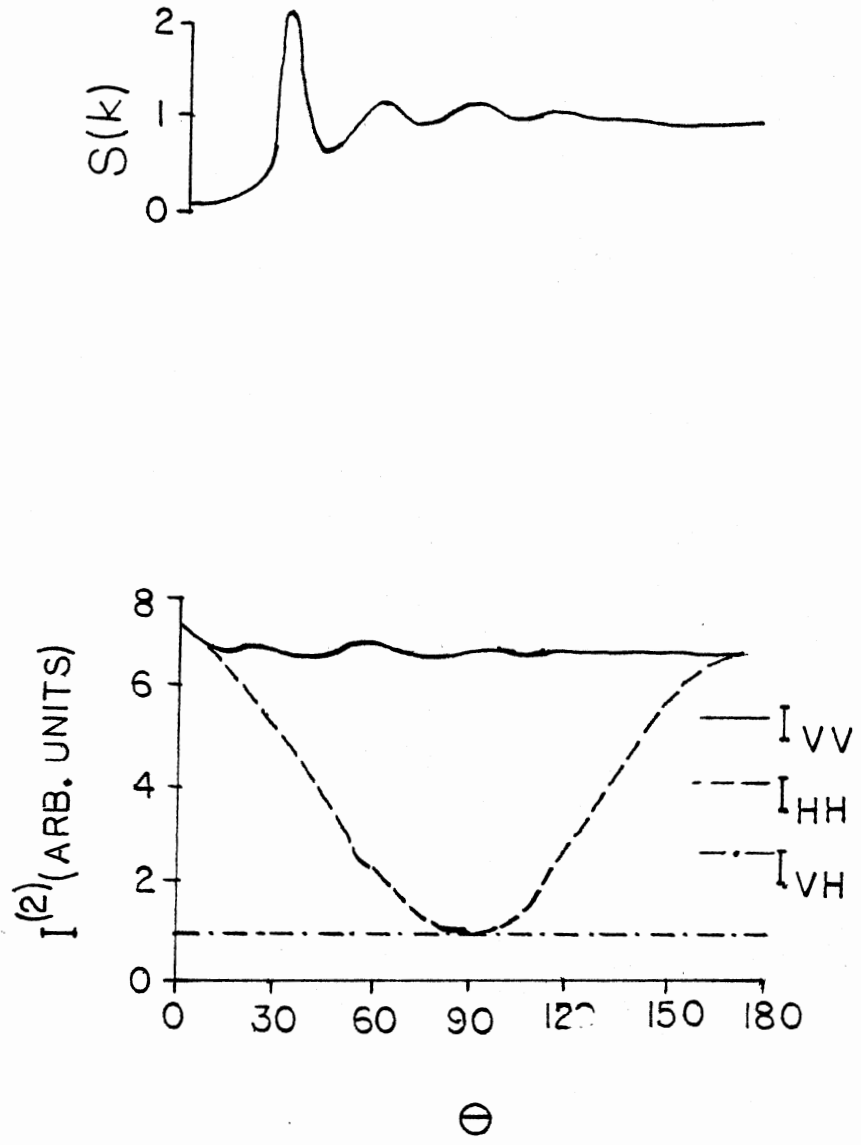

Figure 6. Static Structure Factor and Double Scattered Intensities for a System of Interacting Colloidal Particles

angular dependence that follows the equation

$$I_{HH}(\theta) = (I_{vv}-I_{HH})\cos\theta + I_{vH} \qquad (3.56)$$

For the experimental system the average scattered intensity for a system of interacting latex spheres was measured. The spheres were of radius .055 μm at a concentration, c = 2.412 x 10^{12} particles/ml. Multiple scattering was present in the sample, however, corrections were made using the method of Gruner and Lehmann (1980). The measured intensity is shown in Figure 6a. The double scattered intensities obtained are shown in Figure 6b. Again we found $I_{vH} = I_{Hv}$. I_{vv} shows the oscillating features of the structure factor, however, the main peak is now at 60^{o} compared to 30^{o} for the single scattered intensity. The cause for this can be understood in the following manner. If the single scattering is strongest at a particular angle, then the double scattered intensity should be strongest at double that angle because the double scattered electric field is written as two successive single scattered events. I_{HH} shows an angular dependence, yet still obeys 3.56 if the angular dependencies are included in I_{vv} and I_{vH}.

The structure factors and double scattered intensities for two other model systems, a delta function on a background and a highly concentrated system, are shown in Figures 7 and 8. These systems show the same general characteristics as the system discussed above.

The normalized double scattered correlation time, $\tau_c = 1/K_1$, determined by 3.54 for the different systems are shown in Figures 9 and 10. The correlation time for noninteracting systems is independent of scattering angle and polarization and is shown as the solid line at $4Dk_o^2\tau_c = 1$. When interactions are present, both an angular and

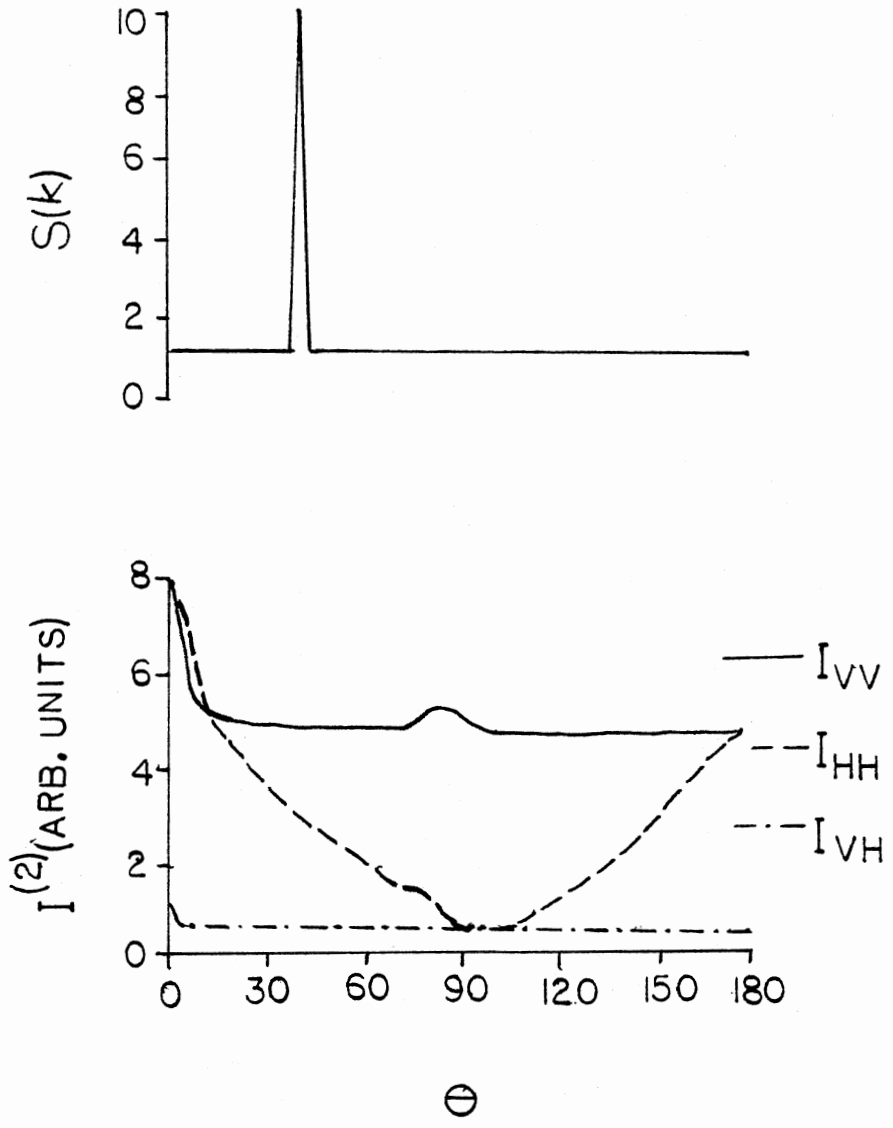

Figure 7. Static Structure Factor and Doubles Scattered Intensities for a Model System of a Delta Function on a Background

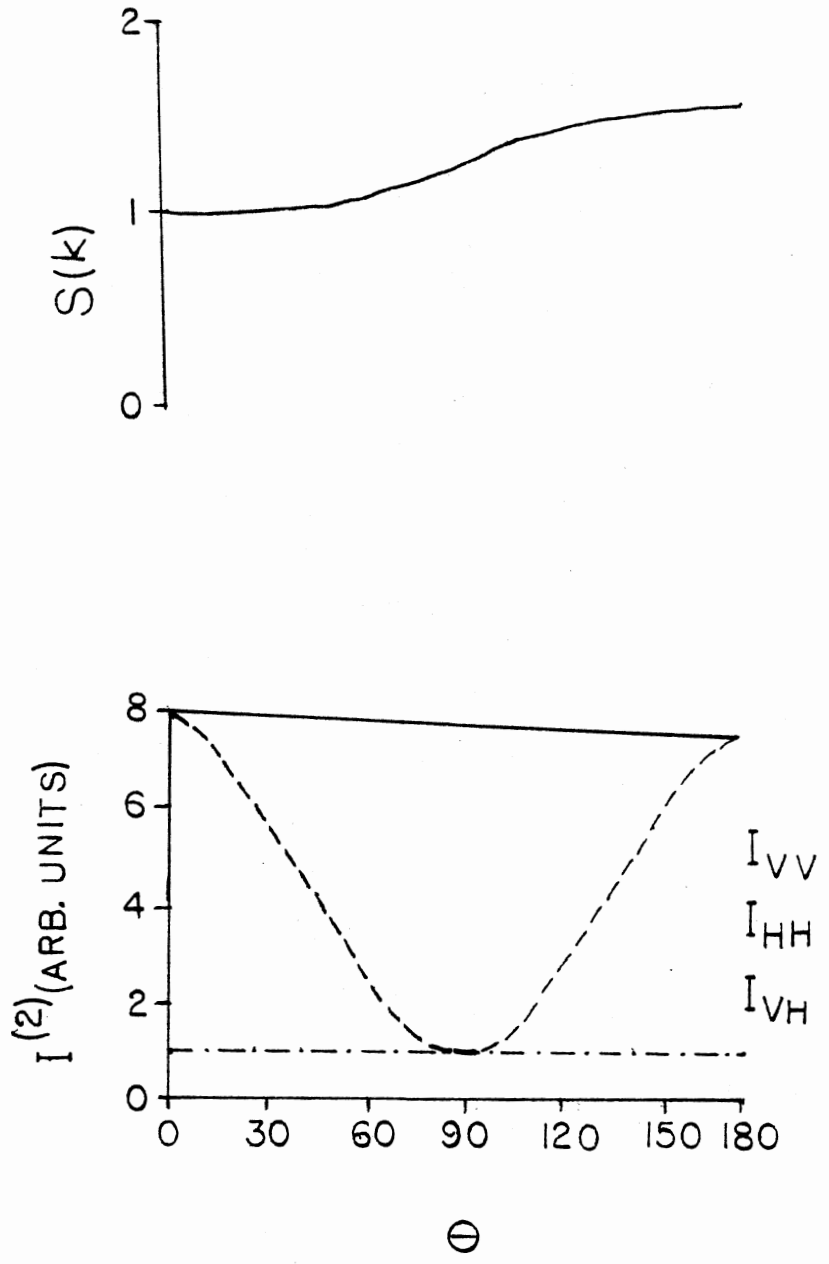

Figure 8. Static Structure Factor and Double Scattered Intensities for a Highly Concentrated Model System

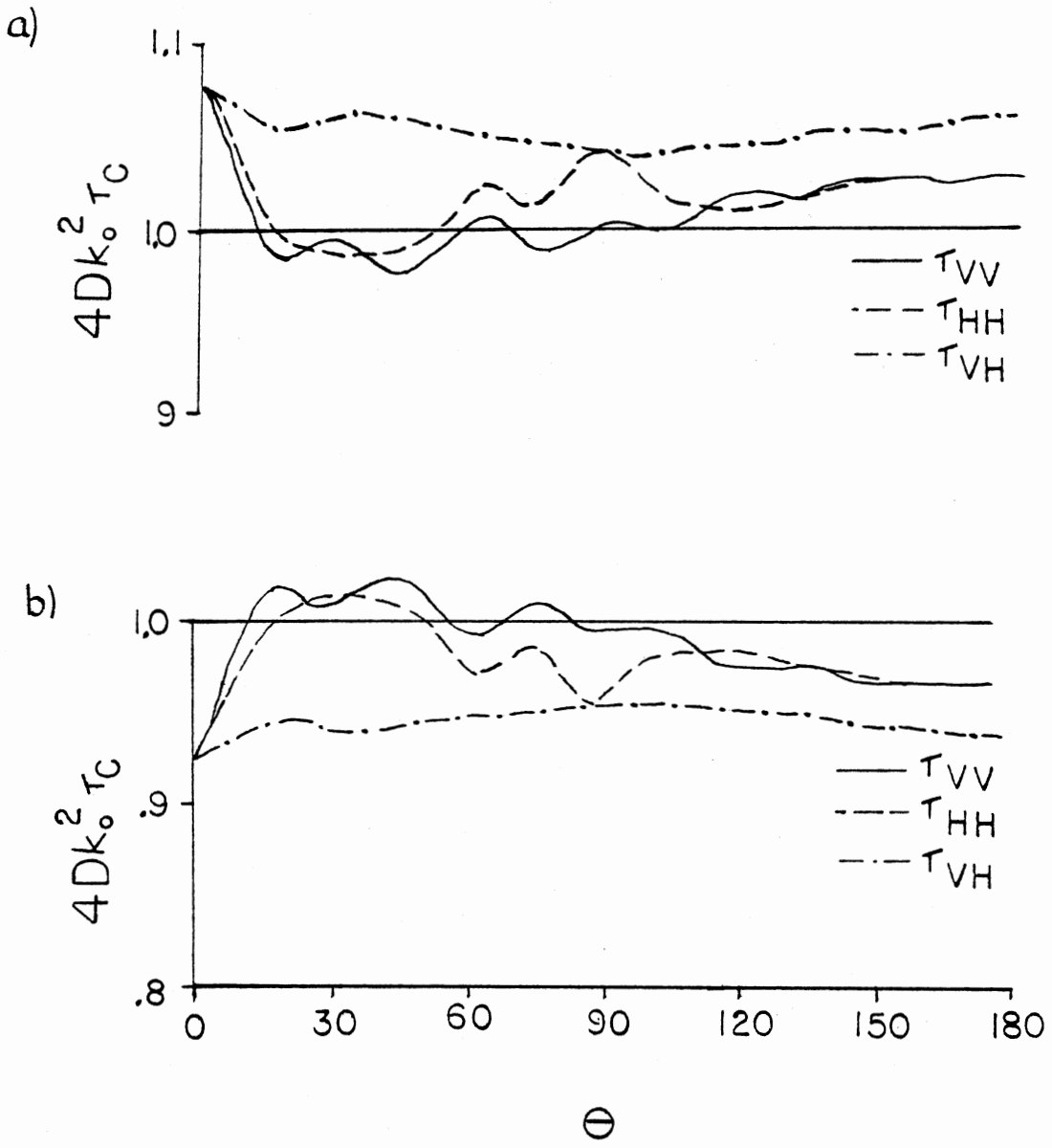

Figure 9. Normalized Correlation Times for the Interacting Colloidal System (a) and the Highly Concentrated Model System (b). The Correlation Time for Non-interacting Particles is Shown as the Solid Line at $4Dk_o^2\tau_c = 1$

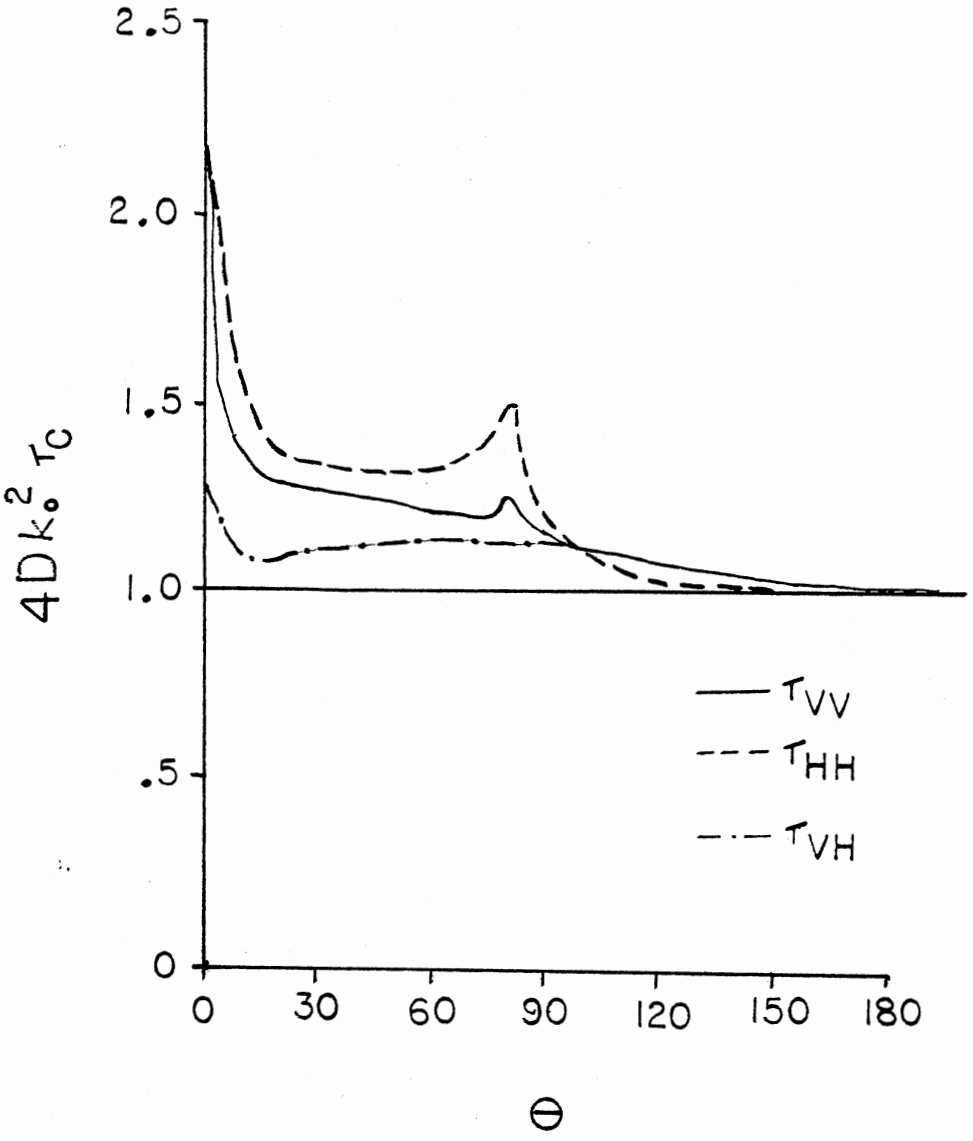

Figure 10. Normalized Correlation Times for the Delta Function on a Background. The Correlation Time for Non-interacting Particles is Shown as the Solid Line at $4Dk_o^2\tau_c = 1$

polarization dependence is seen in the correlation times. In all three cases the VH polarization shows the least angular dependence. This component is relatively constant (≈ 5%) in all but the delta function. The VH polarized correlation time never mimics the VV polarized correlation time. The correlation time in the HH polarization and the VV polarization are similar, but the HH component exhibits a slightly stronger structure.

These points depict the difficulty in working with multiple scattering samples. The VH polarized component is the only polarization that can be measured free of single scattering. Trying to determine the multiple scattered components in the other polarizations from the measured VH component introduces a significant error.

Experimental Observations

To test the theoretical results, the intensity time correlation function and average scattered intensity for aqueous suspensions of latex spheres was measured. Although support for this theory has been reported for non-interacting particles (Sorensen et al. 1976, 1978), more information should be extracted for these systems, and in interacting systems, the possibility of determining the effects of interactions needed to be investigated. Two systems of polystyrene latex spheres suspended in water were used. The latex spheres were of radius .055 μm and very monodisperse (see Chapter IV) so there were no polydispersity problems. The spheres were suspended at a concentration of 2.42×10^{12} particles/ml in doubly distilled water and contained in each of two quartz scattering cells with dimensions .1 cm x 1 cm x 4.5 cm. One of the cells also contained ion exchange resin. The exchange resin removes

excess salt ions from the suspension and allows the suspension to interact (for further comments on exchange resin, see Chapter IV). The focused beam (gauss beam diameter - 0.2 mm) of an Argon-ion laser operating at wavelength, $\lambda = 4880\text{Å}$ was directed lengthwise through the .1 cm side. The optical arrangement is shown in Figure 11. The polarizers are Glan-Thomson prisms with an extinction ratio of 5×10^{-5}. Both prisms were adjustable to pass either vertical or horizontal polarizations. The scattering cell was suspended in a water bath for refractive index matching purposes. The remainder of the apparatus is discussed in Chapter IV.

The calculations presented earlier dealt with the electric field correlation function. In our experiments the intensity correlation function is measured. These two correlation functions are related in a simple manner, the Siegart relation, if the scattered electric field is Gaussian (Pike, 1974). Since the scattering results from many different pairs of scattering events, this assumption should be satisfied for multiple scattering. This point has been discussed by Kelley (1973) and found experimentally true by Colby, Narducci, Bluemel and Beer (1975).

The polarizers were checked both before and after each experiment to insure proper polarizations. This was done by measuring the intensity as a function of the polarizer angle. A typical experimental run is shown in Figure 12. The depolarization ratio was then measured at a scattering angle of 90°. The average scattered intensity was then measured in both polarizations as a function of scattering angle. The depolarization ratio was remeasured to insure sample stability. It varied less than 3% from the initial measurement. The intensity auto-

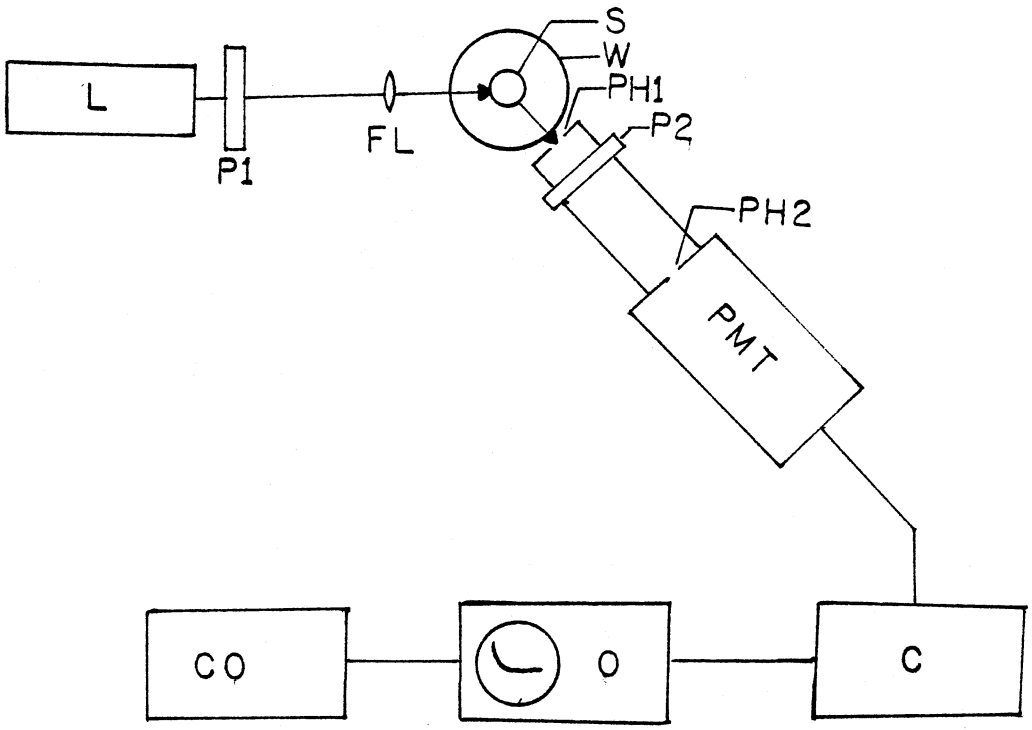

C AUTOCORRELATOR
CO MINI-COMPUTER
FL FOCUSING LENS
L LASER
O OSCILLISCOPE
P POLARIZER(2)
PH PINHOLE(2)
S SAMPLE
W WATER BATH

Figure 11. Dynamic Light Scattering Apparatus and Arrangement for Multiple Scattering Experiments

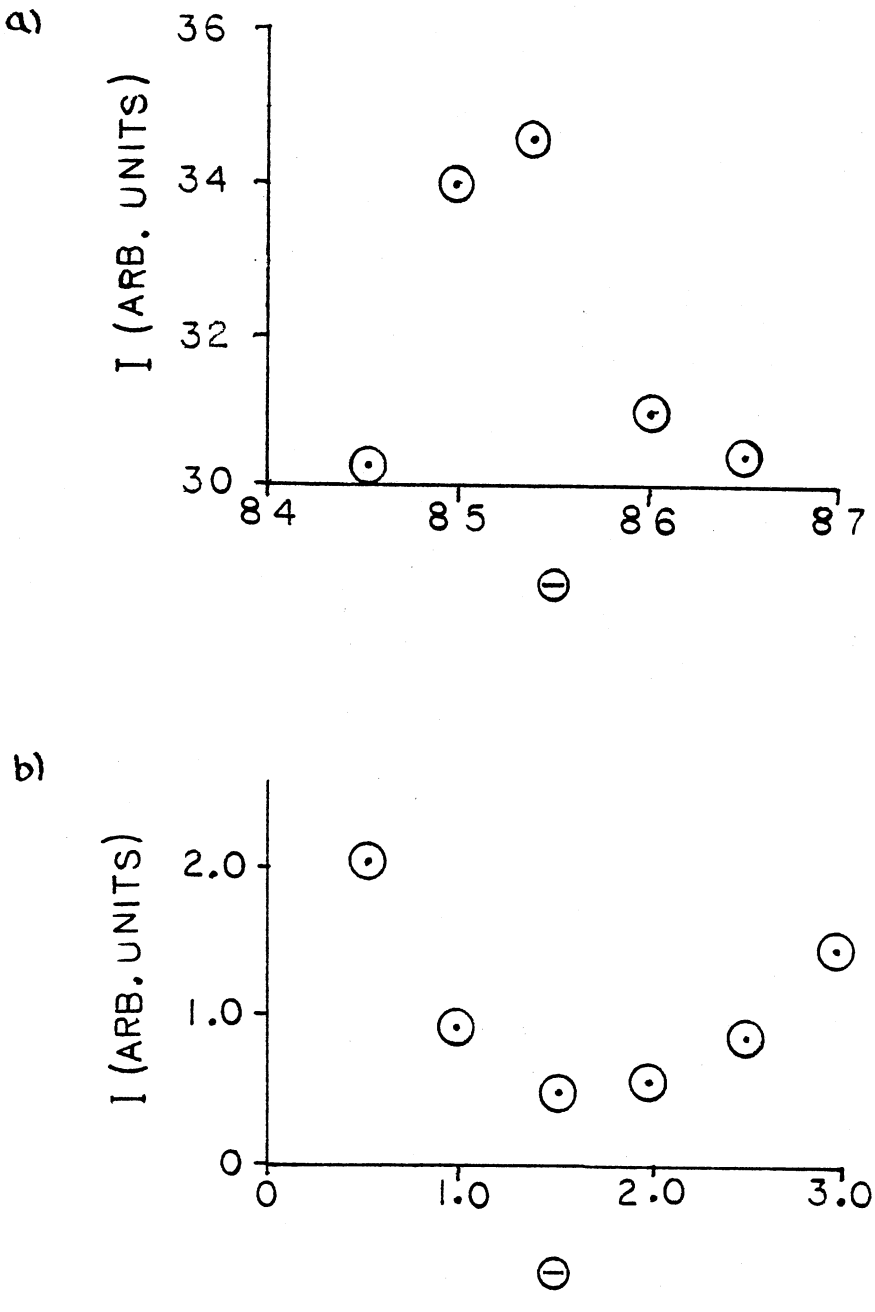

Figure 12. Intensity Passed by Polarizer P2 in the Vertical (a) and Horizontal (b) Polarizations

correlation function was measured next, first in the VV polarization and then in the VH polarization.

For the noninteracting sample the depolarization ratio was determined to be R = .01765 ± 2%. This corresponds to an average number of scattering events, $\bar{n}$ = .3. The average scattered intensities (Figure 13) is constant within experimental error at all scattering angles. The correlation data was fit to the following functional form:

$$\langle \varepsilon^*(r_1,t)\ E(r_1,0) \rangle = \sum_{i=1}^{4} a_i \exp(-\Gamma_i t) \qquad (3.57)$$

The a_i's represent the relative intensity of the ith scattered component with decay rate Γ_i. Figure 14 shows the resulting decay rates in the VV polarization. The solid lines are calculated using Equation (3.31) for i = 2-4. The solid line for single scattering is calculated using $K_1 = 2Dk^2$. The figure shows that the experimental results agree well with the predictions from the multiple scattering theory. Figure 15 shows the decay rates in the VH polarization and again the agreement with theory is quite good. Some of the error is probably due to a small amount of depolarization caused by dust, fingerprints or stresses in the lenses and scattering cell. When the VH polarized correlation function was analyzed using a sum of five exponentials, a small amount (<3%) of the total scattered intensity was due to single scattering.

Table II shows the relative intensities of the four components obtained from the analysis. From these values and the depolarization ratio we may determine the experimental values for the n order depolarization ratios.

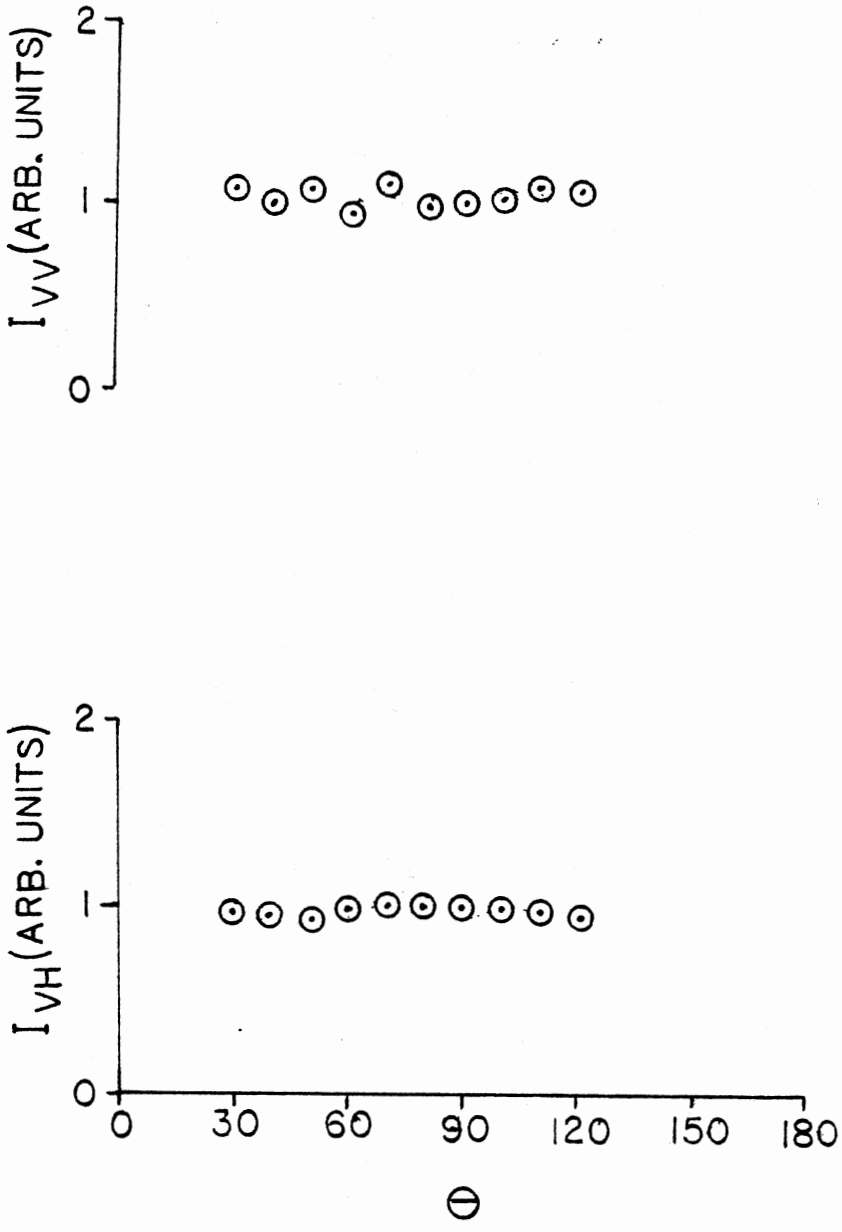

Figure 13. Measured Average Scattered Intensities for a Non-interacting Colloidal Sample

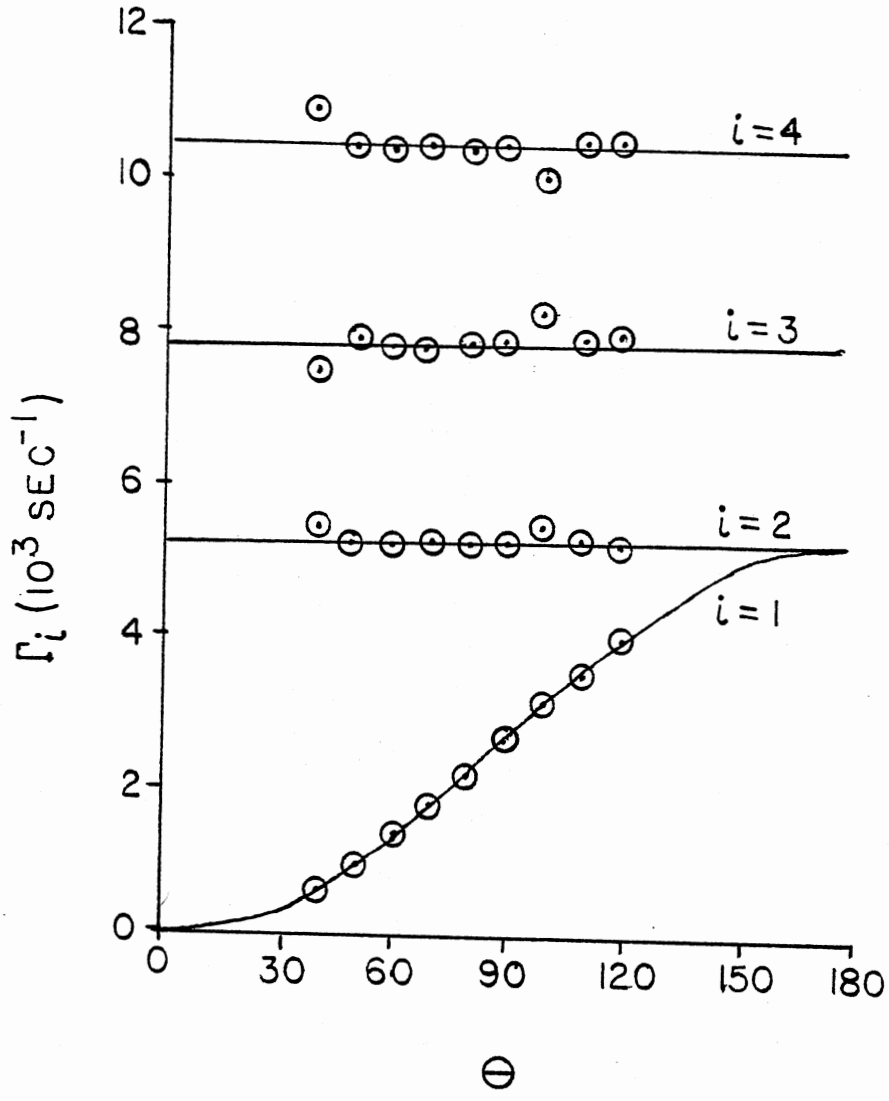

Figure 14. Decay Rates in the VV Polarization for a Non-interacting Sample. Solid Lines are Theoretical Predictions

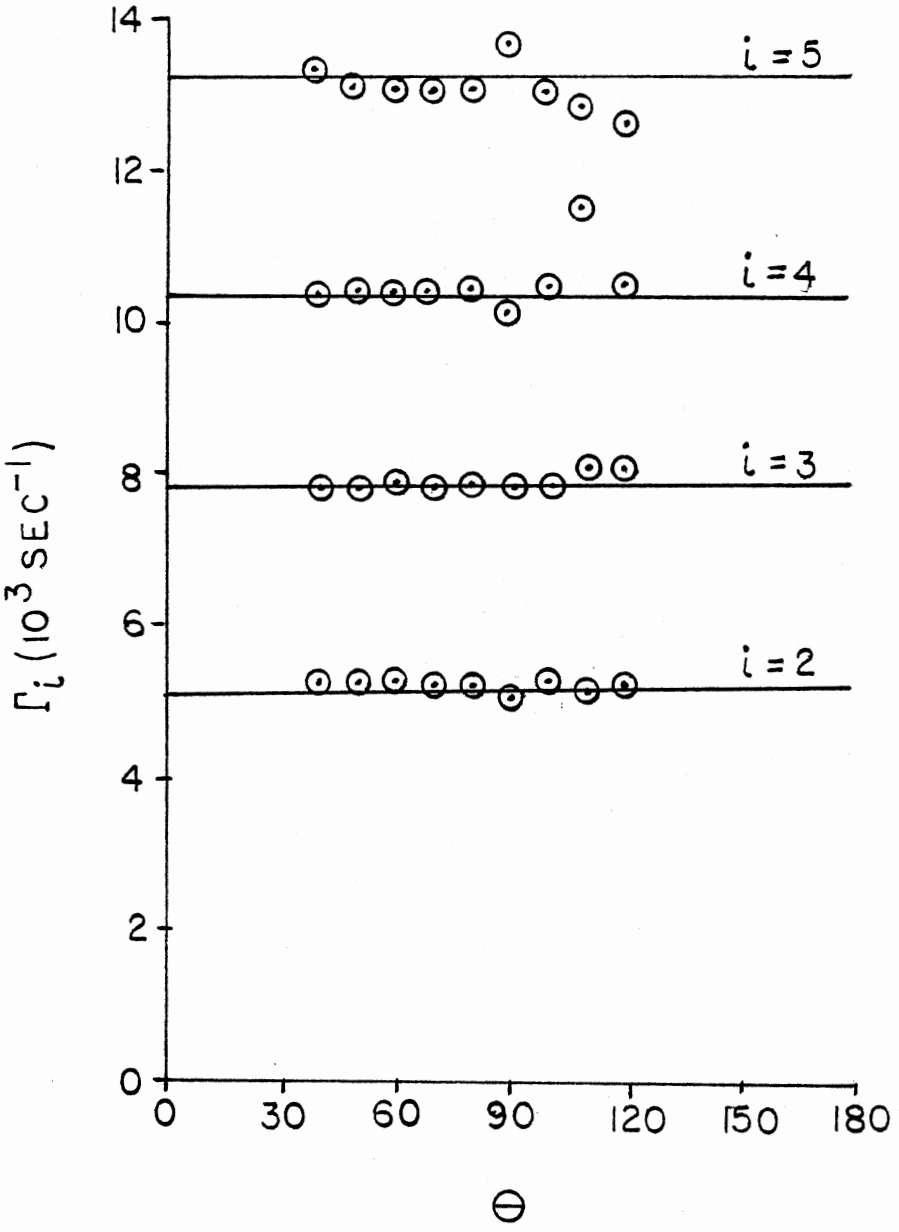

Figure 15. Decay Rates in the VH Polarization for a Non-interacting Sample. Solid Lines are Theoretical Predictions

TABLE II

RELATIVE INTENSITIES OF THE FOUR COMPONENTS OF THE SCATTERED LIGHT

i	$I_{vv}^{(i)}$	$I_{vh}^{(i)}$
1	.8712 ± 2%	----------
2	.1060 ± 13%	.616 ± 5%
3	.0154 ± 13%	.253 ± 9%
4	.0074 ± 15%	.116 ± 9%
5	----------	.034 ± 20%

$$R_n = \frac{R^* I_{vh}^{(n)}}{I_{vv}^{(n)}} \tag{3.58}$$

Using this equation we find

$$R_2 = .103 \pm 14\%$$

$$R_3 = .290 \pm 15\%$$

$$R_4 = .276 \pm 17\%$$

The value for R_2 is lower than the calculated value of .125 and R_3 is higher than the calculated value of .260. These discrepencies are attributed to the slight depolarizations mentioned above, the finite size of the particles, and a non-spherical scattering volume. Since multiple scattering is dependent on the scattering volume in general, and the calculated values are based on a spherical scattering geometry, these differences are not unrealistic. The value of R_4 is low but this is caused by the relative insensitivity of the fitting routine to the fourth order component, as well as the reasons listed above. The good agreement between our experimental values and the theoretical values lends strong support to the theory of multiple scattering in non-interacting particle systems.

The scattering cell with the ion exchange resin was allowed to "cure" for two weeks. By that time it was strongly interacting. The average scattered intensity was monitored for two days to insure that the sample was stable. Once stability was assured the same procedure that was used for the noninteracting sample was followed.

The measured depolarization ratio was R = .03566, which corresponds

to an $\bar{n} = .6$. This higher value must be attributed to the interactions, and R_n is not constant nor truly defined for interacting systems.

Figure 16 shows the intensity for both polarizations. The intensity in the VV polarization is high due to multiple scattering. Gruner and Lehmann (1980) suggest correcting the intensity using the relation

$$I_{vv}^{cor}(\theta) = I_{vv}^{meas}(\theta) - I_{vh}^{meas}(\theta)/R \ . \qquad (3.59)$$

We did not use this correction because the depolarization ratio, R, has an angular dependence.

The intensity in the VH polarization shows a slight downward slope and is caused by high order multiple scattering. The theoretical results for double scattering show a 5% increase at small angles and we suspect higher order effects will increase the slope of the depolarized intensity.

The intensity correlation functions were fit to a sum of four exponentials as in the non-interacting system. However, there didn't seem to be any pattern to the decay rates extracted. This made the separation of the multiple scattering effects from the interaction effects extremely difficult, if not impossible. However, the first cumulant can be extracted. Recall the first cumulant is defined as

$$K_1 = \lim_{t \to o} -\partial/\partial t \frac{\langle E^*(\bar{r}_1,t)\bar{E}(\bar{r}_1,O)\rangle}{\langle \bar{E}^*(\bar{r}_1,O)\bar{E}(\bar{r}_1,O)\rangle}$$

Using 3.57 along with the constraint $\sum_i a_i = 1$, the first cumulant is found to be

$$K_1 = \sum_{i=1}^{4} a_i \Gamma_i \qquad (3.60)$$

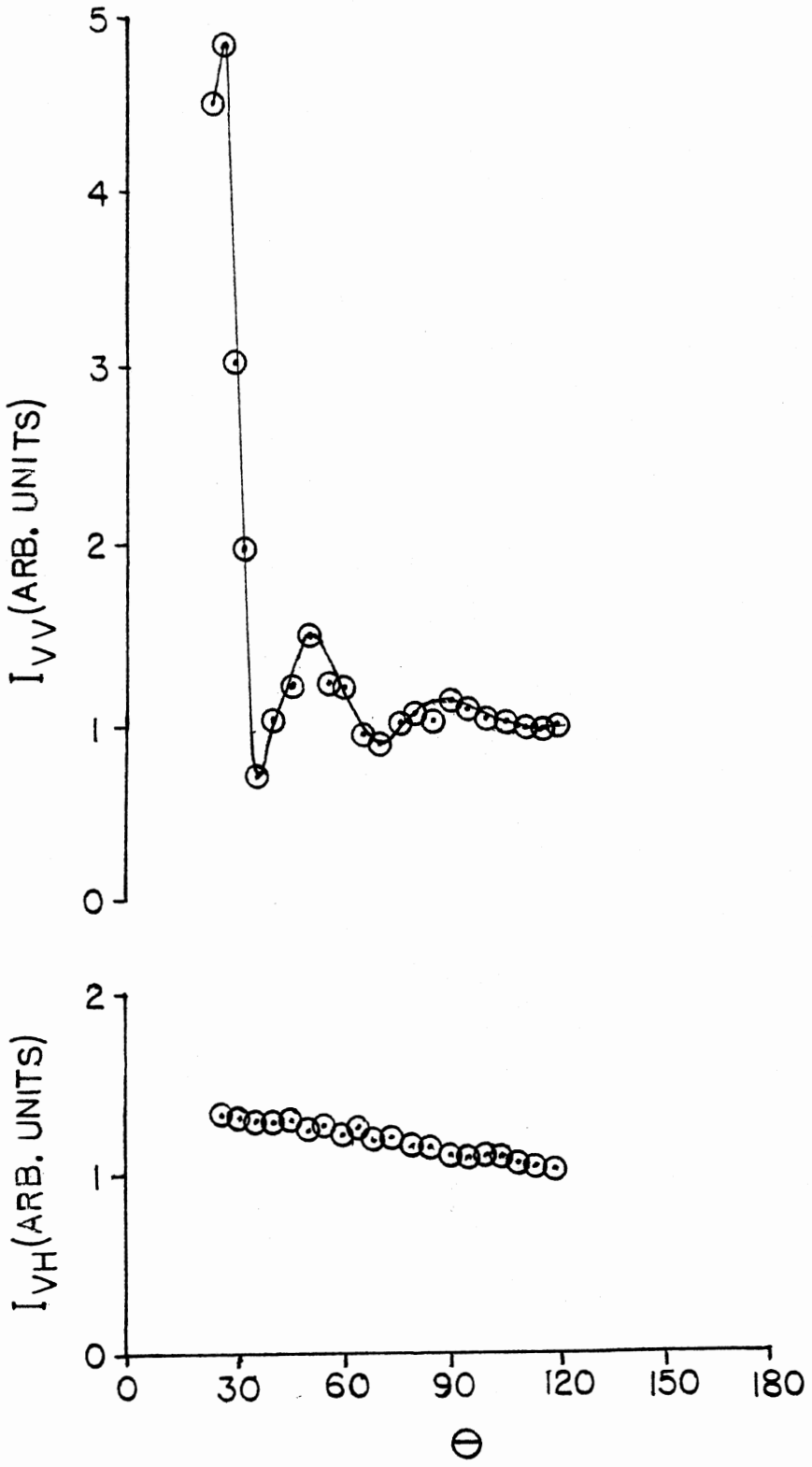

Figure 16. Measured Average Scattered Intensities for an Interacting Colloidal Sample

Figure 17 shows the normalized correlation times for both polarizations. We see in the VV polarization the liquid-like structure expected. It is somewhat reduced at the lower scattering angles and enhanced at the larger angles due to the effects of the multiple scattered field. To understand this consider the noninteracting particle system previously discussed. The single scattered first cumulant varies according to

$$K_1^{(1)} = 2Dk^2 = 4Dk_o^2 \sin^2(\theta/2) .$$

The double scattered first cumulant is constant at $K_1^{(2)} = 4Dk_o^2$. If the intensity of the double scattered component is 10% of the total intensity, the measured first cumulant can be written

$$\bar{K}_1 = .9\ k_1^{(1)} + .1\ K_1^{(2)}$$

or

$$\bar{K}_1 = 4Dk_o^2[.9 \sin^2(\theta/2) + .1]$$

where θ is the scattering angle. Thus as $\theta \to 0$, we see the greatest deviation from the expected value.

In the VH polarized correlation time a slight peak is noticed at 50^o. This angular position is double the single scattered main peak position and could be due to double scattering. The presence of this peak is not predicted by the double scattering theory for interacting particles in the calculations. The absence of it in the calculations may be due to the neglect of double scattering within a single correlation region. However, we do note a slight concavity in K_{1vH} which is seen in the calculations.

Although qualitative agreement is seen between experiment and

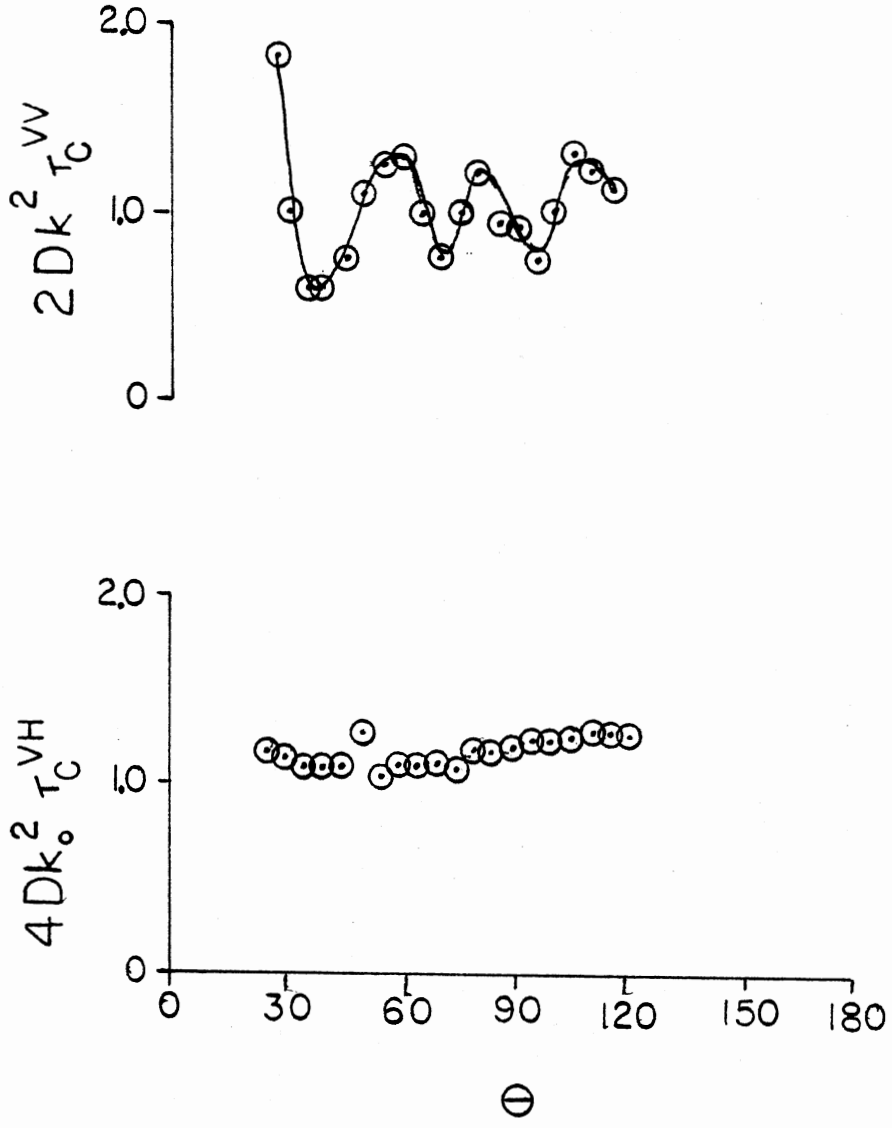

Figure 17. Normalized Correlation Times for an Interacting Colloidal Sample

theory, no reliable method for separating the effects of the interactions from the effects of multiple scattering could be found.

Thin Film Cell

The problem of multiple scattering in interacting systems is difficult to resolve. It was shown that the nonexponentiality of the intensity correlation function is due to two things: multiple scattering and interactions, and that these two effects cannot be reliably separated. The question remains as to what can be done so that concentrated interacting particle systems can be analyzed reliably.

Recently several papers have been published that suggest ways to minimize multiple scattering (Phillies (1981); Siano, Berne and Flynn, 1978; Hurd, 1981). Siano, et al. performed an experiment using a conical cell containing a strongly scattering colloical suspension. They investigated the effects of sample volume on the amount multiple scattering present in the scattered beam. The incident laser beam was directed along the axis of the cone and correlation measurements made at various heights on the axis.

Multiple scattered light was dominant toward the base and the decay rate was 75% greater than expected for single scattering. The discrepancy decreased as measurements were made at smaller cell radii. Thus multiple scattering is less troublesome when the cell's dimensions are reduced. They concluded that when the sample dimensions are much less than the mean free path of a photon, multiple scattering is negligible. This finding led Hurd (1981) to try a thin film cell to reduce the multiple scattering problem. He constrained the colloidal sample in a thin fluid film between optical windows such that one dimension of the

scattering cell was smaller than the photon mean free path. A strongly scattering colloidal sample was placed in the cell and illuminated with a laser beam. The depolarization ratio approached .125 asymptotically for large gap spacings. At a spacing equal to the mean free path of the photon in this sample the depolarization ratio reduced to R = .025. Once assured that multiple scattering was no longer a factor, he used the thin film cell to investigate the lattice dynamics of colloidal crystals.

This method was chosen to reduce multiple scattering to a minimum in the systems we studied. The scattering cell is similar to that of Hurd and is discussed in Chapter IV, as well as a method for determining the gap spacing. To insure that multiple scattering was indeed negligible in the cell, light scattering measurements were performed on a non-interacting particle system.

After the cell was assembled, the gap was measured to be .162 mm ± 2%. The cell was filled with a suspension of .109 μm diameter latex spheres. The intensity autocorrelation function was measured as a function of scattering angle, at two different particle concentrations, $c = 5.67 \times 10^{12}$ and $c = 2.10 \times 10^{13}$. The correlation function was analyzed using a two cumulant fit,

$$\langle E^* E \rangle = A \exp[-K_1 t + K_2 t^2] \qquad (3.61)$$

Figure 18 shows the first cumulant as a function of k^2 for the highest concentration. It exhibits linear behavior as expected for noninteracting particles. A least squares fit was made to determine the best straight line and from the slope of the line, the diameter of the

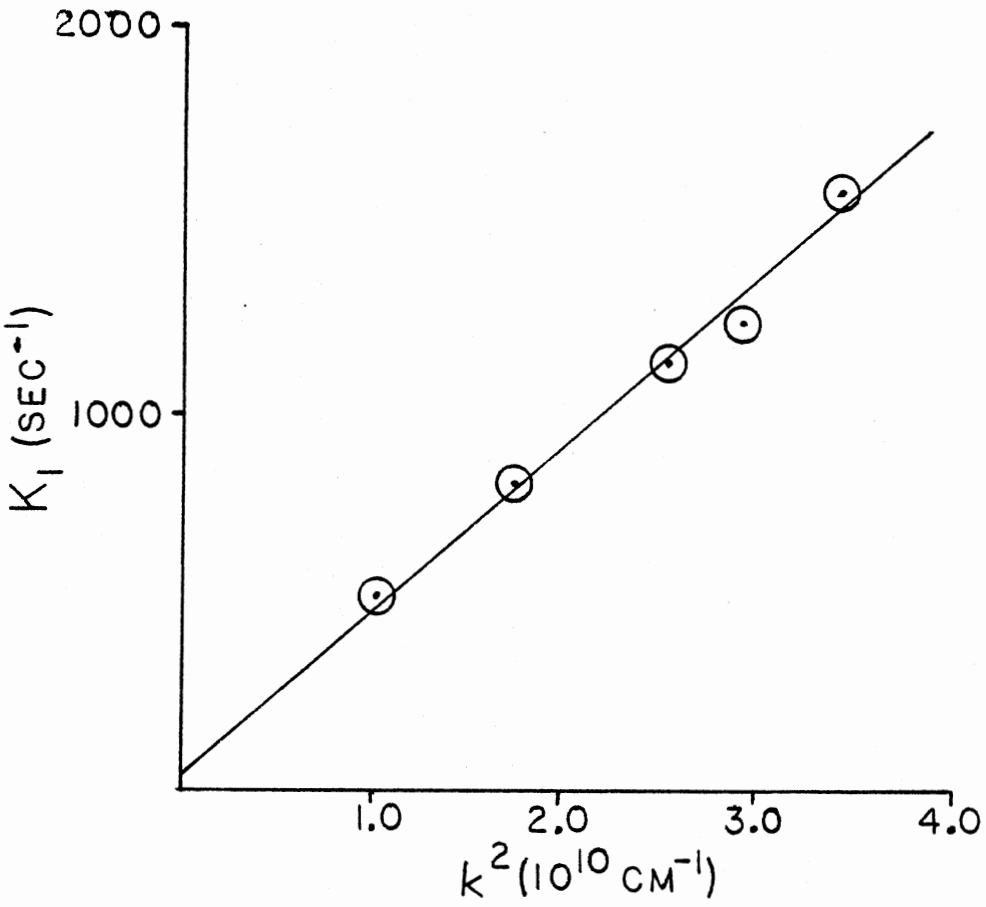

Figure 18. Measured First Cumulant for a Non-interacting Sample in the Thin Film Cell

particles was determined. The diameter was found to be .111 μm ± 2% for both concentrations.

The normalized second cumulant $K_2/2K_1^2 = .025 \pm 10\%$. Thus non-exponentiality is small and negligible even for the concentrations used. Thus multiple scattering is no longer considered a problem. There are several other problems, however, such as cleanliness and nonexponential effects due to interactions with the walls. These and other problems are discussed in Chapter IV.

Conclusions

The model of multiple scattering presented here works well for non-interacting systems. It was shown that the multiple scattered components can be separated from the single scattered component as well as being able to distinguish between the different higher order scattered components. This means that the multiple scattered field's contribution to the intensity correlation function may be subtracted and information from the single scattered field obtained. When interactions are present the nonexponentiality due to the multiple scattered field and the interactions become convoluted and cannot be resolved. Qualitative results may be obtained (Gruner and Lehmann, 1979, 1980), but any quantitative results will be in error.

Thus, to obtain quantitative results, multiple scattering should be reduced to a minimum. We tested a thin film cell and found it easy to use. It also minimized multiple scattering to a satisfactory level.

CHAPTER IV

EXPERIMENTAL APPARATUS AND DATA ACQUISITION

Introduction

This chapter describes the thin film cell, its construction and constraints. A relatively fast and accurate method of determining the gap spacing is presented, as well as the importance of cleanliness.

The next section deals with the sample preparation. A brief summary of the chemistry of latex spheres along with references for a more complete description of their chemistry is given. A discussion on the use of ion exchange as a method of cleaning the latex suspension is also included.

The next two sections are required to aid the understanding of the experiment and the data analysis. Two causes of nonexponentiality, wall effects and polydispersity are examined and shown to be negligible. The optical arrangement as well as a description of the apparatus is included. Finally, a discussion of methods of data analysis is given.

Thin Film Cells

Construction

The thin film cell was constructed as shown in Figure 19. The casing is made of anodized aluminum. The windows are quartz optical flats. Quartz was used to minimize leachable impurities. These

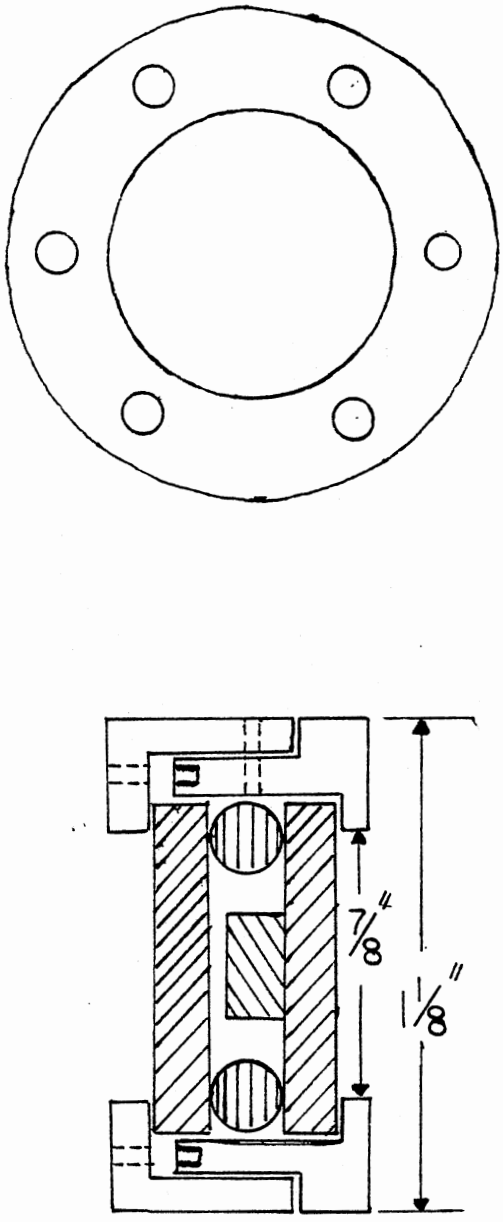

Figure 19. The Thin Film Cell

windows must satisfy two criteria:

1. A large range of scattering angles is desired, so large windows are needed.

2. Cleanliness, which is limited by surface leaching and the diffusion of impurities to the exchange resin calls for small windows.

We used 1" diameter optical flats for the solution containment region and glued a 1/2" diameter flat to one of the larger flats to make the thin film region. With this arrangement, it was possible to probe scattering angles in the range of 30° to 120°.

The O-ring also must serve several purposes. It acts as a spring to press against the optical flat and holds the cell at a constant spacing. It also forms the wall around the perimeter of the cell and must seal effectively against evaporation. We tried a Buna-n rubber O-ring first. This O-ring made a good seal and was resilient enough to keep a constant spacing. However, the rubber leached substantial amounts of impurities into the sample. This caused an instability which could not be tolerated. Next a silica rubber O-ring was tried. It had a higher resiliency than the Buna-n ring and with proper cleaning didn't appear to leach many impurities. Samples made with this O-ring have remained stable over long periods of time.

Gap Measurement

The gap was measured before the colloidal suspension was added to the cell. The measurement is made using a technique developed by Hurd (1981). A collimated laser beam enters the parallel plate cell at an angle θ as shown in Figure 20. Although reflections occur at every interface, only those adjacent to the gap are important.

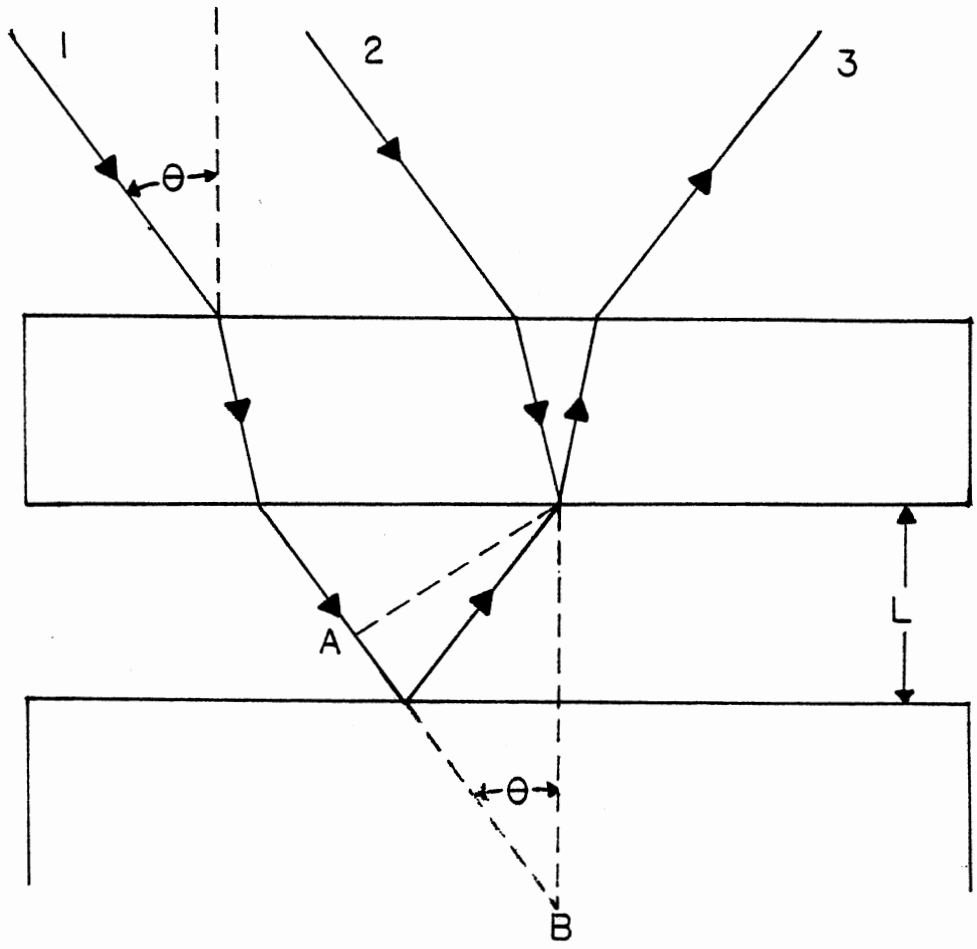

Figure 20. Ray Diagram for Gap Spacing Measurement

The optical path length difference between ray 1 and ray 2 for this air gap is $\overline{AB} + \lambda/2$. The extra $\lambda/2$ accounts for a phase shift suffered by ray 1 when it enters the region with lower index of refraction, the air gap. The length $\overline{AB} = 2L\cos\theta$ so the total path length difference is $2L\cos\theta + \lambda/2$. Destructive interference occurs when this difference is a half-odd integer number of wavelengths. This leads to the relation

$$n = (2L/\lambda)\cos\theta \tag{4.1}$$

where n is the order of interference.

The cell is rotated so that θ increases. Destructive interference will not occur again until θ increases enough that the next lower order of interference is found. To increase the accuracy of the measurement the cell should be rotated through several fringes. Knowing the initial and final angles of incidence, θ_i and θ_f respectively, and the number of fringes passed, Δn, Equation (4.1) can be used to determine the gap spacing, L. The gap spacing is found to be

$$L = \Delta n(\lambda/2)\,[\cos\theta_i - \cos\theta_f]^{-1} \tag{4.2}$$

After finding L, it is reinserted into 4.1 to find the actual order of the interference. The order number is constrained to the nearest integer and the gap spacing is adjusted accordingly. The uncertainty in the measurements is determined by the precision to which the angles are determined. We are able to measure the angles to within $.1^{\circ}$, so the relative error is about 1%. Using this procedure a very accurate measurement of the gap spacing can be made in a few minutes.

Cleanliness

Of great concern in sample preparation is the scattering cell cleanliness. The walls of the sample container constantly leach ionic impurities. In order to reduce the impurities care must be taken in cleaning the sample cell. The parts of the cell that come into contact with the colloidal suspension are boiled in a solution of distilled water and Micro cleaning fluid for one hour. After cooling, the pieces are removed using tongs and rinsed in doubly distilled water. The pieces are then rinsed in spectral grade ethanol to remove any remaining water.

Several other methods of cleaning have been published that require a more vigorous cleaning procedure and more time. We have found the above procedure to be less time consuming and provide sufficient cleanliness to enable the colloidal suspension to interact within a short period of time. The suspensions also remain stable for long periods of time.

Sample Preparation

The latex spheres are purchased commercially from Dow Diagnostics. The ones used in this work have a diameter of .109 ± .0027 μm. The spheres are highly charged when dissolved in water with a typical surface charge density of about 3μ ckm^2. The spheres also carry many ionic impurities, probably from the emulsifier and initiator chemicals. These impurities must be removed in order to increase the Debye length and hence, cause them to interact. For details on the manufacture and cleaning of latex, see McCarvill and Fitch, 1978.

The easiest way to clean latex is by ion exchange. There are three types of commercially available ion exchange resins: cationic, anionic, and mixed bed. They are normally small (500 μm) polystyrene beads that have been surface treated to allow the resin to bind either cations or anions. The ion exchanger releases a H^+ or OH^- into solution depending on the type of resin involved. Most of the released ions will bind together to form non-ionic H_2O.

We have only used monobed resins that have been prepared using the recipe of McCarvill and Fitch (1978). Before the resin is used it is run through a polystyrene sieve (.508 pore size) to remove bead fragments which cause problems when using a thin film cell. The two types of resins are then mixed to form a mixed bed resin.

The latex suspension is prepared and ion exchanged in the following manner. The latex is diluted to a concentration of 5.673×10^{12} particles/ml with water that has been doubly distilled in a quartz still. A small amount (~ 5% by volume) of prepared ion exchange resin is added to the cleaned sample container. The container is then assembled and the gap spacing measured. The gap spacing in these studies was .149 mm. The cell is filled using a needle and syringe to pierce the rubber O-ring through a hole in the aluminum casing. The cell is filled as full as possible to minimize contact with the air.

After filling the sample cell it was laid on its side to maximize contact with the ion exchange resin. Many people suggest agitating the sample to further increase contact with the resin and speed up the cleaning process. We used a smaller amount of resin than normally recommended and did not agitate the sample so that the interaction strength would increase at a slower rate. This enabled us to study the

sample at four different interaction strengths without changing the concentration, temperature, or any other experimental condition.

Measurements

After two days the suspension exhibited a liquid-like structure so autocorrelation measurements were made. After seven days an even stronger structure was seen and measurements were made at this interaction strength. The last time measurements were made was three weeks after the initial filling of the scattering cell. By this time the sample had begun to crystallize and was as close to solid-liquid coexistence obtainable while remaining in the liquid-like state throughout the gap.

Intensity autocorrelation measurements were made as a function of scattering angle at each of the interaction strengths listed above. During the measurements, the normal to the windows of the scattering cell bisected the angle at which the scattered light was detected. This constrained the scattering wave vector, $\bar{k}$, to be parallel to the windows, so only particle motions parallel to the windows contributed to the signal. This is beneficial for two reasons: to reduce flares from the interfaces and to reduce wall effects.

Wall Effects

Wall effects are discussed in detail by Hurd (1981). We deal here only with the portions relevant to our experiment. Hurd shows that the amount of the wall effect is characterized by the ratio of the gap spacing to the particle radius, L/a. The effect is less than 5% and is approaching 0% for $L/a \geq 100$. With our gap and particle size the ratio

is L/a = 2300, so wall effects should be minimal. The number of spheres close to the walls will contribute less than 2% of the total scattered intensity. Thus, any effects caused by interactions with the walls of the scattering cell are negligible. In Chapter III it was shown that the measured diffusion constant for a highly concentrated noninteracting particle system in the thin film cell differed by less than 2% from the calculated free diffusion constant. The nonexponentiality was also very small indicating that wall effects were minimal.

Polydispersity

Polydispersity can be a major concern in dynamic light scattering. Pusey (1983) has studied the problem intensively. He investigates scattering power polydispersity and size polydispersity for suspensions of hard-spherical particles. He concludes that for relatively high volume fractions and fairly narrow distributions, the intensity correlation function should be composed of two independent modes with well separated decay rates. The faster decaying mode describes collective diffusion and is present even for monodisperse systems. The slower decaying mode describes the exchange of different species.

The measured correlation function and intensity, neglecting interactions, can be described as

$$S^m(\bar{k},t) = A_c \exp[-D_c k^2 t] + A_e \exp[-D_e k^2 t] \quad (4.3)$$

$$S^m(k) = A_c + A_e \quad (4.4)$$

where A_c and A_e are the relative mode amplitudes for the collective diffusion (D_c) and exchange diffusion (D_e) modes respectively. For

interacting systems, the decay becomes more complicated. In the low-k limit the effects of polydispersity are greatest because the static structure factor is small. In this limit the static structure factor for a monodisperse suspension of hard sphere particles is

$$S^I(0) = (1-\phi)^4/(1+2\phi)^2 \tag{4.5}$$

where ϕ is the volume fraction of particles in the suspension. For a polydisperse system in which the particle size distribution is narrow, the measured structure factor, to second order in the deviation in sizes, $\sigma = \overline{\delta a}/\bar{a}$, is given by

$$S^m(0) = S^I(0)\left[1 + \frac{3\sigma^2\phi(4-\phi)}{(1-\phi)^2}\right] \tag{4.6}$$

The collective mode amplitude is given as

$$A_c = S^I(0)\left[1 + \frac{3\sigma^2(7\phi^2 + 8\phi + 3)}{(1 + 2\phi)^2}\right]^{-1} \tag{4.7}$$

This shows that for even narrower distributions, polydispersity can have a significant effect. To see this, consider an example where the deviation, $\sigma = .1$ and the volume fraction, $\phi = .4$. The measured structure factor is then $S^m(0) = 1.12S^I(0)$ and the diffusion mode amplitudes are $A_c = .936\ S^I(0)$ and $A_e = .189S^I(0)$. This means that the exchange mode amplitude is 16% of the total amplitude and definitely has a measurable effect on the intensity and autocorrelation function.

In our studies the volume fraction is $\phi = 3.95 \times 10^{-3}$ and the standard deviation in the particle size is $\sigma = 2.48 \times 10^{-2}$. Using these values we find that the measured structure factor equals the

freely diffusing monodisperse structure factor or $S^m(0) = S^I(0)$. Therefore, polydispersity effects are negligible on the average scattered intensity. The amplitude of the collective diffusion mode is $A_c = .994S^I(0)$. Thus the amplitude of the slow exchange mode is less than 1% and is undetectable in our experiment.

All unwanted causes of non-exponentially in the autocorrelation data have been eliminated. Multiple scattering was reduced by using the thin film cell, wall effects, generated by the thin film cell are negligible, and polydispersity is not a problem.

Apparatus

The scattering apparatus is shown schematically in Figure 21. A 15 mW Spectra-Physics He-Ne laser is used as the incident beam. The beam is focused by lens L1 onto the gap of the scattering cell. The scattered light is collimated by a set of two pinholes to reduce the problem of flares from the interfaces. Pinhole P1 has a diameter of .5 mm and pinhole P2 has a diameter of .38 μm. The pinholes are separated by a cylindrical tube 40 cm long made of aluminum. The tube eliminates stray light entering the collection optics. A telescope is contained in the apparatus after the second pinhole to enable viewing of the scattered light. This allows an easy adjustment of the sample to insure that flares are not present.

The scattered light is directed onto the 1 mm^2 cathode of the PMT-discriminator assembly. The output of the discriminator is fed into a 4-bit 64 channel autocorrelator. The autocorrelator has an analog output that allows a monitoring of the correlation function on an oscilloscope and a digital output that is connected to a PDP 11/10

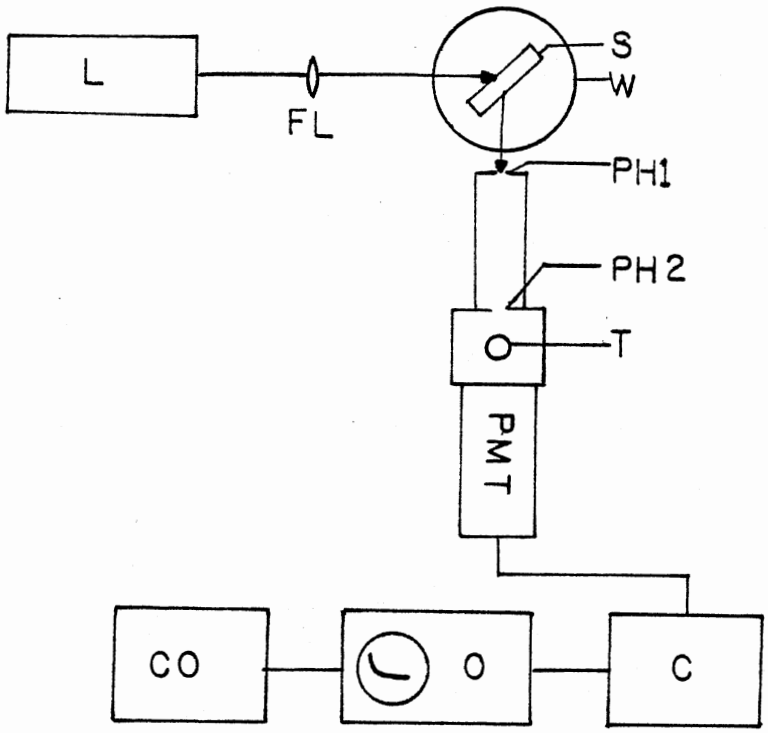

C CORRELATOR
CO COMPUTER
FL FOCUSING LENS
L LASER
O OSCILLISCOPE
PH PINHOLE(2)
S SAMPLE
T TELESCOPE
W WATER BATH

Figure 21. Dynamic Light Scattering Apparatus and Arrangement for Use With the Thin Film Cell

minicomputer. The autocorrelation function is stored on magnetic disks for later analysis.

The scattering cell is suspended in a beaker that had been painted black over half of its inside perimeter. This reduces backward scattering to a minimum and allows the cell to be immersed into a variety of refractive index matching media. The medium extends the k-space available for observation. We found that water gave us a good range in k-space and the other media (mineral oil and air) did not significantly extend this range because of the scattering cell design. With water we were able to look at a range of k values from $k = .7 \times 10^5$ cm^{-1} to 2.2×10^5 cm^{-1}. The scattering cell holder is designed to straddle the beaker and the collection optics. It allows a rotation of the cell and has a Vernier scale which is accurate to $.1^{o}$.

Data Analysis

The intensity autocorrelation functions were originally analyzed using a cumulant fitting routine. The cumulants are defined as

$$\ln[\langle E^{*}E\rangle] = \sum_{m=1}^{\infty} K_m(-t)^m/m! \qquad (4.8)$$

where K_m is the mth order cumulant. For noninteracting monodisperse systems $K_m = 0$ for $m \geq 2$ and corresponds to a single exponential. Thus the k_m's give us a measure of the nonexponentiality of the decay. The reason for using this methid was to obtain a good measure of K_1 by fitting the correlation function to two cumulants. In practice it is difficult to extract higher order cumulants and attempting to do so increases the error in K_1 and K_2 (Chu, 1983; Koppell, 1972). In this particular case, the two cumulants did not fit the data well as

evidenced by the pattern in the residuals. The residuals are defined as the deviation of the fitted function from the measured data. Since the function did not fit the data well, a different procedure was needed to measure the first cumulant. A three exponential fitting routine was tried next. It should be noted that this routine also converts the intensity autocorrelation function to the electric field autocorrelation function using the Siegart relation

$$\langle I^*I \rangle = 1 + \langle E^*E \rangle^2 \tag{4.9}$$

Electric field correlation function was analyzed using

$$\langle E^*E \rangle = \sum_{i=1}^{3} a_i \exp(-\Gamma_i t) \tag{4.10}$$

using the relative amplitudes, a_i, and the decay rates, Γ_i, the first cumulant can be extracted. The first cumulant is given by (Chapter III)

$$K_1 = \sum_{i=1}^{3} a_i \Gamma_i$$

with the condition $\Sigma\, a_i = 1$. We found that a sum of three exponential decays fit the data much better than the cumulant fit. The three exponential fitting routine was tested on several sets of data. A sample set of data was fit using three different sets of initial values for the amplitudes and decay rates. In all of the trials an analysis of the residuals indicated a good fit to the data. The actual values of the parameters returned by the routine differed between the fits, yet the first cumulant varied less than 2%. Thus this is the procedure that was chosen to extract a reliable first cumulant.

Several methods were also tried to determine the area under the correlation function, A. The first and most obvious way was to use the results of the three exponential fit. The area is an interaction of the electric field correlation function over all time. For a sum of exponentials the area is

$$A = \int_o^\infty dt' \left[\sum_{i=1}^{3} a_i \exp(-\Gamma_i t) \right] = \sum_{i=1}^{3} a_i/\Gamma_i \qquad (4.11)$$

Again there is the condition $\Sigma\, a_i = 1$.

This method appeared to work well and was also the choice of Gruner and Lehmann (1979), but the area found in this manner is very sensitive to the amplitudes and decay rates. Slight changes in the values of these parameters caused variations in the area of about 10-15% although no change was seen in K1. The problem lies in the weighting of the data. The short times are weighted heavier due to the increased noise as the background is reached. The fitting routine is less sensitive to changes in the slow decays. The slow decays, although a minor component in the first cumulant, are a major component in the area calculations. Therefore, a more reliable way of determining the area is needed.

A straight forward integration of the electric field correlation function was then used to determine the area. The integration is done numerically using a 3-point Langrangian interpolation procedure. Using the first cumulant obtained from the three exponential fit, the area is corrected to include t=0. It is difficult, however, to correct for the long time end. It is better to make sure the data extends well into the background. Doing this causes a greater error in the initial decay, but this problem is resolved by taking data over a range of delay times. This insures an accurate measure of both the first cumulant and the area.

The area measured in this manner differed at most 10% from the values obtained using the three exponential fit. As a check of the numerical integration procedure, it was used on a noninteracting particle system. In a system of noninteracting particles the electric field autocorrelation function should decay as a single exponential and the product of the area and the first cumulant should equal 1. This held true to within 5%. Thus this procedure is the best procedure to accurately determine both the first cumulant and the area.

CHAPTER V

RESULTS AND CONCLUSIONS

The main purpose of this thesis is to measure the memory effects on systems of interacting particles. The electric field correlation function was measured at three different interaction strengths. The three different strengths are denoted system 1-3 where system 1 is the weakest interacting system and system 3 is the strongest.

Figure 22 shows the static structure factors, S(k), for the three systems. The structure factor was calculated from the first cumulant using the relation

$$K_1 = Dk^2/S(k) \tag{5.1}$$

where D is the diffusion coefficient at infinite dilution and k the scattering wave vector. We notice a slight shift in the peak between system 1 and system 2. A small shift like this has been seen in molecular dynamics calculations as the volume fraction of hard spheres is increased. The peak in system 2 is also higher and narrower than that in system 1. The peak in system 3 is somewhat taller and narrower indicating an even stronger interaction than that present in system 2.

The reduced memory functions were determined for the three interacting particle systems as well as a non-interacting particle system. These are shown as a function of k/k_M in Figure 23. The non-interacting

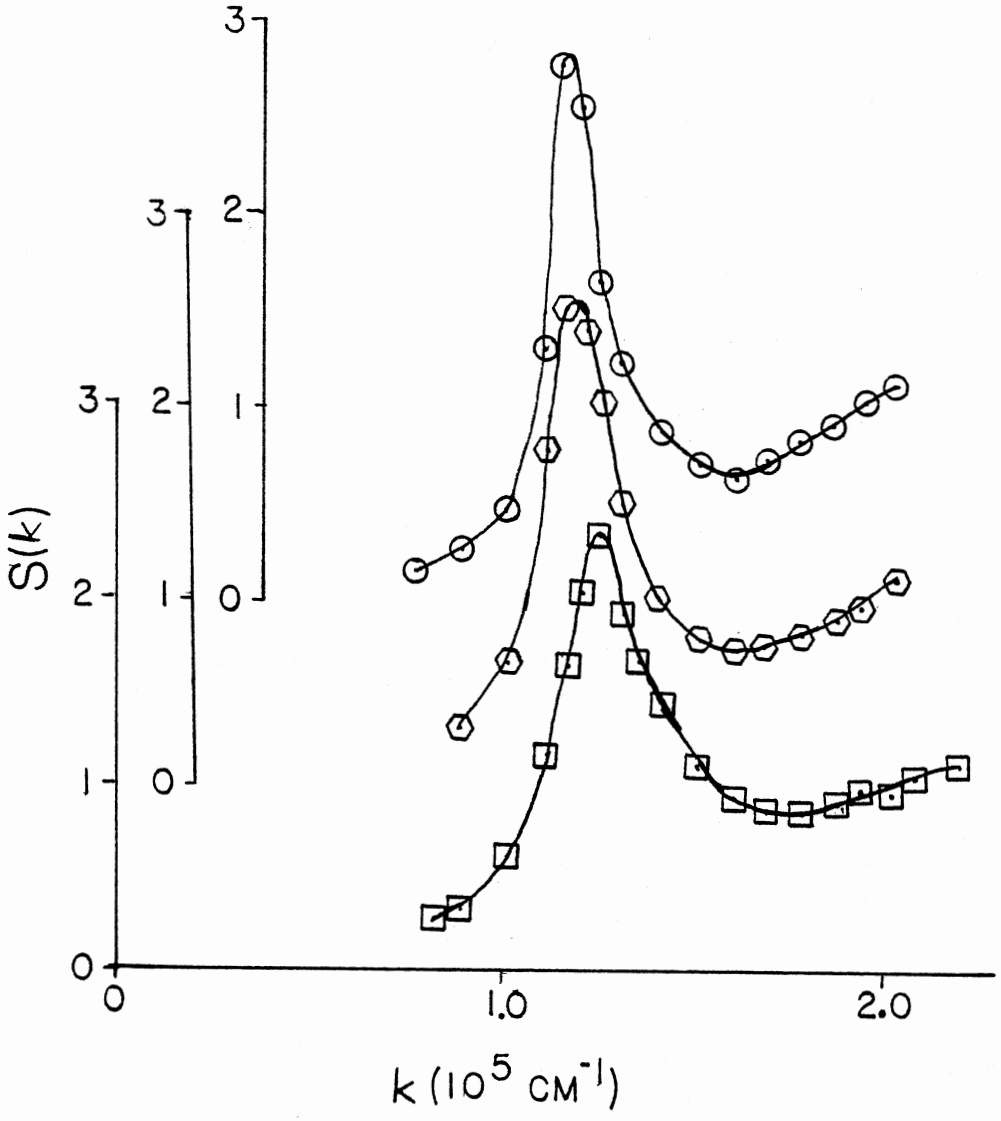

Figure 22. Measured Static Structure Factors for the Three Interacting Systems. □ is System 1, ⬡ is System 2, and O is System 3

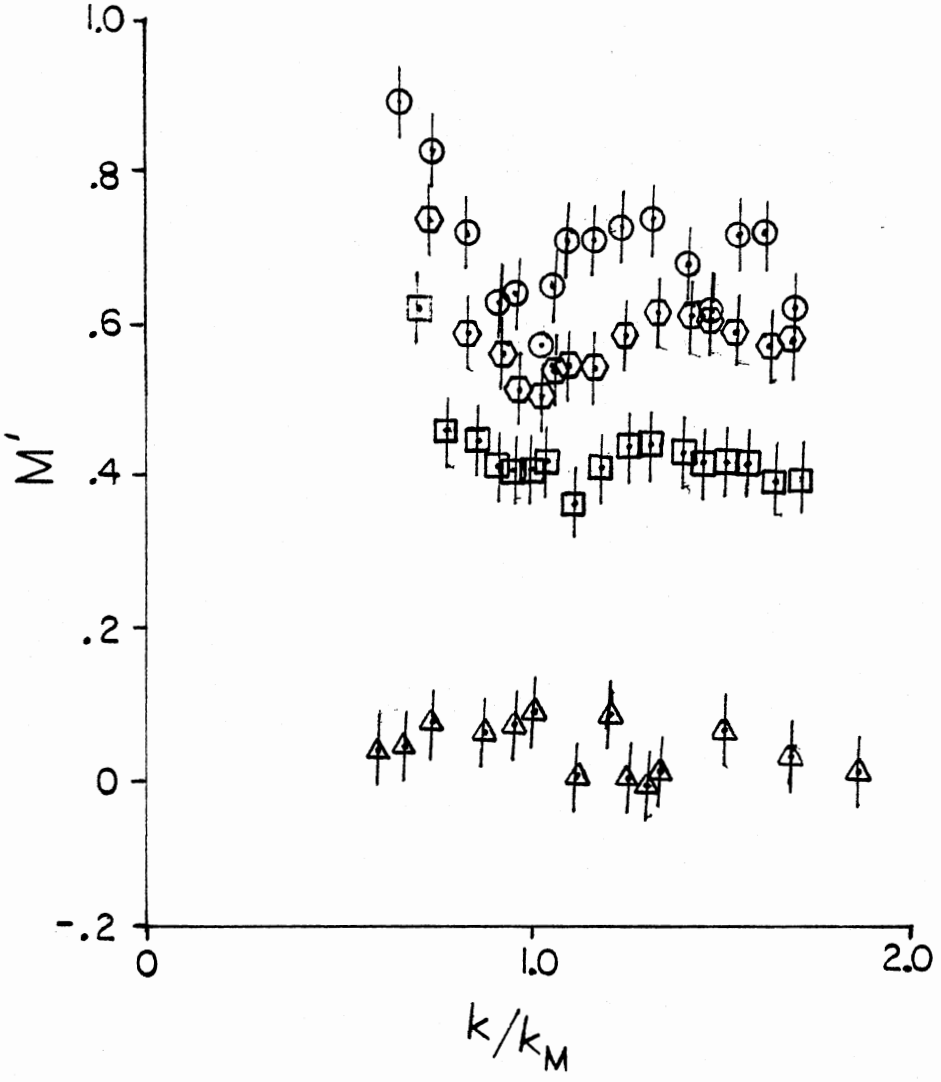

Figure 23. Reduced Memory Functions for the Experimental Systems. Δ is Noninteracting Sample, [] is Sample 1, ⬡ is Sample 2, and O is Sample 3

system should decay as a single exponential and thus have no memory function. By measuring this it gives some idea of the error involved in the determination of M'. M' always appears to be too high which indicates that our determination of the area is always a little high. The average error is about .05 and this value is used for the error bars in the other systems.

The reduced memory function increases as the strength of interaction increases, as expected. M' shows some structure as the interactions strengthen. The reason for this structure is not understood. In Figure 24 the reduced memory function of system 2, representative data of Gruner and Lehmann (1979) and a mode-mode coupling calculation of M' based on Gruner and Lehmann's data (Hess, 1981b) is shown. Instead of a peak at $k \approx k_m$ as seen in Gruner and Lehmann's data, we find a minimum. We suspect that the maximum at this point was caused by multiple scattering in Gruner and Lehmann's sample. This is understood by noting that the single scattered first cumulant is small at $k = k_m$, whereas the multiple scattered first cumulant is still large (see Chapter III). Thus the measured first cumulant will see the effects of multiple scattering most when the single scattered first cumulant is small. Hence, the error in the measured first cumulant will be greater at the peak in the structure factor than in the surrounding points. This in turn causes the measured M' to be higher at this point than the surrounding points as well as higher than M' in the absence of multiple scattering.

Although Hess's calculation does not have a maximum at $k/k_m \approx 1$, neither does it have a minimum. Qualitative agreement is seen between his theoretical and our experimental results. The mode-mode coupling calculation shows structure that is similar to that seen

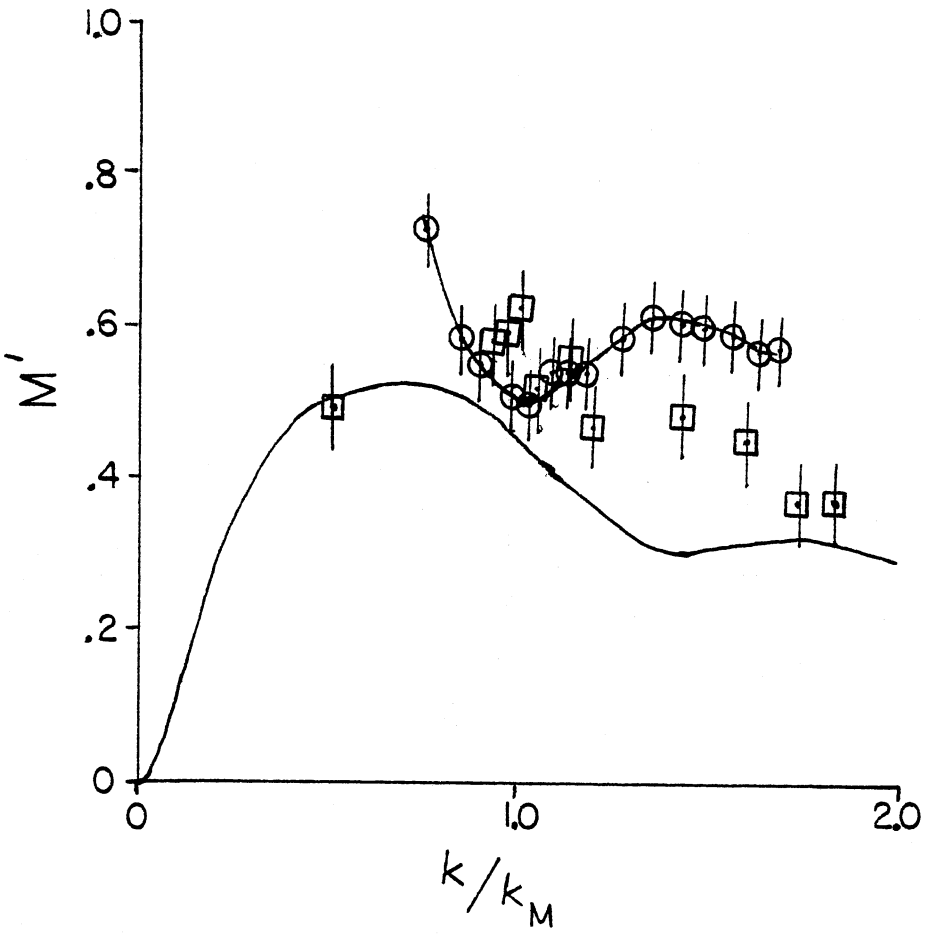

Figure 24. Comparison of Experimental Reduced Memory Function With Theory. O is System 2, [] is Representative Data of Gruner and Lehmann (1979) and the Solid Line is the Theoretical Prediction of Hess (1981b)

experimentally but with a different "frequency". These differences could be caused by not using the static structure factor of system 2 in the calculation as well as deficiencies in the mode-mode coupling model.

The reason for a minimum in M' at $k/k_m \approx 1$ is still not clear. To get a better view of the system, the longitudinal viscosity is found using the FPE result

$$M' = \frac{\eta_{11} k^2/c\xi}{1 + \eta_{11} k^2/c\xi} \tag{5.2}$$

The reason for using the FPE result rather than the SE result is that Hess suggests the SE approach is only valid for $M' << 1$. In Figure 25 the viscosity, η_{11} is plotted on a logarithmic scale. The viscosity is a minimum at $k \approx k_m$. This may be because the particles want to be at this position and small thermal excitations are relatively easy near the minimum in the potential of mean force. Larger movements should be dampened and is seen as a rise in viscosity around this point.

The results presented here, although in great contrast to that of Gruner and Lehmann, provide some insight into systems of interacting particles and the structure of liquids. The longitudinal viscosity increases as the "liquid" approaches crystallization but the structure is as yet not understood. Our data improves on that of Gruner and Lehmann in that the effects of multiple scattering have been eliminated. Also the three experimental systems studied differ only in the strength of the interactions.

We were unable to reach the main peak in M' due to restrictions imposed by our apparatus. An attempt was made to reach the peak by increasing the concentration of colloidal particles. However, the samples

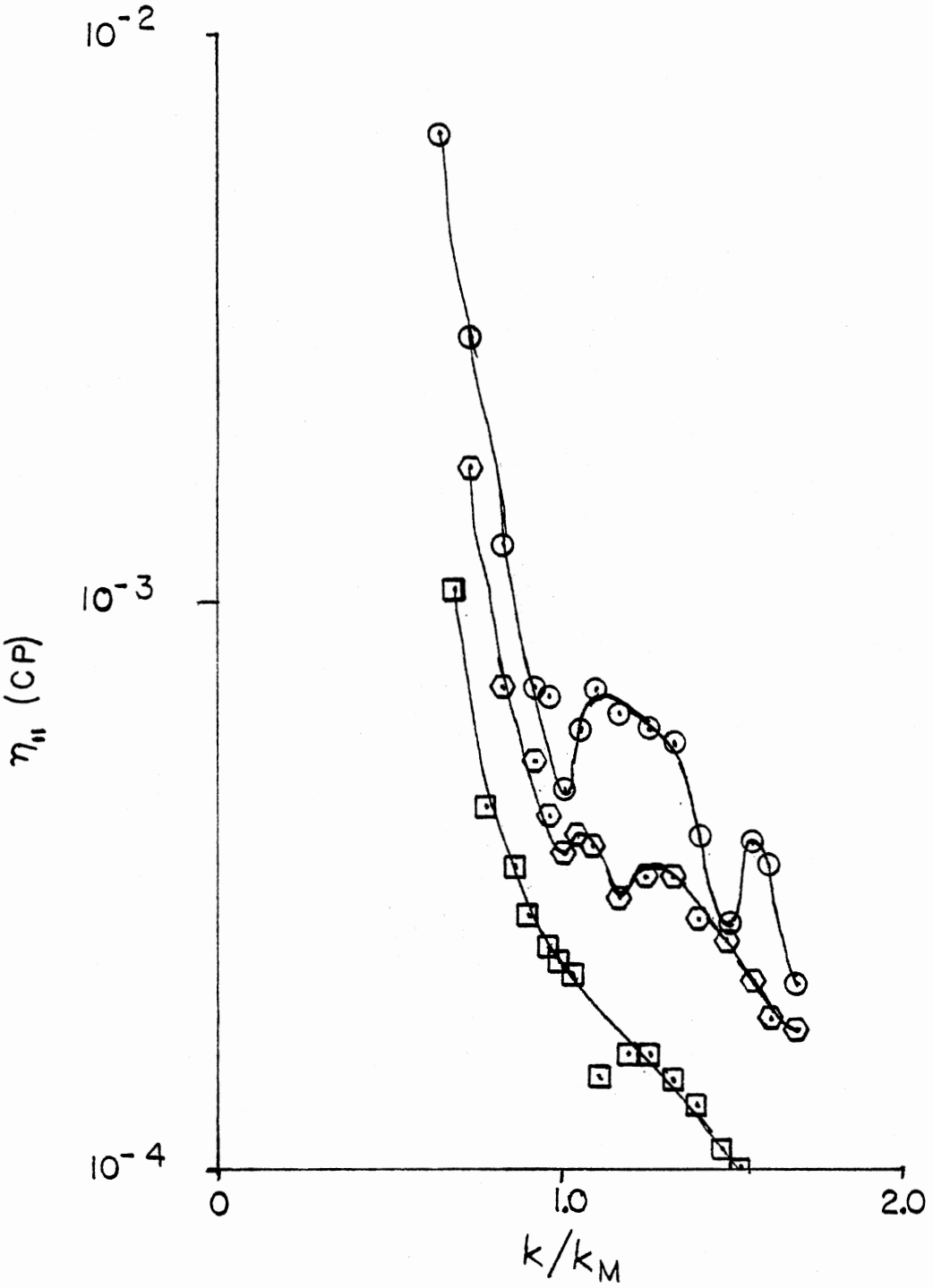

Figure 25. Intrinsic Longitudinal Viscosity for the Three Interacting Systems. [] is Sample 1, ⬡ is Sample 2 and O is Sample 3

were not sufficiently stable in the liquid-like state and crystalized quickly. We feel, however, that the peak should occur before $k/k_m = .5$. From this point it should go to zero as k/k_m goes to zero.

Recently, the FPE results for the intermediate scattering function, $S(k,\omega)$, Eq. (2.11), have been questioned. When the SE is corrected so that the assumption $\eta_{11} k^2/c\xi << 1$ is no longer needed, there should appear a correction to the first cumulant. It becomes

$$K_1 = Dk^2/S(k)(1+A) \tag{5.3}$$

where A is the correction. This correction is not seen in the results of Hess (1981b). However, the disparity can be resolved if under the assumptions used by Hess the longitudinal viscosity can be decomposed into the sum of a constant and a k-ω dependent function so that

$$\eta_{11}(k,\omega) = \eta^{o}_{11} + \eta'_{11}(k,\omega) \tag{5.4}$$

In this case the first cumulant would agree with that of the corrected SE with $A \propto \eta^{o}_{11}$. If this is true and the correction is small, then the results presented here are valid.

This gives us an idea as to what further work needs to be done in this area. Theoretical models need to be investigated in order to find an explanation for the structure in the longitudinal viscosity. Experimentally, the procedure and apparatus used in this study needs to be improved so that the region $k/k_m = .1 - .7$ can be reached. The averaged scattered intensity should also be measured and compared to the static structure factor obtained from the first cumulant. This would give a measure of the correction factor A and possibly η^{o}_{11}.

Thus there remains a great deal to be done to better understand the physics of simple liquids and the method of dynamic light scattering used on aqueous suspensions of latex spheres appears to be a very promising approach.

A SELECTED BIBLIOGRAPHY

Ackerson, B. J., J. Chem. Phys. 64, 242 (1976).

Ackerson, B. J., J. Chem. Phys. 69, 684 (1978).

Altenberger, A. R., Optica Acta 27, 345 (1980).

Berne, B. J., Photon Correlation Spectroscopy and Velocimetry, Plenum Press, N. Y. (1977).

Berne, B. J. and R. Pecora, Dynamic Light Scattering, John Wiley and Sons, N. Y. (1976).

Bøe, A. and O. Lohne, Phys. Rev. A 27, 2023 (1978).

Brown, J. C., P. N. Pusey, J. W. Goodwin, and R. H. Ottewill, J. Phys. A: Math. Gen. 8, 664 (1975).

Colby, P. C., L. M. Narducci, V. Bluemel, and J. Beer, Phys. Rev. A 12, 1530 (1975).

Chu, B., The Application of Laser Light Scattering to the Study of Biological Motion, Plenum Press, N. Y., in press.

Dieterich, W. and I. Peschel, Physica 95A, 208 (1979).

Egelstaff, P. A., An Introduction to the Liquid State, Academic Press, London, N. Y. (1967).

Gruner, F. and W. Lehmann, J. Phys. A: Math. Gen. 12, L303 (1979).

Gruner, F. and W. Lehmann, J. Phys. A: Math. Gen. 13, 2155 (1980).

Hanson, J. P. and I. R. McDonald, Theory of Simple Liquids, Academic Press, London, N. Y. (1976).

Hess, W., Physica 107A, 190 (1981a).

Hess, W., J. Phys. A. 14, L145 (1981b).

Hess, W. and R. Klein, Physica 105A, 552 (1981).

Hurd, A. J., R. C. Mockler, and W. J. O'Sullivan, Proc. 4th Int'l. Conf. Photon Correlation Techniques in Fluid Mechanics, Stanford University Press, Stanford University (1980).

Hurd, A. J., "The Lattice Dynamics of Colloidal Crystals" (Unpub. Ph.D. Dissertation, University of Colorado, 1981).

Kelley, H. C., J. Phys. A. 6, 353 (1973).

Koppel, D. E., J. Chem. Phys. 57, 4814 (1972).

Kubo, R., Rep. Prog. Phys. 29, 255 (1966).

Martin, P. C., Statistical Mechanics of Equilibrium and Non-Equilibrium, North-Holland Publ., Amsterdam (1965).

Martin, P. C., Measurements and Correlation Functions, Gordon and Breach Science Publ., N. Y. (1968).

McCarvill, W. T. and R. M. Fitch, J. Coll. Interface Sci. 64, 403 (1978).

Phillies, G. D. J., Phys. Rev. A. 24, 1939 (1981).

Pike, E. R., Photon Correlation and Light Beating Spectroscopy, Plenum Press, N. Y. (1974).

Pusey, P. N., J. Phys. A: Math. Gen. 8, 1433 (1975).

Pusey, P. N. and R. J. A. Tough, Dynamic Light Scattering and Velocimetry, Plenum Press, N. Y. (1981).

Pusey, P. N., to be published.

Schaefer, D. W. and B. J. Ackerson, Phys. Rev. Lett. 35, 1448 (1975).

Schofield, P., Physics of Simple Liquids, North-Holland Publ. Amsterdam (1968).

Siano, D. B., B. J. Berne, and G. W. Flynn, J. Coll. Interface Sci. 63, 282 (1978).

Sorensen, C. M., R. C. Mockler, and W. J. O'Sullivan, Phys. Rev. A. 14, 1520 (1976).

Sorensen, C. M., R. C. Mockler, and W. J. O'Sullivan, Phys. Rev. A. 17, 2030 (1978).

Titulaer, U. M., Physica 91A, 321 (1978).

Uhlenbeck, G. E. and G. W. Ford, Lectures in Statistical Mechanics, American Mathematical Society, Providence R. I. (1963).

Wilemski, G., J. Stat. Phys. 14, 153 (1976).

VITA

Thomas Warren Taylor

Candidate for the Degree of

Doctor of Philosophy

Thesis: DYNAMIC LIGHT SCATTERING FROM A SYSTEM OF INTERACTING COLLOIDAL PARTICLES

Major Field: Physics

Biographical:

Personal Data: Born in Tulsa, Oklahoma, June 13, 1955, the son of Mrs. Georgia Beasley and the late Dr. Thomas W. Taylor.

Education: Graduated from Atlanta High School, Atlanta, Texas, in May, 1973; received Bachelor of Science degree in physics from Lamar University in 1977; completed requirements for Doctor of Philosophy degree at Oklahoma State University in July, 1983.

Professional Experience: Teaching Assistant, Department of Physics, Lamar University, 1974-1977; NSF Undergraduate Research Participant, 1976; Graduate Teaching Assistant, Department of Physics, Oklahoma State University, 1977-1982; Participated in NATO Advanced Study Institute on the Application of Light Scattering to the Study of Biological Motion, Maratea, Italy, 1982; Graduate Research Assistant, Department of Physics, Oklahoma State University, 1982-1983.